INTERCELLULAR JUNCTIONS AND TUBULOBULBAR COMPLEXES BETWEEN SERTOLI CELLS IN PRIMARY CULTURE AND *IN VIVO*

by

Aarati Sriram

M.Sc., Simon Fraser University, 2014

A THESIS SUBMITTED IN PARTIAL FULFILLMENT OF

THE REQUIREMENTS FOR THE DEGREE OF

DOCTOR OF PHILOSOPHY

in

THE FACULTY OF GRADUATE AND POSTDOCTORAL STUDIES

(Cell and Developmental Biology)

THE UNIVERSITY OF BRITISH COLUMBIA

(Vancouver)

August 2019

The following individuals certify that they have read, and recommend to the Faculty of Graduate and Postdoctoral Studies for acceptance, the dissertation entitled:

Intercellular junctions and tubulobulbar complexes between Sertoli cells in primary culture and *in vivo*

submitted by Aarati Sriram in partial fulfillment of the requirements for

the degree of Doctor of Philosophy

in Cell and Developmental Biology

Examining Committee:

Dr. Wayne Vogl, Cell and Developmental Biology
Supervisor

Dr. Julian Guttman, Cellular Microbiology
Supervisory Committee Member

Dr. Lacey Samuels, Botany
Supervisory Committee Member

Dr. Hakima Moukhles, Cellular and Physiological Sciences
University Examiner

Dr. Calvin Yip, Biochemistry
University Examiner

Additional Supervisory Committee Members:

Dr. Calvin D. Roskelley, Cellular and Physiological Sciences
Supervisory Committee Member

Abstract

Tubulobulbar complexes (TBCs) are actin-rich structures that form at intercellular junctions in the seminiferous epithelium of the mammalian testis. Massive intercellular junctions form at the base of the epithelium where Sertoli cells are connected to each other, and at the apex where Sertoli cells are connected to mature spermatids. TBCs are proposed to be responsible for internalizing these intact junctions during spermiation at the apex and during the translocation of spermatocytes from basal to adluminal compartments near the base of the epithelium. A growing body of evidence indicates that apical TBCs internalize tissue specific adhesion junctions at the apex of the epithelium and are involved in sperm release. In comparison, relatively little is known about basal TBC function and spermatocyte translocation. This thesis explores the hypothesis that the presence of spermatogenic cells influences the structure of TBCs at basal junctions between Sertoli cells *in vitro*. A primary Sertoli-germ cell co-culture system was optimized and used to explore TBC structure *in vitro*. In the seminiferous epithelium, if basal TBCs are responsible for internalizing junctions, then interfering with TBC structure or formation should lead to delayed translocation of spermatocytes and increased mass of basal intercellular junctions. An *in vivo* ribonucleic acid interference (RNAi) procedure was optimized to knockdown cortactin, a component of TBCs, and the morphological differences on basal TBCs were observed. This work is a necessary prelude to future work to evaluate the role of basal TBCs during spermatocyte translocation. Finally, this thesis shows that disruption of actin at basal TBCs results in the same altered TBC structure as has been observed at apical sites.

Lay Summary

The research discussed in this thesis focuses on unique structures termed tubulobulbar complexes (TBCs), which are involved in removing cell-to-cell attachments in the mammalian testis during the development of germ cells and release of sperm. To date there have been few detailed studies of the role of TBCs in germ cell movement within the testis. This thesis provides evidence that when germ cells are grown in culture with supporting cells of the testis, TBCs that more closely resemble those in tissue are present than when these germ cells are absent from the cultures. Moreover, results of studies are presented that are a prerequisite to testing the hypothesis that TBCs are part of the mechanism by which the next generation of germ cells move deeper into the epithelium. Finally, this study provides evidence that the cytoskeleton (cell skeleton) surrounding TBCs is necessary for maintaining normal TBC structure.

Preface

Chapter 2: The isolation, culture, and characterization of differences in growth and morphology of Sertoli cells isolated from 20 and 30-day-old rats

Aarati Sriram was involved in optimizing experimental methods, execution of experiments, maintaining primary Sertoli cell cultures, image acquisition using light and confocal microscopy and data analysis. Min Du initially provided training on basic primary culture techniques. Athena Huynh (Nghi Huynh), John Shadarevian, and Diana Djaksigulova contributed to execution of experiments and image acquisition using light and confocal microscopy. Prunveer Palia contributed to image acquisition and data analysis. Dr. A. Wayne Vogl was involved in designing the research project, maintaining the animal breeding colonies at the animal care facility, the surgical removal of testes from animals, processing tissue for electron microscopy and acquiring light and electron micrographs. Dr. Calvin D. Roskelley and Pamela Dean provided their laboratory biosafety cabinet and other essential equipment required to perform all cell culture experiments. Dr. A. F Parlow provided rat follicle-stimulating hormone for all cell culture experiments. Chapter 2 was written by me and edited by Dr. A. Wayne Vogl.

Chapter 3: The co-culture of spermatogenic cells with Sertoli cells promotes formation of basal tubulobulbar complexes *in vitro*

Aarati Sriram was involved in optimizing experimental methods, execution of experiments, maintaining primary Sertoli-germ cell co-cultures, image acquisition using light and confocal microscopy and data analysis. Athena Huynh (Nghi Huynh), John Shadarevian, Diana Djaksigulova and Prunveer Palia contributed to execution of experiments and image acquisition using light and confocal microscopy. Prunveer Palia also contributed to data analysis. Dr. A. Wayne Vogl was involved in design of research, maintaining the animal breeding colonies at the

animal care facility, the surgical removal of testes from animals, processing tissue for electron microscopy and acquiring light and electron micrographs. Dr. Calvin D. Roskelley and Pamela Dean provided their laboratory biosafety cabinet and other essential equipment required to perform all cell culture experiments. Chapter 3 was written by me and edited by Dr. A. Wayne Vogl.

Chapter 4: Optimizing an *in vivo* RNAi technique to study basal junction turnover in the seminiferous epithelium

Aarati Sriram was involved in optimizing experimental methods, execution of experiments including injecting animals with RNAi reagents, image acquisition using confocal microscopy and data analysis. Prunveer Palia, John Shadarevian, Diana Djaksigulova and Athena Huynh (Nghi Huynh) contributed to execution of experiments and image acquisition. Prunveer Palia also contributed to data analysis. Dr. A. Wayne Vogl was involved in design of experiment, handling and maintaining animals at animal care facility prior to, during and post injections, processing tissue for electron and fluorescence microscopy and acquiring light and electron micrographs. Dr. Calvin D. Roskelley and Pamela Dean provided their laboratory biosafety cabinet and other essential equipment required to prepare reagents for *in vivo* siRNA experiments. Dr. Geoffrey L. Hammond's laboratory provided their digital imaging system for imaging all blots by chemiluminescence. Dr. Ed Conway's laboratory provided their cryo-microtome for obtaining sections for immunohistochemical analysis. Chapter 4 was written by me and edited by Dr. A Wayne Vogl.

Chapter 5: Actin disruption results in altered morphology of basal tubulobulbar complexes in rat seminiferous epithelium

Published in The Anatomical Record, June 27, 2016. Aarati Sriram, Kevin R. P. Lyon, Clement Dallas Ho, Nghi Huynh and A. Wayne Vogl

Aarati Sriram was involved in optimizing experimental methods, execution of experiments, processing tissue for electron microscopy, acquiring electron micrographs, data analysis, writing and editing of manuscript. Kevin R. P. Lyon contributed to processing tissue for electron microscopy, execution of experiments, acquiring electron micrographs, data analysis, writing and editing of manuscript. Athena Huynh (Nghi Huynh) and Clement Dallas Ho contributed to processing tissue for electron microscopy and acquiring electron micrographs. Dr. A. Wayne Vogl was involved in design of the experiment, handling and maintaining animals at the animal care facility, conducting *ex vivo* perfusion of rat testes, processing tissue for electron microscopy, acquiring electron micrographs and editing of manuscript. Chapter 5 is an adaptation of my manuscript with minor changes to the text, organization of content and addition of a new figure.

The use of animals in this study has been approved by the Animal Care Committee of the University of British Columbia. Approved animal care protocols are A16-0069, breeding A15-0046, and biosafety B15-0071.

Table of Contents

List of Tables

List of Figures

List of Symbols

% - percent

© - copyright

°C – degree Celsius

III - 3

IV – 4

V – 5

VII - 7

VIII – 8

IX – 9

X - 10

™ - trademark

List of Abbreviations

α6β1 – alpha-6-beta-1

µg - microgram

µl – microlitre

µm – micrometer

µM - micromolar

Y3 – gamma 3

x g – times Earth's gravitational force

2D – two-dimensional

3D – three-dimensional

^{59}Fe – isotope of iron

ADIP – afadin DIL-domain-interacting protein

AP2 – adaptor protein 2

ARP2/3 – actin-related protein 2/3

BSA – bovine serum albumin

BTB – blood-testis barrier

Ca^{2+} - calcium ion

$CaCl_2$ – calcium chloride

CAR – coxsackievirus and adenovirus receptor

cm^2 – square centimeter

CO_2 – carbon dioxide

Cttn – cortactin

DAPI – 4', 6-diamidino-2-phenylindole

ddH_2O – double-distilled water

DMEM – Dulbecco's modified eagle medium

DMSO – dimethyl sulfoxide

DNase – deoxyribonuclease

E-cadherin – epithelial cadherin

ECL - electrochemiluminescence

ECM – extracellular matrix

EDTA – ethylenediaminetetraacetic acid

EEA1 – early endosomal antigen 1

EGF – epidermal growth factor

ER – endoplasmic reticulum

ESs – ectoplasmic specializations

F-actin – filamentous actin

FBS – fetal bovine serum

FSH – follicle-stimulating hormone

g - grams

GDNF – glial cell derived neurotrophic factor

h – hour

HCl – hydrochloric acid

IgG – immunoglobulin G

JAM-1 – junctional adhesion molecule-1

KCl – potassium chloride

kDa – kilodaltons

kg – kilogram

KH_2PO_4 – potassium dihydrogen phosphate

kV – kilovolt

LAMP1 – lysosomal associated membrane protein 1

LIF – leukemia inhibitory factor

M – molar

mg – milligram

Mg^{2+} - magnesium ion

$MgSO_4$ – magnesium sulfate

min – minute

ml – milliliter

mM – millimolar

mRNA – messenger ribonucleic acid

N-cadherin – neural cadherin

N-WASP – neuronal wiskott-aldrich syndrome protein

N/P – nitrogen to phosphate ratio

Na – sodium

NaCl – sodium chloride

$NaHCO_3$ – sodium bicarbonate

ng – nanogram

nm – nanometer

NMIgG – normal mouse immunoglobulin

NRIgG – normal rabbit immunoglobulin

O_2 – oxygen

OCT – optimal cutting temperature

OCT 3 / 4 – octamer-binding transcription factor 3 / 4

pAJ – punctate adherens junction

PBS – phosphate-buffered saline

PDGF – platelet-derived growth factor

PEI - polyethylenimine

pH – potential hydrogen

PLZF – promyelocytic leukemia zinc finger

PND – postnatal day

PVDF – polyvinylidene difluoride

qPCR – quantitative polymerase chain reaction

Rab5 – ras-related protein Rab-5

RBM – reconstituted basement membrane

RIPA – radioimmunoprecipitation assay buffer

RNA – ribonucleic acid

RNase – ribonuclease

RNAi – ribonucleic acid interference

RPM – revolutions per minute

SACS – soft agar culture system

SALL4- sal-like protein 4

SCP-3 – synaptonemal complex protein 3

SDS – sodium dodecyl sulfate

SFDM – serum-free defined medium

siRNA – small interfering ribonucleic acid

SSCs – spermatogonial stem cells

TBCs – tubulobulbar complexes

TBST – tris-buffered saline tween 20

TPBS – tris phosphate-buffered saline

U/ml – units per milliliter

ZO – zonula occludens

Acknowledgements

I would like to express my deepest gratitude to my supervisor, Dr. Wayne Vogl, for his guidance, encouragement and support. It has been an honor to work with you.

I am ever grateful to my committee members, Dr. Julian Guttman, Dr. Calvin Roskelley and Dr. Lacey Samuels, who have provided valuable input, guidance and support throughout the research process.

Thanks to my lab mates, Arlo Adams and Kevin Lyon for the great company and constant support. It's been a pleasure working with both of you.

Thanks to my fabulous team of undergraduate research assistants, Athena Huynh, Clement Ho, John Shadarevian, Diana Djaksigulova and Prunveer Palia for all your help and entertaining conversations.

A special thanks to my mom, dad and brother for their unwavering support, love and guidance. None of this would be possible without you. I owe particular thanks to my dear husband, Karthik, who supported me in every way possible throughout my degree. Thanks for all the love and encouragement.

Dedication

To Karthik, Sriram, Jayashree and Rohit for their love and support.

Chapter 1: Introduction

1.1 The mammalian seminiferous epithelium and spermatogenesis

The mammalian testis contains a tubular compartment surrounded by an interstitial compartment. The interstitium is the space between the tubules and contains lymphatics, blood vessels, connective tissue and steroidogenic Leydig cells that produce testosterone. The tubular compartment is comprised of numerous tiny convoluted tubules termed seminiferous tubules. The tubules are enclosed by a layer of contractile peritubular myoid cells that are separated from the epithelium lining the inside of the tubules by a basal lamina.

Spermatogenesis, the production of male gametes, occurs in the most complex epithelium in the body known as the seminiferous epithelium. This epithelium lines the seminiferous tubules of the mammalian testis and is made up of Sertoli cells and spermatogenic cells (Fig. 1.1). The Italian physiologist and histologist, Enrico Sertoli, was the first to discover Sertoli cells in 1865[1,2]. He described their appearance as cells with long cytoplasmic arms that wrapped germ cells and postulated that the intricate physical association with developing germ cells was linked to the process of spermatogenesis. Later, in the mid 1960s – 1970s, investigators closely examined and described the ultrastructural relationship between Sertoli-Sertoli and Sertoli-germ cells using data produced by transmission electron microscopes[2]. The tall and somewhat columnar Sertoli cells are the major architectural units of the seminiferous epithelium and generally do not divide. They span the entire width of the epithelium, from the basal lamina to the lumen of the tubule and provide mechanical support and nourishment for the spermatogenic cells throughout their development, thereby functioning as 'nurse cells'[1,3,4]. Near the base of the epithelium, massive junction complexes connect neighboring Sertoli cells to each other (Fig. 1.1) and divide the epithelium into a basal compartment below the junctions, and an adluminal compartment above[5].

Unlike Sertoli cells, spermatogenic cells are proliferative and undergo differentiation. Spermatogenic cells lie in between and are attached to Sertoli cells (Fig. 1.1) and begin their journey of maturation with diploid spermatogonia in the stem cell niche at the base of the epithelium. Through a series of mitotic divisions, these cells produce spermatocytes that then enter meiosis. The leptotene spermatocytes pass through basal Sertoli cell junction complexes and translocate upwards into the adluminal compartment where they complete meiosis and become haploid spermatids[6]. The spermatids elongate and mature in apical invaginations or crypts of Sertoli cells. The spermatids are firmly anchored to Sertoli cell crypts by large adherens junctions (Fig. 1.1). Eventually, the mature spermatids are released into the lumen as spermatozoa and enter the duct system of the male reproductive tract. As they are released from the epithelium, their excess cytoplasm is removed and endocytosed by Sertoli cells[7].

1.2 Intercellular adhesion junctions in epithelial cells

Junctional complexes mediate cell-cell contact and communication and help hold cells together in epithelial tissue. These junctional complexes consist of tight junctions, gap junctions, desmosomes and adherens junctions. Each of these major types of cell junctions have different functions and are made up of trans-membrane proteins that help cells form contact with neighboring cells.

1.2.1 Tight junctions

Tight junctions are a type of cell-cell junction between epithelial cells that form a barrier between different compartments of the body. They are generally present in the most apical regions of epithelial cells. Tight junctions regulate the diffusion between compartments of ions and molecules based on their size and charge[8]. Occludins[9,10] and claudins[11,12] and immunoglobulin superfamily members, junctional adhesion molecules (JAM-1)[13] and the

coxsackievirus and adenovirus receptor (CAR)[14] are the different types of integral membrane proteins found at tight junctions. In addition to barrier functions, both occludins and claudins are also involved in signalling and cell-cell adhesion. Both of these proteins consist of four trans-membrane domains, two intracellular and two extracellular domains[15]. Occludin and claudin bind to cytoplasmic adaptor proteins such as zonula occludens (ZO-1, ZO-2 and ZO-3), which help stabilize and link the junctions to the cell's internal actin cytoskeleton[15,16].

Tight junctions are necessary for maintaining barrier function in various types of tissues. They play an important role in forming the blood-brain barrier, which restricts the diffusion of compounds from blood to the brain. The tight junctions that form this barrier connect capillary endothelial cells within cerebral blood vessels. The blood-retina barrier functions in a similar manner and is also composed exclusively of tight junctions between retinal capillary endothelial cells[17]. The blood-testis barrier (BTB) is one of the tightest tissue barriers in the mammalian body[5,18]. Between neighboring Sertoli cells at the base of the seminiferous epithelium, tight junctions together with adherens junctions, gap junctions and desmosome-like junctions form massive junction complexes[17] (Fig. 1.1) that separate basal from adluminal compartments of the epithelium. Tight junctions within these complexes contribute to forming the BTB.

1.2.2 Gap junctions

Gap junctions are formed by intercellular channels that connect the cytoplasm of adjacent cells and permit the exchange of small molecules (up to 1 kDa) and ions. They are involved in regulating cellular communication and enhance electrical and metabolic coupling between cells. The gap junction channels are composed of the connexin family of integral membrane proteins. A group of six connexins (each with four transmembrane domains) form a connexon hemichannel[19] and two connexon hemichannels, one on each cell, form a channel that permits exchange of various substances across the intercellular space[19,20]. These channels can exist in

an open or closed conformation depending on response to metabolic signals[21,22]. Connexins form associations with the scaffolding protein, ZO-1, to recruit signalling proteins[23] and interact with the underlying cytoskeleton[24].

1.2.3 Desmosomes

Desmosomes (macula adherens junctions) are cell-cell adhesion junctions that connect adjacent cells intracellularly to intermediate filaments and strongly hold cells together. They maintain tissue integrity by providing mechanical strength and resisting shearing forces[21]. Typical desmosomes are made up of the cadherin family of transmembrane proteins, desmoglein and desmocollin and these adhesion molecules are ultimately linked to intermediate filaments via adaptor proteins (plakoglobin, plakophillin and desmoplakin)[15].

1.2.4 Adherens junctions

Adherens junctions are intercellular protein complexes that are generally located below tight junctions and form mechanical attachments between the sides of adjacent epithelial cells. They are involved in providing support and maintaining tissue structure. Adherens junctions usually appear as small zones or belt-like junctions around the entire cell and are called zonula adherens[25]. These junctions are primarily composed of the homophilic cadherin family of transmembrane proteins, typically E-cadherin in many epithelia[21]. The extracellular segments of cadherins in adjacent cells bind to each other and the cytoplasmic tails of cadherins bind to catenins forming the cadherin-catenin complex[26]. Catenins are adaptor proteins that link cadherins to the surrounding actin cytoskeleton. The proper functioning and morphology of cadherins is highly dependent on the presence of Ca^{2+}. In addition to cadherins, nectins are another group of adhesion junction proteins, but are Ca^{2+} independent. They bind to the underlying actin cytoskeleton via the adaptor protein afadin[16,25,27] that organizes their connection

by interacting with binding proteins such as ponsin and afadin DIL-domain-interacting protein (ADIP)[28,29]. Nectin molecules form either homotypic or heterotypic junctions with molecules in neighboring cells. Adherens junctions are also composed of the heterotypic interacting proteins, integrins that help facilitate cell-extracellular matrix adhesion either directly or via scaffolding proteins. Adherens junctions can also occur focally in cells where they are termed punctate adherens junctions (pAJ) or *puncta adhaerentia*[30].

1.3 Junction complexes in the seminiferous epithelium

A variety of intercellular junctions are present in the seminiferous epithelium that interact with different elements of the cytoskeleton (actin filaments, microtubules and intermediate filaments)[31,32]. Intercellular adherens junctions termed ectoplasmic specializations (ESs), tight junctions, gap junctions and desmosome-like junctions occur in basal regions of the epithelium[33] (Fig. 1.1), not at the apex as they do in columnar cells of other types of epithelia. At the apex of the epithelium, mainly ESs are present around apical crypts where Sertoli cells are attached to the heads of spermatids[34] (Fig. 1.1).

1.3.1 Ectoplasmic specializations

Sertoli cells are attached to each other and to spermatogenic cells by large actin-rich intercellular adhesion junctions (Fig. 1.1) called ectoplasmic specializations (ESs)[35]. ESs are testis-specific[36] and are tripartite structures characterized by a layer of actin filaments packed into hexagonal arrays between an attached cistern of endoplasmic reticulum (ER) on one side of the actin layer and the Sertoli cell plasma membrane on the other[33,37,38]. They form at two major locations in the seminiferous epithelium (Fig. 1.1). The first location is at the base of the epithelium as part of the basal junction complex linking neighboring Sertoli cells (homotypic junction) (Fig. 1.1) and the second location is at apical sites where Sertoli cells are attached to

elongate spermatids (heterotypic junction) (Fig. 1.1). Integral membrane adhesion molecules that mediate cell-cell adhesion such as nectin-2[27] and α6β1 integrin[39] have been localized at ESs in Sertoli cells. The ligand for α6β1 integrin is reported to be Ɣ3 laminin[40] and for nectin-2 is either nectin-3 (heterotypic junction) in spermatids[27] or another nectin-2 (homotypic junction) in the adjacent Sertoli cell[27,39]. N-cadherin has also been reported to be present at ESs[41], though their presence at these sites still remains unclear[42]. At the base of the epithelium, ESs are part of the large belt-like junction complexes that also include tight, gap and desmosome-like junctions[33]. The major integral membrane protein involved in forming tight junctions in the seminiferous epithelium is claudin-11 (oligodendrocyte-specific protein)[5,43], although as the new junctions form, claudin-3 is present first before being replaced by claudin-11 as the junction matures[44]. The most abundant gap junction protein present at basal junction complexes is connexin-43[20,45,46].

ESs have gained a lot of interest in recent years, as they are considered primary targets for the development of male contraceptives[37,47]. A thorough understanding of the biology and regulation of the junction complexes is therefore very important for developing effective male contraceptives and potentially identifying new targets for these contraceptives in the future.

1.4 Junction turnover generally in cells

Intercellular junctions in cells are not static structures and their timely assembly and disassembly is important during normal physiological processes such as morphogenesis, epithelial renewal, movement of cells between compartments and tumor progression. Internalization of tight and adhesion junctions in cells generally involves detachment from ligands on adjacent cells, followed by endocytosis of junction molecules separately into each cell via clathrin/caveolin-mediated endocytosis[48–51] or macropinocytosis[52]. In contrast, gap

junctions are internalized as intact junctions in double membrane vesicles by one of the cells in a clathrin-dependent manner[53,54].

1.5 Junction turnover in the seminiferous epithelium

The cyclic turnover of massive intercellular junctions and related changes in the cytoskeleton plays a pivotal role during two major morphogenic events that occur during spermatogenesis – (1) movement of the next generation of spermatocytes from basal to adluminal compartments of the seminiferous epithelium, and (2) release of elongated spermatids at the apex. During spermatogenesis, basal junction complexes disassemble above and reassemble below spermatocytes (Fig. 1.1), thereby maintaining the Sertoli cell permeability barrier[6,55]. At the apex of the epithelium, the removal of junctions at attachment sites between mature spermatids and Sertoli cells allows for the release of mature spermatids into the duct system of the male reproductive tract. New junctions are formed with earlier step spermatids situated deeper in the epithelium. Junction turnover occurs at specific stages in the seminiferous epithelium and these have been well described and are easily identifiable in the rat[6,56].

1.5.1 Tubulobulbar complexes, their basic architecture and molecular components

During extensive tissue remodeling in the seminiferous epithelium, Sertoli cells form unique clathrin/actin-based endocytic structures termed tubulobulbar complexes (TBCs) that develop at both apical and basal junction sites (Fig. 1.1) and internalize intact intercellular junctions into Sertoli cells[36,57–61]. The appearance of TBCs coincides with the disappearance of ESs[62]. Their formation at basal sites precedes spermatocyte translocation[4,58] and at apical sites TBCs appear prior to sperm release[62]. Several other functions have also been proposed for TBCs, which include, elimination of excess cytoplasm from spermatids prior to release[4], shaping of

spermatid head[63] and anchoring elongate spermatids to the seminiferous epithelium[62,64]. Only the junction internalization hypothesis accounts for the presence of TBCs both at apical junctions between Sertoli cells and spermatids and at basal sites at junctions between neighboring Sertoli cells.

TBCs are initiated as clathrin-coated pits at intercellular junctions and consist of elongate tubular extensions (generally of 2-3 μm in length) that project from a Sertoli cell or a spermatid into corresponding invaginations of a neighboring Sertoli cell[62,65] (Fig. 1.1). TBCs have three distinct regions (Fig. 1.2): a long proximal tubule, a swollen bulb and a short distal tubule that is capped with a clathrin-coated pit[62,66]. The ends of TBCs are associated with numerous small vesicles. A network of actin filaments cuffs the proximal and distal tubules[66,67] and the bulb is closely associated with cisternae of the ER (Fig. 1.2). As TBCs mature, the bulbar region eventually undergoes scission at its root from the junction[68], coalesce with other internalized bulbs and enters endosomal compartments of Sertoli cells and is degraded[62]. It is unclear what happens to the clathrin coated pits and distal tubules during scission of the bulb.

Previous work in our lab has identified numerous molecular components present at TBCs (Fig. 1.2) that are involved in actin assembly and polymerization as well as clathrin-based endocytosis. Actin[38] and actin-related proteins such as, neuronal wiskott-aldrich syndrome protein (N-WASP)[60], actin-related protein 2/3 (Arp2/3)[60,69], cortactin[60], cofilin[70] and paxillin[71] are localized at tubular membrane cores of TBCs. The network of actin filaments is surrounded by an outer shell composed of plectin and spectrin[72]. The coated pit contains clathrin and related clathrin-mediated endocytic proteins[57,60]. Proteins associated with membrane curvature and scission such as amphiphysin and dynamin[73,74] also are localized at TBCs. The bulbous region of TBCs are associated with the endosomal marker ras-related protein Rab5 (Rab5), and large vesicles present at the ends of TBCs contain early endosomal antigen 1 (EEA1) and lysosomal associated membrane protein 1 (LAMP1)[36,57,61,75]. Extensive membrane contact sites form

between the Sertoli cell plasma membrane and ER at the bulbs[76]. Calcium regulatory machinery has recently been reported to be present at these sites[76].

1.5.2 The role of actin at tubulobulbar complexes

Actin filament networks are an integral component of TBCs. Previous research has shown that perturbation of the testis with cytochalasin D, an inhibitor of actin polymerization[77], impacted the surrounding actin network[68], resulting in short, swollen and abnormally-shaped TBCs at apical junction sites between Sertoli cells and spermatids[68]. Based on these results, it has been proposed that the polymerization of the actin networks associated with TBCs is involved with the formation, elongation and maintenance of tubular regions of the complex[68,78] and depolymerization of the networks is associated with formation, expansion and eventual scission of the bulb during junction turnover[68].

1.5.3 Tubulobulbar complexes internalize junctions

Previous work in our lab has revealed that TBCs contain junction proteins and are associated with markers of endocytosis. The distal ends of TBCs at apical sites contain the adhesion junction proteins, nectin-2[36,74,78], α6β1 integrin[42,61] and nectin-3[36]. Electron microscopy images have also shown the presence of intact junctions (with attached membranes) within TBCs.

In the rat, basal TBCs are largely present at early stages (IV and V) of spermatogenesis well before spermatocytes begin to translocate through basal junction complexes (stage VIII)[4]. This suggests that basal junction turnover begins well before the next generation of spermatocytes move upwards in the seminiferous epithelium[58]. Ultrastructurally identifiable tight, gap, and adhesion junctions[4] and their representative proteins, claudin-11 (tight junction), connexin-43 (gap junction) and nectin-2 (adhesion junction) are present in basal TBCs[57]. The

endosomal markers EEA1, Rab5 and LAMP1 occur at or adjacent to the distal ends of TBCs[36,42,57,61]. The presence of junction proteins and markers of endocytosis within TBCs are consistent with the hypothesis that TBCs internalize intercellular junctions in the seminiferous epithelium.

1.5.4 Apical and basal tubulobulbar complexes

TBCs have been studied most intensely at apical sites of attachment between Sertoli cells and mature spermatids. A growing body of evidence supports the conclusion that TBCs that form at apical sites internalize intercellular junctions between mature spermatids and Sertoli cells[36,42,61] and that their proper functioning is critical for normal spermiation[69,73,79]. Perturbing the formation or structure of apical TBCs results in inhibition of junction internalization and prevents or delays sperm release at the apex[69,73,79].

Although basal TBCs also internalize intercellular junctions[33,57,62] and have been suggested to play a role in spermatocyte translocation[57], they have been much less studied and largely ignored compared to apical TBCs for a number of reasons. Apical TBCs are much easier to study compared to basal TBCs because they are (1) more numerous, (2) form clusters in specific regions adjacent to spermatid heads, and (3) together with spermatid heads, can be easily isolated from the seminiferous epithelium for visualization at high resolution[42]. In comparison, basal TBCs are more difficult to visualize as they often occur in folds or pockets within the intercellular junctions, making it challenging to distinguish them from actin containing ESs of the junction complex[4] using conventional fluorescence microscopy. Basal TBCs do not cluster at any specific or predictable locations in the basal junction complex. In addition, basal TBCs cannot be isolated and fragmented away from the seminiferous epithelium for visualization. As a result, relatively little is known about the regulation of basal TBCs and their role in spermatocyte translocation from one epithelial compartment to another. Recently, our lab

was the first to demonstrate that TBCs develop at basal junctions in morphologically differentiated primary cultures of Sertoli cells[57]. This *in vitro* culture system provides a useful tool for experimental manipulation of TBCs and for studying basal junction remodeling in Sertoli cells.

1.6 Morphologically similar structures to tubulobulbar complexes

Although TBCs are unique to the seminiferous epithelium, they are similar in morphology and molecular composition to clathrin-based endocytosis machinery present generally in cells[58,80]. TBCs have the molecular signature of clathrin-coated pits with extremely long necks; hence, it is likely that they evolved from the basic clathrin-mediated endocytosis mechanism. TBCs also morphologically resemble podosomes in osteoclasts[81] in that they both consist of tubular membranes surrounded by a network of actin filaments. However, TBCs differ from clathrin-coated pits and podosomes in that they exist at intercellular junctions and are formed by two attached plasma membranes of cells as opposed to invagination of a single membrane.

1.7 Overall objectives and chapter aims

TBCs are dynamic actin-related tubular membrane structures that develop at both apical and basal compartments during junction disassembly. Although the link between apical TBCs and sperm release has been established[69,73,79], basal TBCs have yet to be linked directly to the mechanism of spermatocyte translocation. The focus of this thesis is to explore the role of basal TBCs in the internalization of basal junction complexes. The seminiferous epithelium of the rat testis is an ideal model system to conduct this research as basal intercellular junctions are large and easy to visualize, stages of the epithelium have been well defined morphologically and temporally, and the molecular composition and structure both of junctions and of TBCs have been well documented.

The overall objectives of this thesis are to: 1) develop and optimize procedures both *in vivo* and *in vitro* that will help characterize the biological function of basal TBCs and eventually link them to spermatocyte translocation and 2) determine if the function of actin networks at apical and basal TBCs are the same. To meet the first objective, three aims were explored based on the hypothesis that basal TBC-mediated disassembly of intercellular junctions is necessary for spermatocyte translocation from basal to adluminal compartments of the seminiferous epithelium. These specific aims include:

1. To first establish a morphologically differentiated primary Sertoli cell culture.
2. To co-culture early spermatogenic cells with the established primary Sertoli cell culture system and determine if this stimulates junction remodeling by observing developed basal TBCs at the basal junction complex.
3. To optimize and establish a long-term *in vivo* ribonucleic acid interference (RNAi) knockdown procedure to perturb the formation of basal TBCs and observe the effect on them at the morphological level, and eventually enable testing the hypothesis that TBC function is part of the mechanism of spermatocyte translocation through basal junction complexes in the seminiferous epithelium.

Chapter 2 addresses aim 1 and describes the successful establishment of a morphologically differentiated primary Sertoli cell culture from 20-day-old rats that was developed to be used for co-culture studies with spermatogenic cells. Also, it demonstrates the *in vitro* formation of seminiferous cords when Sertoli cells are isolated from slightly more mature animals. Chapter 3 presents the development of a Sertoli-germ cell co-culture to study basal junction remodeling and provides evidence for the development of basal TBCs at these junctions. Also, it provides the first qualitative data indicating that the presence of germ cells may affect the morphology of TBCs. Chapter 4 presents the work on optimizing an *in vivo* RNAi approach to studying the role of TBCs in spermatocyte translocation. If basal TBCs are responsible for internalizing intact

intercellular junctions, then interfering with their structure or formation should prevent junction turnover and lead to delayed translocation of spermatocytes into the adluminal compartment of the epithelium. The experiments discussed in this chapter are crucial to eventually linking basal TBC function to the turnover of the BTB and spermatocyte translocation in the future. In an attempt to begin exploring the function of basal TBCs, an *in vivo* RNAi technique was optimized to alter the expression of cortactin (molecular component of TBC) (Fig. 1.2) in the seminiferous epithelium and prevent TBCs from forming. Finally, chapter 5 of this thesis explores the effects of actin network perturbation on the morphology of basal TBCs in seminiferous tubules. This study is related to the second objective, which is to determine if the role of actin networks at apical and basal TBCs are the same. The results from this project verify the hypothesis that the actin networks at both apical and basal TBCs have similar functions in the seminiferous epithelium.

The results from this thesis contribute to the development of an *in vitro* co-culture system for studying basal junction turnover. Importantly, they also form the foundation for doing crucial *in vivo* experiments to test the hypothesis that basal TBCs are necessary for normal turnover of the BTB and for spermatocyte translocation.

1.8 Chapter 1 Figures

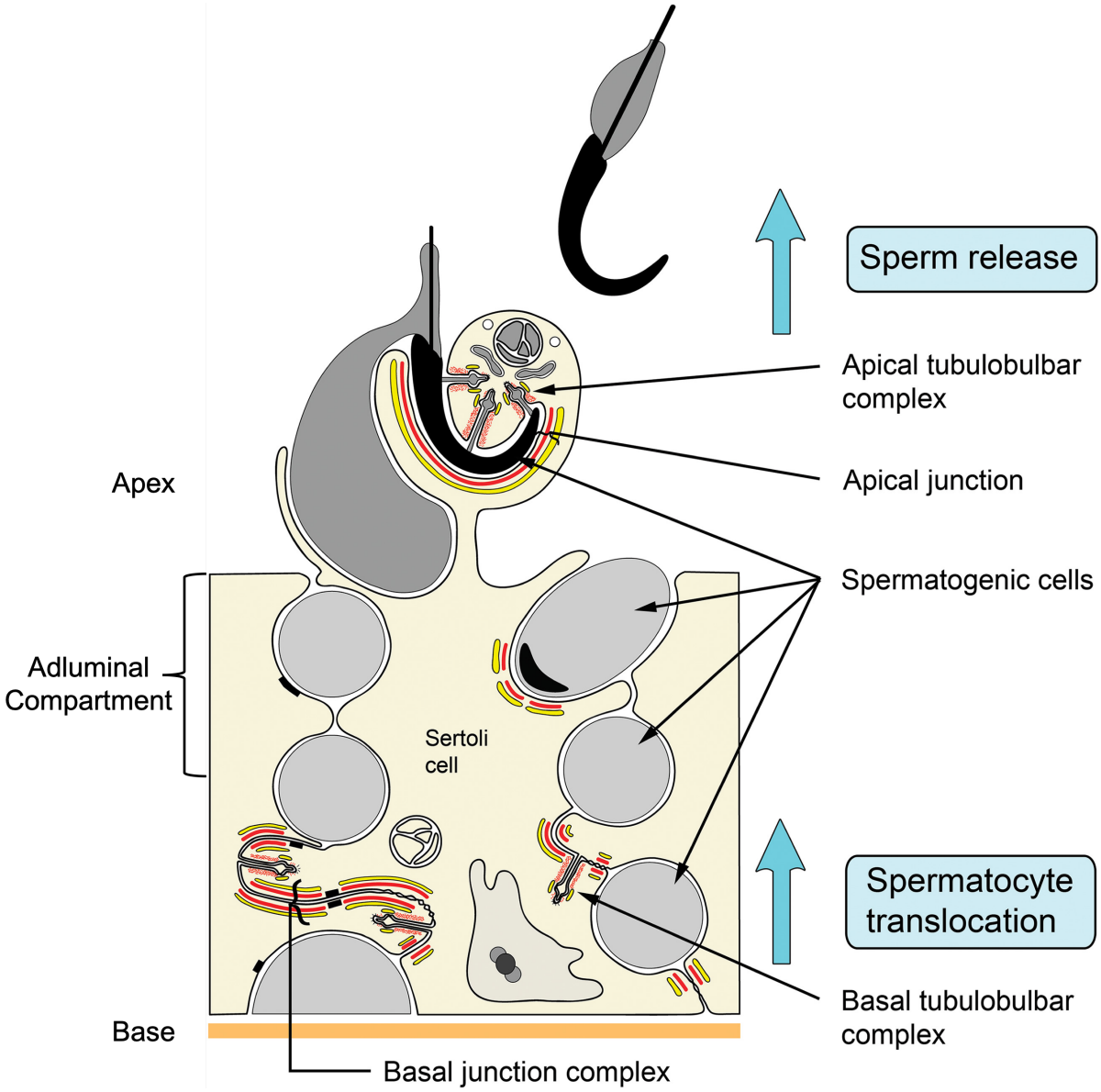

Figure 1.1 Schematic diagram showing the position of junction complexes and tubulobulbar complexes in seminiferous epithelium of the rat.
Basal junction complexes occur between neighboring Sertoli cells at the base of the epithelium. Tubulobulbar complexes form at basal junction complexes to internalize junctions and allow spermatocyte translocation to occur. Apical tubulobulbar complexes form at apical adhesion junctions to remove junction proteins, which anchor the spermatid to the epithelium. The removal of these junctions results in sperm release. Actin filaments are shown in red, and yellow represents the endoplasmic reticulum. Figure 1.1 from © Adams, Sriram, & Vogl (2018)[82]. Internalization of Intact intercellular Junctions in the Testis by Clathrin/Actin-Mediated Endocytic Structures: Tubulobulbar Complexes. The Anatomical Record, 301(12) 2080-2085. Page 2081. Adapted with permission from publisher.

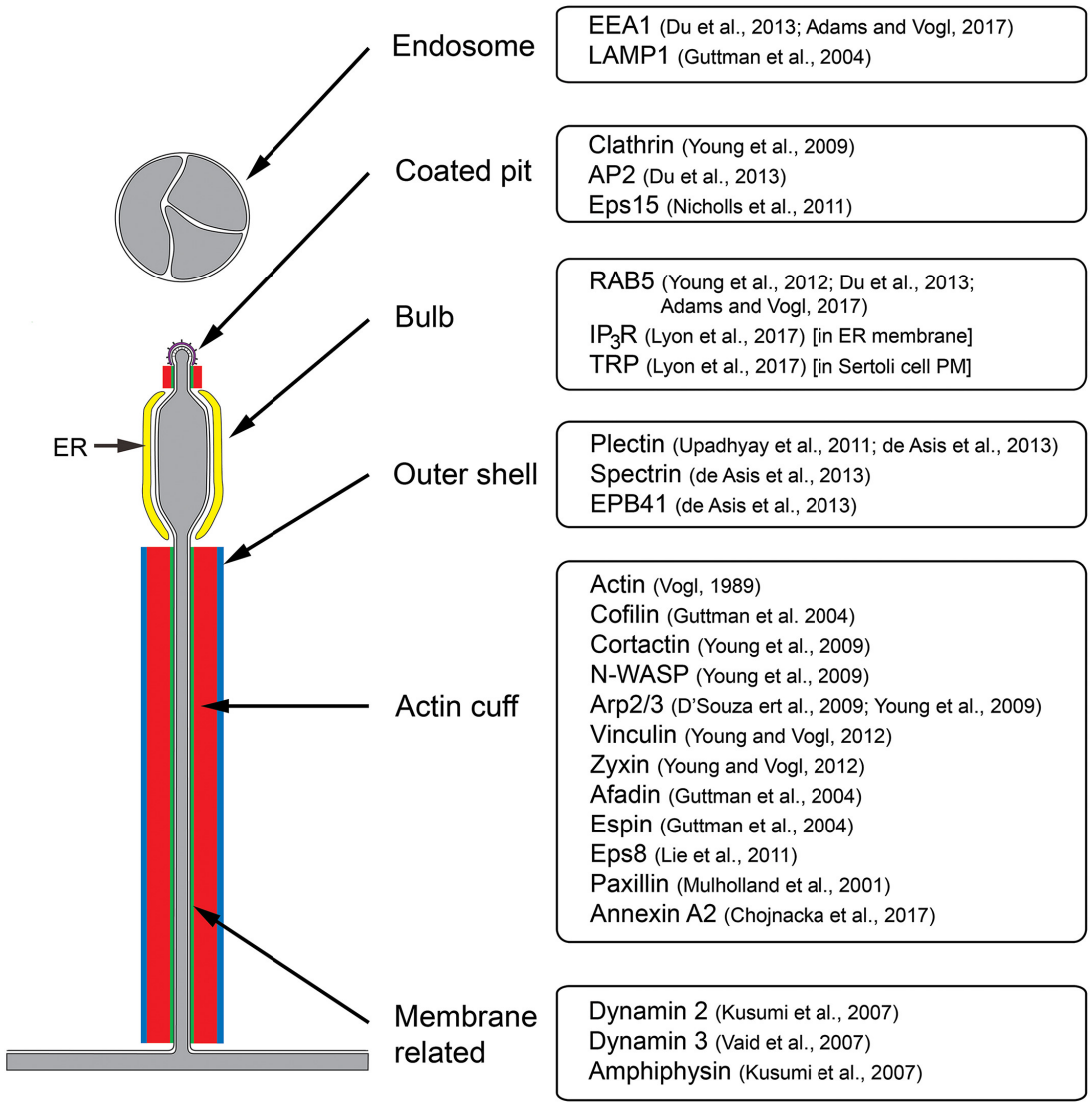

Figure 1.2 Schematic diagram showing the various components of a tubulobulbar complex and the associated proteins with each region.
Numerous molecular components that are either involved in actin assembly, actin polymerization, or clathrin-mediated endocytosis are present at tubulobulbar complexes. The tubular regions are cuffed by a network of actin filaments and are associated with membrane curvature and scission related proteins (dynamin and amphiphysin). The actin cuffs are surrounded by an outer shell composed of plectin and spectrin. The bulb region is in close association with endoplasmic reticulum and endosomal markers. The coated pit contains clathrin and related proteins. After scission, the endosome is associated with endosomal and lysosomal markers (EEA1 and LAMP1). Figure 1.2 from © Adams, Sriram, & Vogl (2018)[82]. Internalization of Intact intercellular Junctions in the Testis by Clathrin/Actin-Mediated Endocytic Structures: Tubulobulbar Complexes. The Anatomical Record, 301(12) 2080-2085. Page 2084. Adapted with permission from publisher.

Chapter 2: The isolation, culture, and characterization of the differences in growth and morphology of Sertoli cells isolated from 20 and 30-day-old rats

2.1 Background

Primary Sertoli cell cultures have long been used as a research tool to study Sertoli cell structure and function, hormone responsiveness, polarized secretion of proteins and the integrity of the blood-testis barrier[83–90]. Earlier methods of culturing Sertoli cells from testicular tissue involved mechanical agitation and chemical digestion of cells, followed by plating cells onto to the bottom of glass culture dishes[84,85], on top of individual matrix components[91,92] or on uncoated plastic[93]. When Sertoli cells are cultured on plastic, they do not retain their columnar shape and appear flat and non-polarized[83,92–94]. Later, modifications were made that included growing Sertoli cells on top of Matrigel™ to enhance cell attachment and growth[95]. Matrigel™ is a porous reconstituted basement membrane (RBM) preparation that is extracted from mouse tumors rich in extracellular matrix proteins such as laminin, type IV collagen, entactin, heparan sulfate proteoglycan, and epidermal growth factor[96].

The development of Sertoli cell cultures on permeable supports (impregnated with Matrigel™) within bicameral culture chambers (Fig. 2.1)[83,94,97,98] resulted in a more representative model of the compartmentalization that occurs *in vivo*[5]. With these modifications, the *in viv*o histotypic features of Sertoli cells were better preserved[87,95] and the cells were able to maintain a morphologically differentiated phenotype *in vitro* for an extended period of time[83,94]. A paper by Suárez-Quian and Onoda[88] describes a general procedure for isolating and culturing Sertoli cells from rat testicular tissue with the use of Matrigel™-coated inserts suspended in bicameral culture chambers. The protocols for isolation of Sertoli cells from other animals[99–101] and humans[102] are very similar. Sertoli cells for primary culture preparations are generally isolated from young immature rats (around 10 to 30 days of age), and the cultures are

largely comprised of Sertoli cells and contain negligible amounts of connective tissue, other somatic (Leydig and Peritubular cells) and germ cells. At 10 to 30 days of postnatal development in rats, Sertoli cells are non-proliferative[103] and tight junctions between Sertoli cells have already begun to form[104]. Enriched populations of Sertoli cells are obtained after sequential enzymatic treatment of testes, which ensures removal of interstitial and residual peritubular cells. The isolated Sertoli cells are maintained in culture in serum-free defined medium (SFDM)[105] containing essential hormones and vitamins[106]. The presence of follicle-stimulating hormone (FSH) and testosterone in SFDM regulates Sertoli cell function[106] and helps promote the formation of ectoplasmic specializations (ESs) and extensive adherens junctions in immature rat Sertoli cells *in vitro*[107]. Sertoli cells remain viable and can be cultured in this manner for at least two weeks. A brief hypotonic shock treatment is used to keep germ cell contamination to a minimum and improve the purity of Sertoli cells[108].

The extracellular matrix (ECM) can greatly influence the growth, morphology and behavior of epithelial cells in culture. The ECM contains specific cell surface receptors that belong to the integrin[109] family of proteins that help transduce signals that regulate cell behavior, and also help mediate the adhesive interaction of cells by linking the ECM to the cytoskeleton[110]. It has been shown in other systems that the ECM influences the growth and survival of epithelial cells, regulates tissue-specific gene expression via ECM signals and also helps support maintenance and induction of differentiation *in vitro*[111–113]. Similarly, there is considerable evidence that the ECM plays an important role in modulating the function and differentiated phenotype of Sertoli cells *in vitro*. Earlier work by Hadley and colleagues[95], demonstrated that when Sertoli cells are isolated from 10-day-old rats and are cultured on the surface of a thin layer of Matrigel™ (two-dimensional (2D) *in vitro* culture model), they form polarized monolayers with the apical surface of the cells open to culture medium and basal surface of cells attached to Matrigel™. When isolated Sertoli cells are instead mixed with and cultured within a thick layer of Matrigel™ (three-

dimensional (3D) *in vitro* culture model) and then plated, they undergo a dramatic change in morphology and reorganize to form cords, which are, surrounded by Matrigel™[95]. These structures resemble the original tissue from which the cells were isolated. Testis cords are apparent during gestational development of male gonads (between embryonic day 13 and day 15 in rats)[114] and are the precursor structures to seminiferous tubules. The aggregation of Sertoli cells into cords is the earliest visible sign of male gonadal differentiation. These primary cultures displayed tight junctions and tight junction proteins between neighboring Sertoli cells that compartmentalized the cords into basal and adluminal compartments[95]. Since then, a number of research groups have developed various 3D *in vitro* culture models using Matrigel™ or other supportive scaffolds, to generate testicular organoids *in vitro* from dissociated testicular tissue[115-123]. Recently, a novel three-layer gradient system was established in which rat testicular cells were cultured in Matrigel™ suspended between two cell-free layers of Matrigel™ to increase the surface area available for *in vitro* cord formation[124]. As these 3D culture systems more closely model the testicular microenvironment, they are commonly used to study testicular organogenesis and development, complex interactions between different testicular cell types and germ cell differentiation *in vitro*[124].

To date, various 2D and 3D primary Sertoli cell culture systems have been reported in the literature. Several laboratories, including our own[57] have had some success in improving the 2D *in vitro* culture system. Significantly, our lab was the first to demonstrate that tubulobulbar complexes (TBCs) develop at basal junctions in morphologically differentiated primary cultures of Sertoli cells, although they are not identical to those formed *in vivo*[57]. This observation indicated that with further refinements, involving co-culturing with germ cells, this cell culture system would provide a valuable tool for studying basal junction remodeling *in vitro*. Hence, the main aim of this study was to establish a 2D morphologically differentiated primary culture of Sertoli cells so that it could eventually be used for co-culturing with germ cells. This chapter

discusses the isolation of Sertoli cells from 20-day-old rats and the successful establishment of a primary Sertoli cell culture with polarized monolayers and basal junction complexes. In addition, it demonstrates the *in vitro* formation of cord-like structures that occur when Sertoli cells are isolated from slightly older rats (30-day-old rats). This finding differs from what has previously been reported in literature. So far, cords or testicular organoid formation has only been shown to occur in 3D culture conditions. In the developed culture system, Sertoli cells isolated from 30-day-old rats reorganize to form cords surrounded by Matrigel™ when plated on the surface of a layer of Matrigel™ (2D *in vitro* culture model) as opposed to being mixed and cultured within Matrigel™ (3D *in vitro* culture model).

2.2 Materials and Methods

2.2.1 Animals

All animals used in the experiments were reproductively active male Sprague Dawley rats (*Rattus norvegicus*), obtained from Charles River Laboratories (Sherbrooke, QC, Canada). The rats were maintained and used according to guidelines established by the Canadian Council on Animal Care, and the protocols approved by the Animal Care Committee of the University of British Columbia. Twenty-day-old and thirty-day-old rats were obtained from a breeding colony maintained at the animal care facility. A total of four pups were used for each Sertoli cell isolation experiment.

2.2.2 Primary Sertoli cell culture

Primary Sertoli cell cultures were prepared based on established protocols[57,88] with some modifications**.** A day prior to isolating Sertoli cells, cell culture plates were prepared by adding cell culture inserts (Transwell permeable supports with membranes containing 1-µm-sized

pores) (Falcon® A Corning Brand, Corning, NY, USA) into the wells of Falcon™ 24-well Multiwell plate(s) (Falcon® A Corning Brand). 50 µl of undiluted Matrigel™ (BD Biosciences, Mississauga, ON, Canada) was used to coat each insert membrane, and it was allowed to polymerize at 37^{o}C for 1 h, followed by placing it in a 34^{o}C incubator with media overnight. Figure 2.1 shows a schematic diagram of the primary Sertoli cell culture setup.

Sertoli cells were isolated from fresh rat testicular tissue by placing the rat pups under deep anesthesia with isoflurane, and the animals were then euthanized by decapitation. The isolated testes were immediately decapsulated, minced into a fine slurry, and transferred to a sterile dissociation flask (Fisher Scientific, Ottawa, ON, Canada) for enzyme digestion. All of the enzymatic digestions of testicular tissues were conducted in sterile glass dissociation flasks, which were swirled in a MaxQ™ 7000 water bath orbital shaker (ThermoFisher Scientific, Fife, WA, USA), set to 37^{o}C and 110 RPM. The testicular tissues were first enzymatically digested in enzyme solution 1 (trypsin/deoxyribonuclease (DNase)) for 25 min, followed by the addition of 20 ml of Dulbecco's modified eagle medium/nutrient mixture F12 (DMEM/F12) (Millipore Sigma, Oakville, ON, Canada) containing 10% fetal bovine serum (FBS) in order to stop trypsin activity. The trypsin-DNase digestion is required for removing interstitial cells and obtaining isolated tubules. The digested tissues were centrifuged at 188 *x g* for 5 min at room temperature, and the supernatant was removed, leaving a loose pellet. The pellet was washed twice with 10 ml of washing solution (DMEM/F12 containing L-glutamine and antibiotic agents). After washing, the pellet was resuspended in enzyme solution 2 (collagenase/hyaluronidase/DNase) and underwent enzymatic digestion for 40 min to remove residual peritubular cells. No FBS treatment was conducted following the second enzymatic digestion. The digested tissue was centrifuged at 120 *x g* for 4 min at room temperature, and the supernatant was removed, leaving a dense pellet. The pellet was washed twice with 10 ml of washing solution. After washing, the pellet was resuspended in enzyme solution 3 (trypsin/EDTA), and underwent enzymatic

digestion for 15 min. The digestion of cells with Trypsin/EDTA yields aggregates of Sertoli and germ cells. After digestion, 20 ml of DMEM/F12 containing 10% FBS was added in order to stop trypsin activity. The digested tissues were centrifuged at 188 *x g* for 5 min at room temperature, and the supernatant was removed, leaving a dense pellet. The pellet was washed twice with 10 ml of washing solution. After washing, the pellet was resuspended in 5 ml of serum-free defined medium (SFDM)[105]. The cell suspension was diluted and seeded onto cell culture inserts at a high cell density of 1.3 x 10^6 cells/0.2 ml SFDM, and 0.8 ml of SFDM was added to the wells of the cell culture plates. The cells were incubated at 34^{o}C in 5% CO_2. The cell culture media was replenished every 48 h to maintain Sertoli cells and wash away any non-adhering or loosely attached germ cells.

The cells were treated with a brief hypotonic wash after two days of culturing to lyse large amounts of any contaminating germ cells[108]. The hypotonic wash solution was composed of 10 mM Tris-HCl (Millipore Sigma) at pH 7.5. The hypotonic wash lasted for 2 min[125]. The duration of the hypotonic treatment has to be short as it can cause deleterious effects to the isolated Sertoli cells and result in significant loss of cells[125]. After the wash, fresh SFDM was added, and the cell culture plate was gently shaken to loosen any lysed germ cells. Finally, SFDM containing debris was removed, and replaced with fresh SFDM. Sertoli cells were maintained in SFDM for a week or a total of 9 days prior to being fixed and processed for immunofluorescence or transmission electron microscopy.

2.2.3 Composition of serum-free defined medium

SFDM was prepared based on established protocols[57,105] by adding the following reagents at the indicated concentrations to DMEM/F12 culture medium (Millipore Sigma): 10 µg/ml insulin (ThermoFisher Scientific), 5.5 µg/ml transferrin (ThermoFisher Scientific), 6.7 ng/ml sodium selenite (ThermoFisher Scientific), 100 U/ml penicillin (ThermoFisher Scientific), 0.1 mg/ml

streptomycin (ThermoFisher Scientific), 2 mM L-glutamine (ThermoFisher Scientific), 250 ng/ml Fungizone (ThermoFisher Scientific), 50 ng/ml vitamin A (Millipore Sigma), 200 ng/ml vitamin E (Millipore Sigma), 10^{-9} M hydrocortisone (Millipore Sigma), 10^{-7} M testosterone (Millipore Sigma), 10^{-8} M estradiol (Millipore Sigma), 100 ng/ml rat FSH (Courtesy of Dr. A. F. Parlow, National Hormone and Peptide Program, Torrance, CA, USA), 3 µg/ml cytosine β-D-arabinofuranoside (Millipore Sigma) and 10 ng/ml recombinant human epidermal growth factor (EGF) (Millipore Sigma).

2.2.4 Composition of enzyme solutions

20 ml of three different enzyme solutions, named 1, 2 and 3 were used for sequential digestions of testicular tissue and these were prepared based on established protocols[57,88]. Enzyme solution 1 was composed of DMEM/F12 containing 1.5 mg/ml trypsin (StemCell Technologies, Vancouver, BC, Canada), 40 µg/ml crude DNase I (Millipore Sigma), 250 ng/ml Fungizone (ThermoFisher Scientific), 100 U/ml penicillin (ThermoFisher Scientific), and 0.1 mg/ml of streptomycin (ThermoFisher Scientific). Enzyme solution 2 was composed of DMEM/F12 containing 2 mg/ml collagenase type I (Invitrogen, Burlington, ON, Canada), 2 mg/ml hyaluronidase type I-S (Millipore Sigma), 40 µg/ml crude DNase I, 250 ng/ml Fungizone, 100 U/ml penicillin, and 0.1 mg/ml streptomycin. Enzyme solution 3 was composed of Ca^{2+}-free/Mg^{2+}-free Dulbecco phosphate-buffered saline (StemCell Technologies) containing 0.5 mg/ml trypsin, 0.1 mg/ml EDTA (Fischer Scientific), 4 mM dextrose (Fischer Scientific), 250 ng/ml Fungizone, 100 U/ml penicillin, and 0.1 mg/ml streptomycin.

2.2.5 Immunofluorescence of primary Sertoli cell cultures

After a week or nine days of culturing, Sertoli cells were fixed with 3% paraformaldehyde (Millipore Sigma) in PBS (150 mM NaCl, 4.0 mM Na/KPO_4 and 5 mM KCl, pH 7.3) for 30 min at

room temperature by replacing the media inside and outside of the cell culture inserts with fixative. Then, the cells were washed 3 times, 10 min each with TPBS/0.1% bovine serum albumin (BSA) (Millipore Sigma) buffer (0.05% Tween 20 (Millipore Sigma), pH 7.3). The membranes were cut from cell culture inserts with a scalpel and immediately submerged in cold acetone for 5 min to permeabilize the cells. The cells were washed 3 times, 10 min each with TPBS/0.1% BSA buffer, followed by blocking for 1 h at room temperature with TPBS/1% BSA buffer. Primary antibody solution was added to the membranes and stored at 4^{o}C overnight. The next day, the membranes were washed 3 times, 10 min each with TPBS/0.1% BSA. Secondary antibody solution was added to the membranes and the cells were labeled for 1 h in a 37^{o}C incubator. Following incubation, the cells were washed 3 times, 10 min each with TPBS/0.1% BSA. In addition, when required, cells were stained with either phalloidin or DAPI (4'6-Diamidino-2-Phenylindole, Dihydrochloride). Finally, the membranes were mounted on glass slides in VectaShield mounting medium without DAPI (Vector Laboratories, Burlington, ON, Canada).

All the primary antibodies and stains used in the experiments were diluted to working concentrations in TPBS/0.1% BSA buffer. The primary antibody used to stain tight junctions was rabbit polyclonal anti-oligodendrocyte specific protein (anti-claudin-11) (Abcam, Cambridge, MA, USA) at a working concentration of 0.0025 mg/ml. Normal rabbit IgG (NRIgG) (Millipore Sigma) was diluted to the same working concentration used for the primary antibody. The secondary antibody, Alexa Fluor™ 488 goat-anti-rabbit (ThermoFisher Scientific) was used at 1:100 dilutions. Alexa Fluor™ 633 Phalloidin (ThermoFisher Scientific) was diluted 7.5:100 to stain F-actin in cultured Sertoli cells. DAPI (ThermoFisher Scientific) was diluted 1:1000 to stain nuclei and chromosomes.

Z-stacks of cultured Sertoli cells were obtained using a Leica TCS SP5 Confocal laser-scanning microscope (Leica Microsystems Inc., Concord, Ontario, Canada). All fluorescence

microscopy images were subsequently analyzed and processed using ImageJ software[126]. The Z-project function on ImageJ was used to create a max projection image of the slices, which was a composite of the various stains from Z-stacks. To show the position of claudin-11 with respect to basal regions of cultured cells, slices were selected such that it represented the whole Z-stack (from top to bottom). The step sizes for each of the slices on the Z-stacks were in increments of 0.1 µm. The 3D images of the Z-stack were created using the 3D-project function on ImageJ.

2.2.6 Light and electron microscopy

The cultured Sertoli cells were fixed using 1.5% paraformaldehyde/1.5% glutaraldehyde/0.1 M sodium cacodylate (Electron Microscopy Sciences, Hatfield, PA, USA), pH 7.3 for 3 h at room temperature by replacing the media inside and outside of the cell culture inserts with a fixative. The membranes were cut from the insert in fixative using a scalpel and transferred to a scintillation vial containing 0.1 M sodium cacodylate, pH 7.3 and were allowed to sit overnight or until further processing. The next day, the membranes were washed 2 times, 10 min each with 0.1 M sodium cacodylate, and placed on ice for 1 h with 1% osmium tetroxide/0.1 M sodium cacodylate (Electron Microscopy Sciences). Then, the membranes were washed 3 times, 10 min each with ddH_2O and stained for 1 h at room temperature with 1% aqueous uranyl acetate (Electron Microscopy Sciences). After another set of washes with ddH_2O (3 times, 10 min each), the membranes were dehydrated with increasing concentration series of ethyl alcohol ending in 100% and following this treated 2 times, 30 min each with 100% propylene oxide. The membranes were then left overnight in 1:1 propylene oxide: polybed. The membranes were treated 2 times, 1 h each with 100% polybed and were finally embedded in fresh 100% polybed (Electron Microscopy Sciences) in embedding capsules and placed in a 60^{o}C oven for 24 h.

Sections were evaluated and photographed using a Zeiss imager or a FEI Tecnai G2 Spirit electron microscope.

2.3 Results

2.3.1 Only Sertoli cells cultured at high density mimic *in vivo* conditions

Primary cultures of Sertoli cells isolated from 20-day-old rats and grown on top of Matrigel™ established a morphologically differentiated phenotype that was highly dependent on cell density. Sertoli cells seeded at low cell density (1.3×10^5) did not form a confluent monolayer with cells appearing sparsely distributed and non-polarized (Fig. 2.2 A). At medium cell densities (4.1×10^5), cells remained non-confluent with frequently interrupting gaps and moved into clumps (Fig. 2.2 B). In contrast, primary cultures of Sertoli cells cultured at high cell density (1.3×10^6) formed a confluent layer within 24 – 48 h of plating, with cells having a cuboidal-columnar shape (Fig. 2.2, C and D). These cells organized to form a monolayer interrupted by areas where cells formed focal clumps. Sertoli cells within the monolayer were basally attached to Matrigel™ and had an apical surface opened to media (Fig. 2.2, C and D). The columnar heights of the cells varied from low to high in different regions of the monolayer. Often the more columnar cells folded over the tops of adjacent cells giving the appearance of a multilayered epithelium. Sertoli cells within this culture system were generally polarized with nuclei and tissue specific junction networks (ESs) located basally. The Sertoli cell nuclei were irregularly oval in shape with their long axis oriented perpendicular to the plane of growth (Fig. 2.2, C and D). The primary cultures were predominantly comprised of Sertoli cells with very few contaminating germ or peritubular myoid cells. Germ cells, if present, appeared necrotic due to hypotonic shock treatment and were often attached to the upper surface of the monolayer.

2.3.2 Characterization of primary Sertoli cell culture from 20-day-old rats

Ultrastructural analysis revealed that ESs were present when Sertoli cells were seeded at low, medium and high cell densities. Sertoli cells seeded at low or medium cell densities formed short basal junctions with discontinuous associated endoplasmic reticulum (ER) connections (Fig. 2.3, A and B). At high cell densities, cultures displayed long and well-developed ESs between neighboring Sertoli cells, with morphologically identifiable tight junctions (membrane kisses) and prominent actin networks (Fig. 2.3 D). The integrity of the neighboring ER was well preserved (Fig. 2.3 C). ESs between adjacent Sertoli cells were consistently located in the basolateral region of the monolayer next to Matrigel™.

When stained with phalloidin, actin networks in primary cultures of Sertoli cells displayed an intricate honeycomb-like pattern that formed circumferential rings at cell peripheries (Fig. 2.4, A and B). Claudin-11 staining outlined the periphery of Sertoli cells in regions known to contain basal junction complexes, confirming the presence of tight junctions in similar regions to the actin networks (Fig. 2.5, A and B). Tight junctions within cultured Sertoli cells were present specifically in basal regions (Fig. 2.5, A and B). Primary (Fig. 2.5 C) and secondary antibody (Fig. 2.5 D) controls confirmed the specificity of the antibody targeting claudin-11.

2.3.3 Primary Sertoli cell cultures from 30-day-old rats form cords with a morphologically differentiated phenotype

When the age of rats used for isolating Sertoli cells is 30-days-old, the cells respond much differently to the same culture conditions than cells from slightly younger animals. Sertoli cells isolated from 30-day-old rats and cultured on top of Matrigel™ rapidly re-aggregated to form a condensed mass from which elongated cords of cells projected into the surrounding remodeled Matrigel™ (Fig. 2.6, A, B and C). The Sertoli cells within the cords were highly polarized, columnar and their irregularly shaped nuclei were located basally around the periphery of the

cords (Fig. 2.6, D, E and F). The cordlike aggregates did not form a single prominent central lumen *in vitro*.

Intercellular junctions appeared and formed long and well developed ESs at the base of Sertoli cells (Fig. 2.7, A and B). Ultrastructural analysis revealed that actin networks, ER, and membrane kisses indicative of tight junctions, were present within the junction complexes (Fig. 2.7 A). In addition, claudin-11 staining confirmed the presence of numerous tight junctions within the cords (Fig. 2.8).

2.4 Discussion

Primary Sertoli cells cultured on top of Matrigel™, established and maintained a morphologically differentiated phenotype *in vitro*. Sertoli cells isolated from 20-day-old rats formed a monolayer with the heights of cells varying from low to high in different regions of the insert. A high seeding density (1.3×10^6) was required for the cells to be tightly packed and form a confluent monolayer. Sertoli cell polarization was indicated by the tall columnar morphology of cells and their basally located nuclei. Furthermore, the presence of well-developed Sertoli cell specific ESs and ultrastructurally observable tight and gap junctions as part of the junction complexes indicated Sertoli cell differentiation *in vitro*. The staining pattern of the tight junction protein, claudin-11, using confocal microscopy confirmed that tight junctions occurred specifically at basal regions of cultured Sertoli cells. The high seeding density caused Sertoli cells to occasionally stack up on top of each other and form focal clumps in certain regions. Hence, Sertoli cells did not form a perfect monolayer *in vitro*. Sertoli cells seeded at low or medium densities only formed clumps with frequent gaps between the clumps that were devoid of cells. Therefore, it was established that only Sertoli cells cultured at a high-density formed confluent monolayers with intact and specialized junctions that closely mimic *in vivo* conditions and hence are the best for conducting co-culture experiments.

It was observed that when the age of rats used for isolating Sertoli cells were slightly older (30-days-old), the cells responded much differently to the same culture conditions *in vitro*. Sertoli cells isolated from 30-day-old rats and plated on the surface of Matrigel™ did not form monolayers but instead rapidly reorganized to form a central mass with testicular cord-like structures emanating from the mass into the surrounding Matrigel™. The enzymatically dissociated testicular cells displayed the ability to self-organize into cord-like structures that resembled the tissue from which the cells were isolated. Sertoli cells within the cords were columnar and highly polarized. In addition, claudin-11 expression confirmed the presence of junctions between Sertoli cells in the cords.

The difference in morphology between these cultures can be attributed to the maturational stage of the rats, since all other factors were similar. The testes of 20 and 30-day-old rats are comprised of distinct populations of Sertoli cells, which are at different stages of testicular development. It is evident from the results that the maturation status of Sertoli cells plays a significant role in how cells respond *in vitro*. Within a few days in culture, Sertoli cells isolated from 30-day-old rats underwent compaction and aggregated at the center of the insert to form irregular spherical structures. Compared to Sertoli cells isolated from 20-day-old rats, they were more capable of colonizing and remodeling the underlying Matrigel™. In order to support cord formation, the cells manipulated the Matrigel™ and used it as a 3D supportive matrix that surrounded the cords.

Hadley and coworkers had earlier demonstrated that *in vitro* cord formation only occurs when isolated Sertoli cells are mixed and cultured within Matrigel™[95]. In contrast in this study I demonstrate a more improved maintenance of the Sertoli cell phenotype within testicular cords when Sertoli cells isolated from 30-day-old rats are plated on the surface of Matrigel™ (2D culture conditions). However, in the developed cultures, the cords that formed were atypical as they were devoid of germ cells (due to hypotonic shock treatment) and lacked a single defined

central lumen. In the future, further progression and development of cords in this culture system would be possible by co-culturing with other testicular cell types such as germ cells[95,123,124] or peritubular myoid cells[117,127,128].

The main aim of this study was to establish a primary Sertoli cell culture system that could be used for co-culturing with germ cells to investigate the process of basal junction remodeling *in vitro*. The primary Sertoli cell culture system with cells plated at high density successfully established using 20-day-old rats provides easy access to both apical and basal compartments for experimental manipulation. Hence, this culture system was used for co-culture studies, as discussed in the next chapter. In conclusion, these findings present two improved primary Sertoli cell culture systems that more closely resemble the *in vivo* phenotype and may in the future provide a more effective model for studying testicular organogenesis and junction turnover.

2.5 Chapter 2 Figures

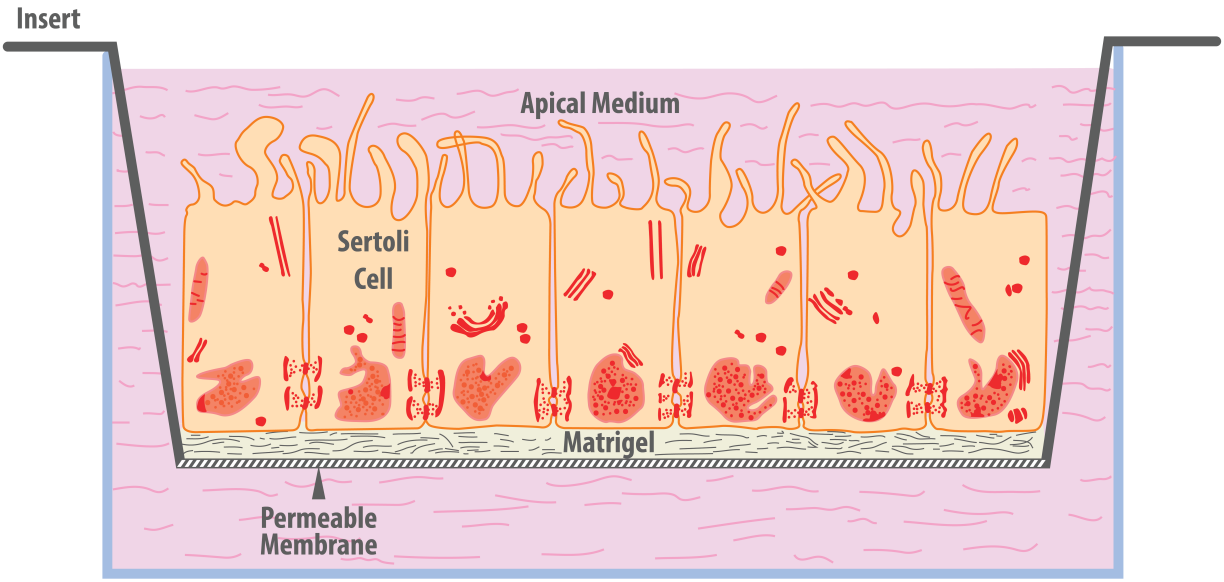

Figure 2.1 *In vitro* primary Sertoli cell culture setup.
Cell culture inserts with membranes containing 1-µm-sized pores, were coated with Matrigel™ and added to wells of a falcon 24-well multiwell plate. This transwell setup was used to mimic the *in vivo* environment. Isolated Sertoli cells were plated at a high density of 1.3 x 10^6 cells/0.2 ml on Matrigel™ and cultured in serum-free defined medium. Media was added to the inner and outer chambers and was changed every 48 h. Figure 2.1 was modified from © Djakiew *et al*. (1986)[98]. Transferrin-Mediated Transcellular Transport of ^{59}Fe Across Confluent Epithelial Sheets of Sertoli Cells Grown in Bicameral Cell Culture Chambers. Journal of Andrology, 7(6), 355-66. Page 357. Adapted with permission from publisher.

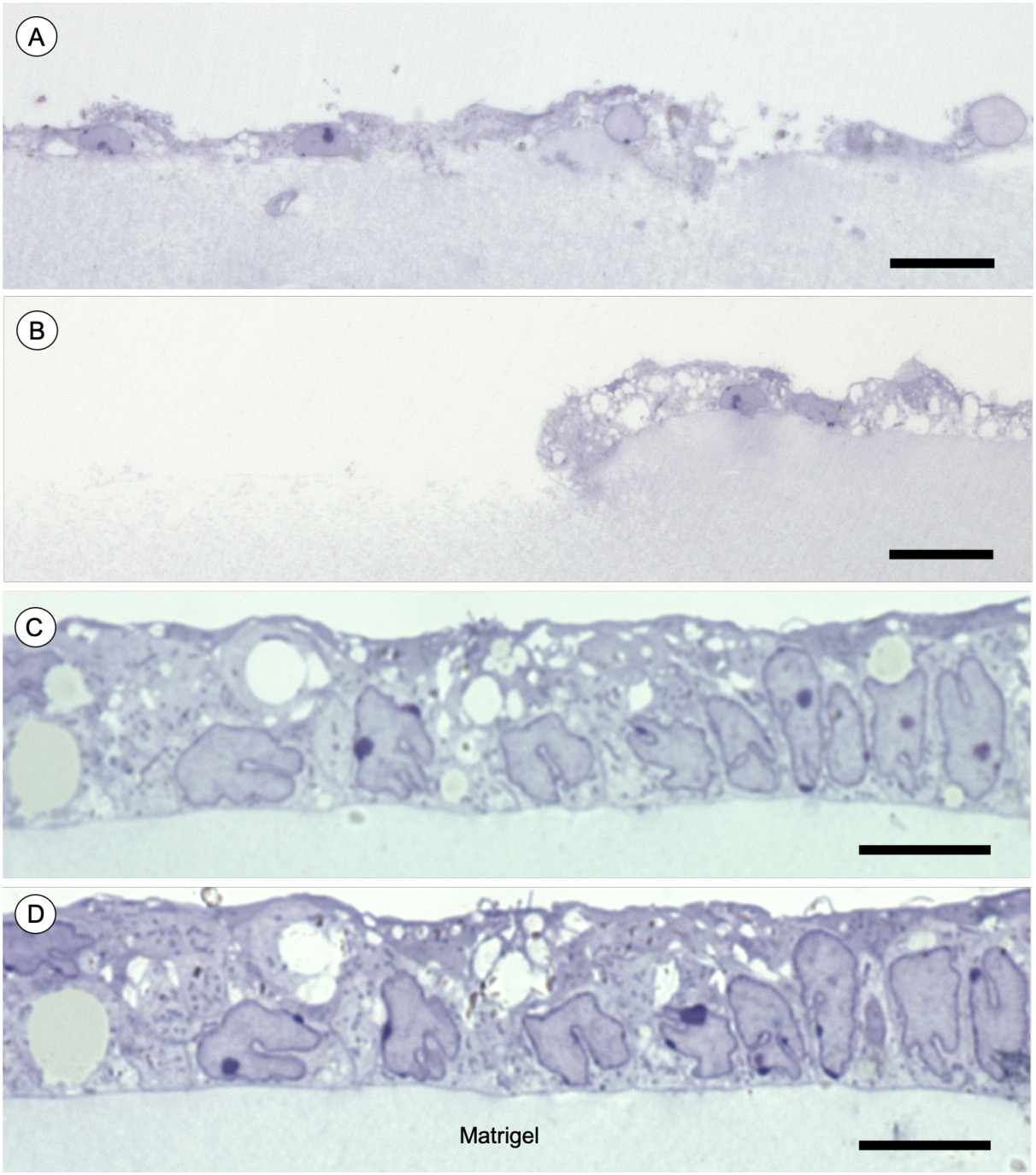

Figure 2.2 Light micrographs of Sertoli cells cultured at low, medium, and high cell densities.
(A) Cultures plated at low (1.3 x 10^5) cell density did not form a confluent monolayer. (B) At medium (4.1 x 10^5) cell density, cells remained non-confluent with frequently interrupted gaps. (C, D) At high (1.3 x 10^6) cell density, cultures developed the most confluent monolayers with cells having a columnar shape and nuclei located basally. (A) and (B) were captured at 40X magnification and (C) and (D) were captured at 100X magnification. For (A, B), Bars = 20 μm and for (C, D), Bars = 10 μm.

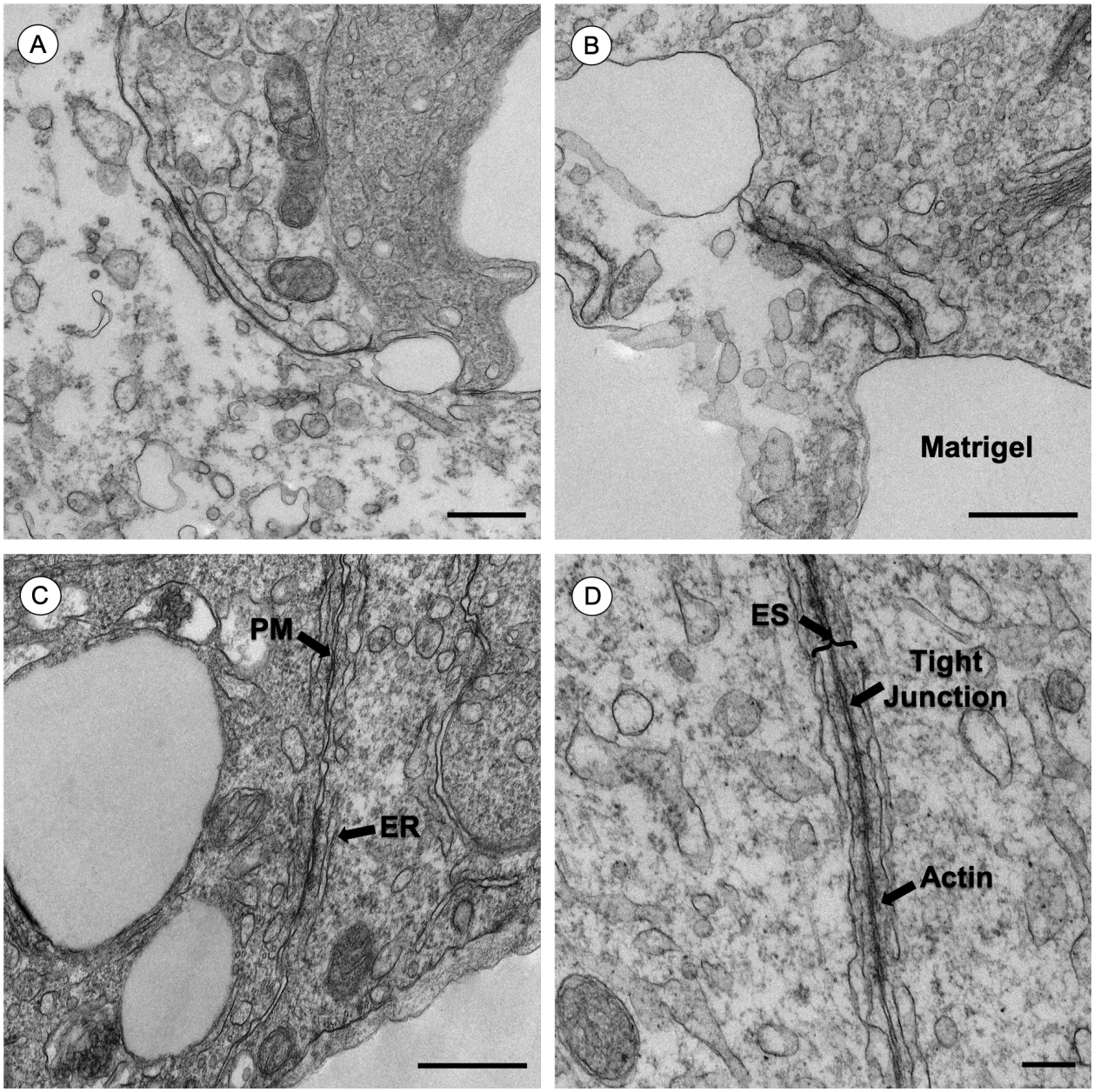

Figure 2.3 Transmission electron micrographs of primary Sertoli cell cultures plated at varying densities.
At low (1.3 x 10^5) and medium (4.1 x 10^5) cell densities (A and B, respectively), cultures showed short basal junction complexes with discontinuous endoplasmic reticulum (ER) connections. At high (1.3 x 10^6) cell density, cultures displayed long and well-developed ectoplasmic specializations (ESs) (C and D) with morphologically identifiable tight junctions and actin networks (D). The integrity of the neighboring ER was well preserved (C). Bars = 500 nm.

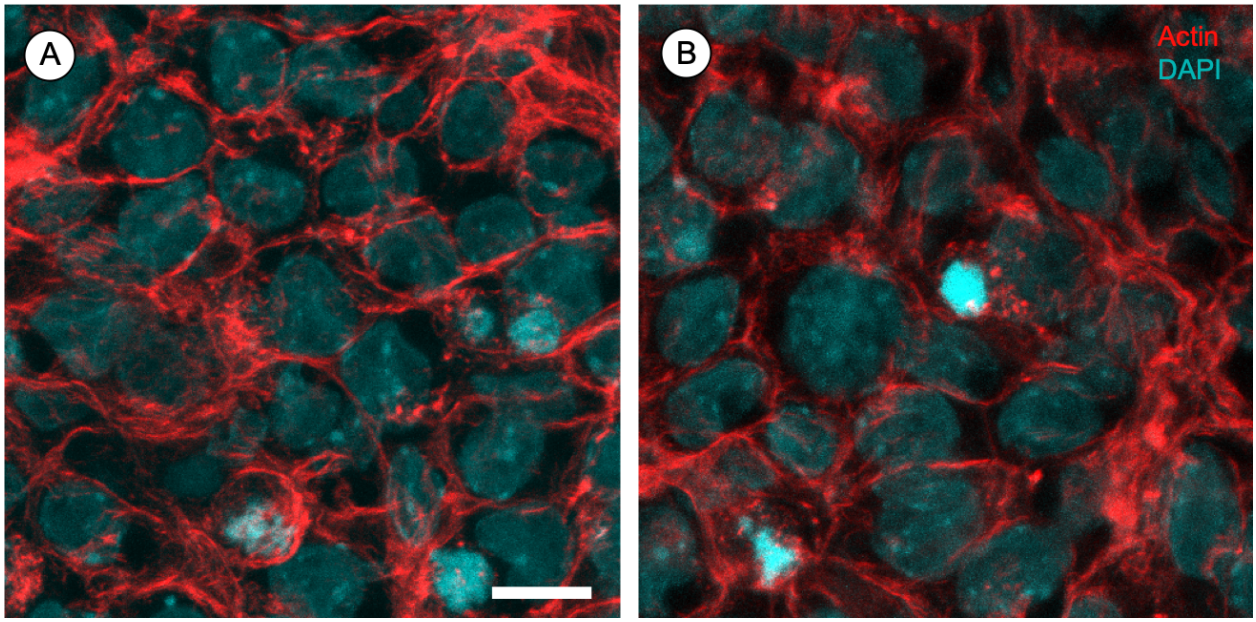

Figure 2.4 Organization of actin cytoskeleton in Sertoli cells cultured from 20-day-old rats.
Actin networks in morphologically differentiated primary cultures of Sertoli cells formed a honeycomb pattern (A, B). Phalloidin was used to stain F-actin (red) and cell nuclei were stained with DAPI (blue). (A, B) are maximum intensity projections of Z-stacks of immunofluorescently labeled Sertoli cell cultures. Bar = 10 μm.

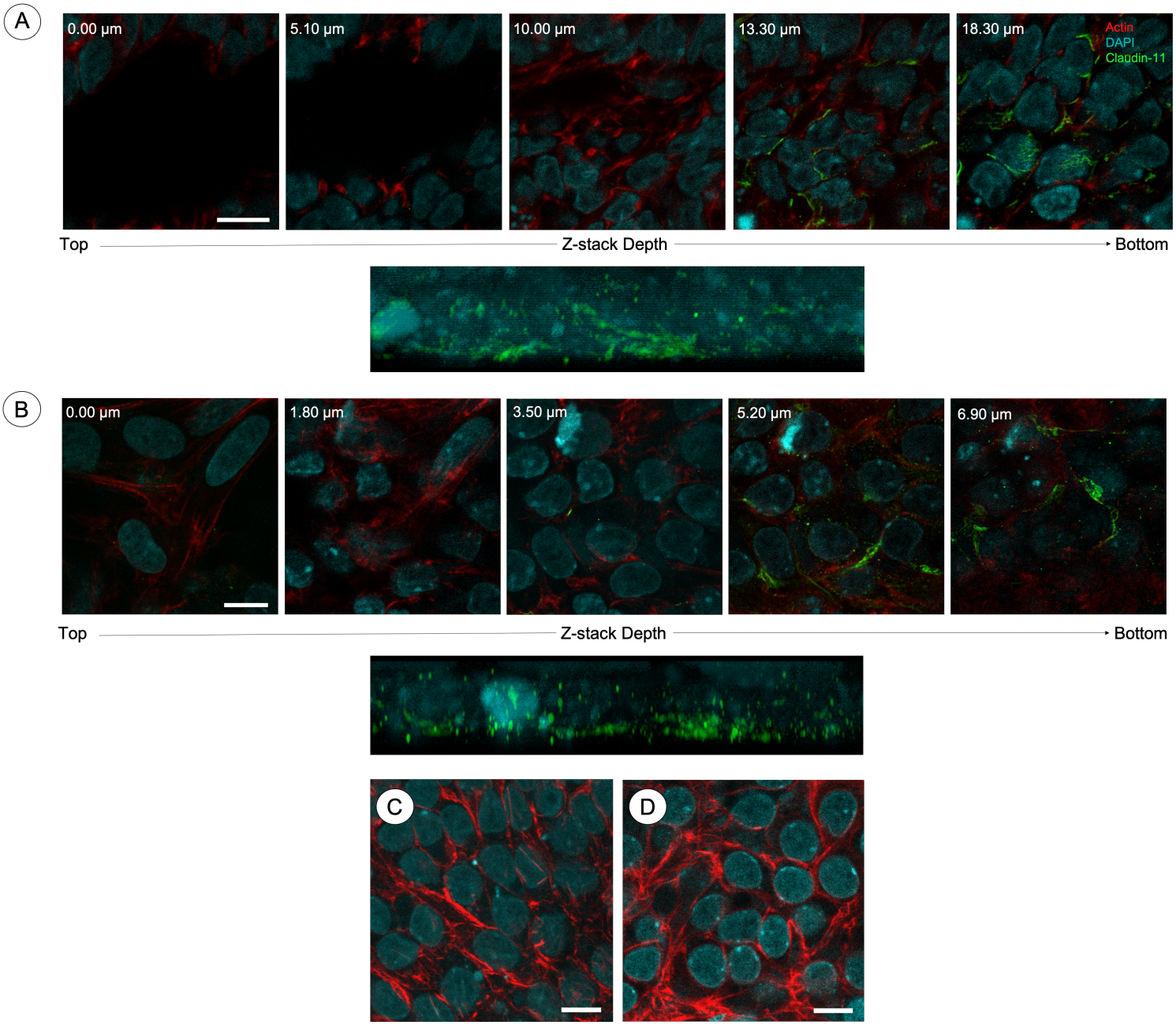

Figure 2.5 Confocal images of cultured Sertoli cells from 20-day-old rats labeled for claudin-11.

Sertoli cells cultured for 1 week were fixed and immunoprobed for the tight junction protein, claudin-11. Slices representing whole Z-stacks from top to bottom as well as 3D representations are shown. For (A), total slices = 263 out of which 5 slices were selected approximately every 50 slices apart at the indicated increments. For (B), total slices = 94 out of which 5 slices were selected approximately every 23 slices apart at the indicated increments. Claudin-11 staining (green) confirmed the presence of tight junctions specifically in basal regions of cultured cells (A, B). Filamentous actin was stained with phalloidin (red) and nuclei of Sertoli cells were stained with DAPI (blue). (C) shows NRIgG control for claudin-11 staining and (D) shows secondary antibody control. Bars = 10 µm.

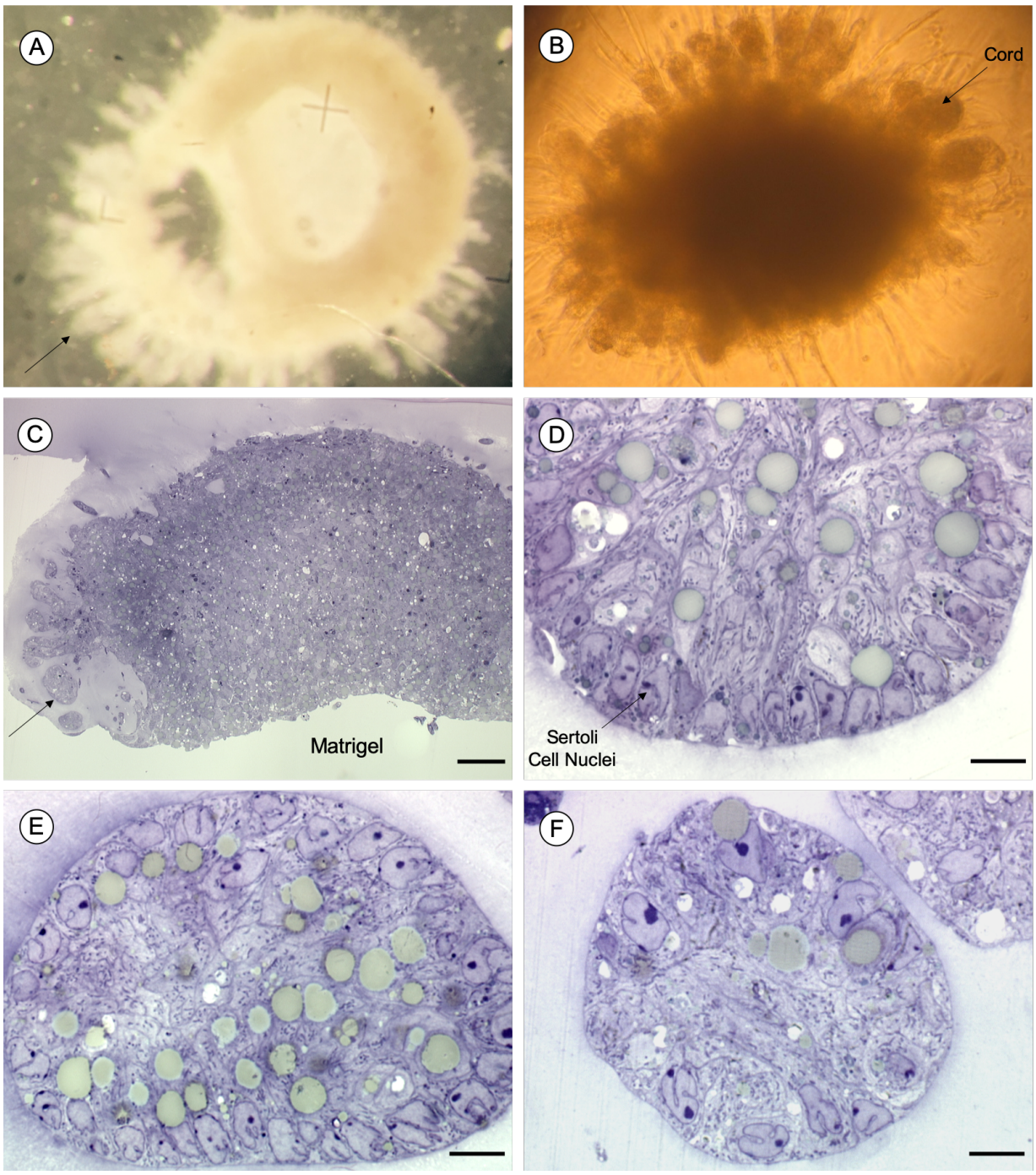

Figure 2.6 Morphology of Sertoli cells cultured from 30-day-old rats.
Sertoli cells isolated from 30-day-old rats reorganized to form a condensed mass from which cylindrical cords of cells (arrows) projected into the surrounding remodeled Matrigel™ (A, B, C). Sertoli cells within the cords were columnar with nuclei located basally around the periphery of cords (D, E, F). (C) was captured at 10X magnification and Bar = 100 µm. (D – F) were captured at 100X magnification and Bars = 10 µm.

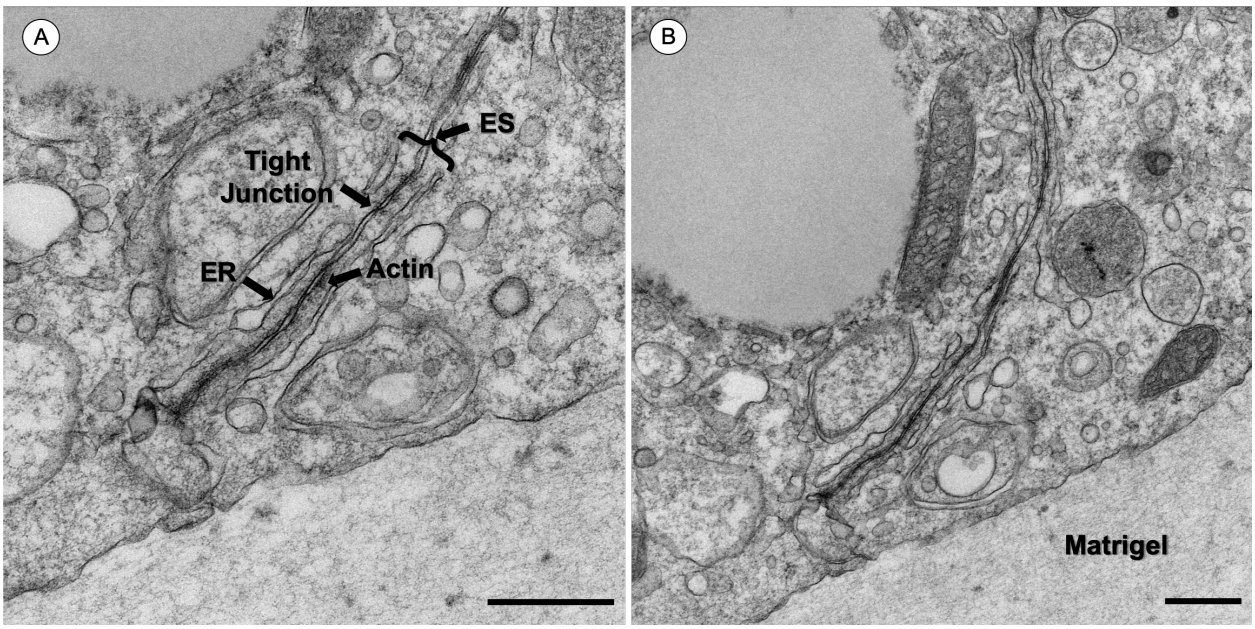

Figure 2.7 Electron micrographs of basal junction complexes within seminiferous cords *in vitro*.
Sertoli cells within the cords formed long, well-developed ectoplasmic specializations (ESs) (A, B) with identifiable tight junctions, actin networks and endoplasmic reticulum (ER) (A). Bars = 500 nm.

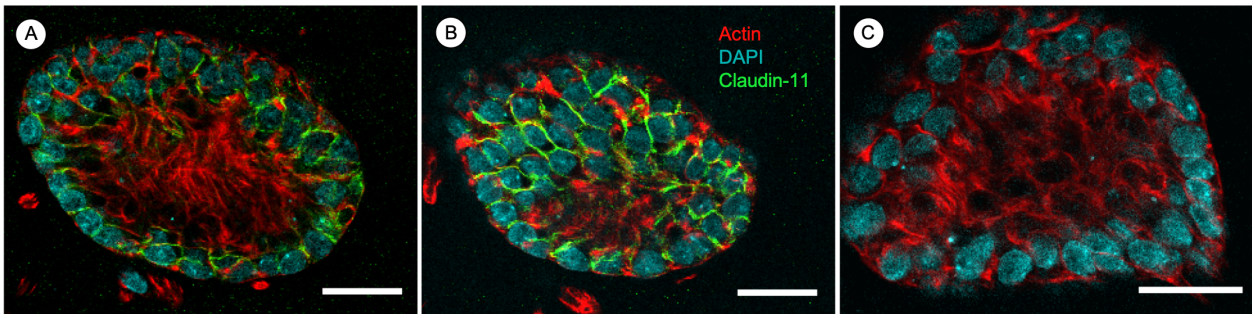

Figure 2.8 Confocal micrographs of cultured Sertoli cells from 30-day-old rats labeled for claudin-11.
Filamentous actin was stained with phalloidin (red) and the nuclei of Sertoli cells were stained with DAPI (blue). Claudin-11 staining (green) confirmed the presence of tight junctions within the cords (A, B). (C) shows NRIgG control for claudin-11 staining. Bars = 30 µm.

Chapter 3: The co-culture of spermatogonia with Sertoli cells promotes formation of basal tubulobulbar complexes *in vitro*

3.1 Background

In the testis, the interaction between Sertoli cells and germ cells is integral for spermatogenesis to occur. Sertoli cells provide structural support and produce soluble factors necessary for germ cell survival and differentiation[1,129]. Spermatogonial stem cells (SSCs) continuously maintain spermatogenesis in adult mammals by giving rise to differentiating daughter cells that enter meiosis and develop into spermatozoa[130,131]. Also, SSCs are responsible for maintaining the stem cell pool by way of active self-renewal. In the mammalian testis, SSCs are located on the basement membrane of the seminiferous epithelium and are surrounded by Sertoli cells that provide growth factors such as glial cell line-derived neurotrophic factor (GDNF), leukemia inhibitory factor (LIF), platelet-derived growth factor (PDGF) and extrinsic stimuli for SSC survival and proliferation[1,132,133]. The Sertoli cells limit the expansion of the spermatogonial population and allow a certain number of germ cells to reside in the seminiferous tubules, thereby controlling the extent of sperm production[134]. This specialized microenvironment formed primarily by Sertoli cells and surrounding Leydig and peritubular myoid cells that supports stem cell self-renewal and differentiation is known as the spermatogonial stem cell niche[135].

Spermatogonia reside on the basal membrane until meiosis occurs. Then, they differentiate into spermatocytes that pass through basal junction complexes and make their way up into the adluminal compartment, where later stages of germ cell differentiation continue to occur[5,55,136].

To date, several investigators have developed Sertoli-germ cell co-cultures to recreate the testicular microenvironment and induce germ cell proliferation and differentiation *in vitro*. Sertoli-germ cell co-cultures are generally difficult to maintain, as isolated germ cells do not survive for

long periods of time *in vitro*[137,138] and many of the culture systems are unable to replicate the complex *in vivo* architectural integrity. Two-dimensional (2D) culture studies using rat models have shown that partial spermatogenesis can be achieved *in vitro* when germ cells are co-cultured with Sertoli cells[139–141]. However, the complex *in vivo* testicular microenvironment with separation of basal and adluminal compartments is not established when cells are cultured on conventional 2D surfaces, and as a result, these cultures often aren't able to support post meiotic spermatogenic processes. The three-dimensional (3D) environment is necessary for supporting germ cell proliferation and differentiation *in vitro* as it more closely mimics the cellular organization and interactions between different cell types in the testis. To date, germ cells have most successfully been shown to differentiate in testicular organ culture systems[142–145] as they are able to maintain the architecture of seminiferous tubules and the interactions between somatic and germ cells. Hadley and co-workers[95] had reported earlier that when Sertoli cells were cultured within Matrigel (3D matrix), Sertoli and germ cells formed compartmentalized cords that supported germ cell differentiation. More recently, the advent of novel 3D culture systems in which small fragments of tissue are cultured in 3D supportive matrix such as soft agar culture system (SACS) or three-layer gradient systems allow for better cell-cell or cell-extracellular matrix (ECM) interaction and induce spermatocytes to differentiate into spermatids/mature spermatozoa *in vitro*[124,146].

The main aim of this study was to co-culture germ cells with Sertoli cells and determine if this stimulates basal junction remodeling by observing basal tubulobulbar complexes (TBCs) at basal junction complexes. This aim is based on the hypothesis that basal-TBC mediated disassembly of intercellular junctions is necessary for spermatocyte translocation from basal to adluminal compartments of the seminiferous epithelium. There is convincing evidence that dynamic TBC formation at basal sites precedes spermatocyte translocation[4] and that basal TBCs are responsible for internalizing intact junctions[33,57,62]. In this study, early germ cells,

namely spermatogonia, were isolated from immature rats using established techniques[147] and were added to the apical surfaces of established primary Sertoli cell culture system. Our lab has previously demonstrated that TBCs develop at basal sites in morphologically differentiated primary cultures of Sertoli cells[57]. The rationale for this study is that in germ cell transplantation experiments[148], where early germ cells (SSCs) from fertile donor mice are injected into seminiferous tubules of infertile recipient mice, donor germ cells move from the luminal compartment and pass through junction complexes to reach the basement membrane where spermatogonia normally reside[149]. Given this, it is predicted that when isolated early germ cells are added to the apical surfaces of primary Sertoli cell cultures, they would induce TBC-mediated junction turnover and migrate to the basal compartment. The established 2D primary Sertoli cell culture system was used as it provides easy experimental access to the luminal compartment for germ cell addition. The findings of this study demonstrate that basal TBCs are present after germ cell addition to primary Sertoli cell cultures and qualitatively appear more mature and more closely resemble TBCs *in vivo* than in primary cultures to which germ cells are not added. By co-culturing with early germ cells, this creates a valuable *in vitro* model for mimicking spermatocyte translocation *in vitro* and for studying basal junction remodeling during this process.

3.2 Materials and Methods

3.2.1 Animals

All animals used in this study were reproductively active male Sprague Dawley rats, obtained from Charles River Laboratories (Sherbrooke, QC, Canada). The rats were maintained and used according to guidelines established by the Canadian Council on Animal Care, and protocols approved by the Animal Care Committee of the University of British Columbia. Sertoli-

germ cell co-culture experiments were conducted using ten-day-old (for germ cell isolation) and twenty-day-old (for Sertoli cell isolation) rat pups obtained from separate breeding colonies maintained at the animal care facility. A total of four animals were used for each Sertoli or germ cell isolation experiment. As controls, Sertoli cells were cultured without the addition of germ cells. Each of the co-culture experiments were performed at least three times.

3.2.2 Germ cell isolation and co-culture setup

Testicular germ cells were isolated from ten-day-old Sprague Dawley rats based on procedures described by Boucheron and coworkers[147] with some modifications. Four rat pups were placed under deep anesthesia with isoflurane, and the animals were then euthanized by decapitation. The isolated testes were quickly decapsulated and minced into a fine slurry in a petri dish containing working solution (Dulbecco's modified eagle medium/nutrient mixture F12 (DMEM/F12) (Millipore Sigma, Oakville, ON, Canada)) containing L-glutamine and antibiotic agents). The seminiferous cords were transferred to a 50 ml falcon tube containing 5 ml of working solution and were allowed to settle to the bottom of the tube. The supernatant was then carefully removed with a pipette and set aside. The resulting seminiferous tubule pellet was incubated in 4.6 ml of working solution, 2.5 ml of collagenase (stock solution 2 mg/ml) (Millipore Sigma), 100 µl of hyaluronidase (stock solution 10 mg/ml) (Millipore Sigma) and 500 µl of deoxyribonuclease I (DNase I) (stock solution 1 mg/ml) (Millipore Sigma) to remove the interstitial cells (myoid and Leydig cells). The sample was gently swirled and transferred to a small sterile dissociation flask (Fisher Scientific, Ottawa, ON, Canada) for 30 min of enzymatic digestion. All of the enzymatic digestions of testicular tissues were conducted in small sterile glass dissociation flasks, which were swirled in a MaxQ™ 7000 water bath orbital shaker (ThermoFisher Scientific, Fife, WA, USA), set to 37^{o}C and 140 RPM. After the first digest, the sample was removed from the shaker and slowly transferred to a 50 ml falcon tube. The tubule

tissue was allowed to settle to the bottom of the tube. The supernatant (containing interstitial cells) was then carefully removed with a pipette without disturbing the partially digested tubules and set aside. Following this, 3 ml of 0.25 % Trypsin-EDTA and 650 µl of DNase I was added to the tubule tissue pellet to dissociate the seminiferous tubules and release the Sertoli and germ cells. The sample was gently swirled and transferred to a small dissociation flask for 20 min of enzymatic digestion. After the second digest, the sample was removed from the shaker and slowly transferred to a 50 ml falcon tube. The tissue was again allowed to settle to the bottom of the tube. The entire supernatant was slowly transferred to a small dissociation flask containing 800 µl of DNase I (to reduce viscosity and cell aggregation) and 20 ml of DMEM/F12 containing 10% fetal bovine serum (FBS) to inhibit proteolytic activity. The sample was gently swirled and placed in the shaking water bath for an additional 10 min of enzymatic digestion. The sample was removed from the shaker after the third digest and transferred to a 50 ml falcon tube. The enzymatically digested cell suspension was gently inverted and poured through a 40-µm-cell strainer (Millipore Sigma) into another new 50 ml falcon tube to remove cell aggregates (containing Sertoli cells) and isolate germ cells. The tube containing filtered cells was then centrifuged at 800 *x g* for 10 min at room temperature. The supernatant was removed and the resulting cell pellet (containing isolated germ cells) was resuspended in 1 ml (for cells isolated from 4 rat pups) of serum-free defined medium (SFDM) (Chapter 2, section 2.2.3). The resulting cell suspension contained primarily spermatogonia. The isolated germ cells (1 ml) were immediately added (200 µl/insert) onto Sertoli cells that had been cultured alone at a high cell density (1.3 x 10^6 cells/cm^2) (Chapter 2, section 2.2.2) for four days to allow for establishment of a functional barrier[150,151].

Sertoli cells were isolated from the testes of 20-day-old rats and cultured as described previously in chapter 2. After 48 h of incubation, these Sertoli cells were exposed to a hypotonic shock treatment to lyse residual germ cells (Chapter 2, section 2.2.2). Isolated germ cells were

added on day five of culture and were co-cultured with Sertoli cells for a period of approximately five days.

3.2.3 Immunofluorescence of Sertoli-germ cell co-cultures

The fixation, labeling protocols and image processing methods for Sertoli-germ cell co-cultures are the same as the ones described in chapter 2 for primary Sertoli cell cultures (Chapter 2, section 2.2.5) with few exceptions. The following mouse monoclonal antibodies (Santa Cruz Biotechnology, Dallas, Texas, USA) were used at a working concentration of 10 µg/ml to stain the following transcription factors that regulate SSC function: synaptonemal complex protein 3 (SCP-3)[152], promyelocytic leukemia zinc finger (PLZF)[153], sal-like protein 4 (Sall4)[153] and octamer-binding transcription factor 3/4 (Oct-3/4)[154]. Normal mouse IgG (NMIgG) (Millipore Sigma) was diluted to the same working concentration used for the primary antibody. The secondary antibody, Alexa Fluor™ 488 goat-anti-mouse (ThermoFisher Scientific) was used at 1:100 dilutions.

3.2.4 Light and electron microscopy

Sertoli-germ cell co-cultures were processed for light and transmission electron microscopy to observe the migration of added germ cells and formation of basal TBCs. The protocols for preparation of Sertoli-germ cell co-cultures for light and electron microscopy are the same as the ones described for primary Sertoli cell cultures in chapter 2, section 2.2.6.

3.3 Results

3.3.1 Interaction between germ cells and Sertoli cells in Sertoli-germ cell co-cultures

The Sertoli-germ cell co-cultures were first assessed by light microscopy to observe the interaction of germ cells with Sertoli cell monolayers and to confirm their entry into the monolayer. In these cultures, the Sertoli cells maintained a morphologically differentiated phenotype with cells maintaining a low to high columnar shape. Germ cells were isolated from 10-day-old rats and this cell preparation contained primarily spermatogonia with few non-germ cell contaminants (Sertoli cell fragments or peritubular cells). When the isolated germ cells were added to primary Sertoli cell cultures, clusters of germ cells were mostly found adhered to apical regions of Sertoli cell monolayers (Fig. 3.1). Some of the added germ cells moved in between Sertoli cells and migrated towards basal regions of the monolayer (Fig. 3.1). A large number of the added germ cells appeared to be degenerating and not viable in the co-cultures.

3.3.2 Immunodetection of germ cell specific markers in Sertoli-germ cell co-cultures

To identify repopulating germ cells in Sertoli-germ cell co-cultures, the following set of germline stem cell markers were tested for their specificity by way of immunofluorescence (Fig. 3.2): SCP-3, PLZF, Oct-3/4 and Sall4. Compared to SCP-3 (Fig. 3.2 A), PLZF (Fig. 3.2 B) and Oct-3/4 (Fig. 3.2 C), Sall4 stained the isolated germ cells with the highest specificity (Fig. 3.2 D). Primary (Fig. 3.2 E) and secondary antibody (Fig. 3.2 F) controls confirmed the binding specificity of Sall4.

Sertoli-germ cell co-cultures fixed and stained for Sall4 confirmed the presence of repopulating germ cells and their entry into the Sertoli cell monolayer (Fig. 3.3 A, B). In contrast, primary cultures of Sertoli cells without germ cells did not stain positive for Sall4 (Fig. 3.3 C).

3.3.3 Basal ectoplasmic specializations in Sertoli-germ cell co-cultures *in vitro*

Ultrastructural analysis revealed that well-developed basal ectoplasmic specializations (ESs) occurred near the base of the monolayer between neighbouring Sertoli cells in these co-cultures (Fig. 3.4 A - D). These structures were characterized by the presence of actin filaments between cisternae of endoplasmic reticulum (ER) and Sertoli cell membrane (Fig. 3.4 E, F). Furthermore, morphologically identifiable tight (Fig. 3.4 E, F) junctions (membrane kisses) were present within the junction complexes.

3.3.4 Evidence of basal tubulobulbar complex formation in Sertoli-germ cell co-cultures and comparison to primary Sertoli cell cultures

Sertoli-germ cell co-cultures were evaluated for the presence of TBCs at basal junctions. In these cultures, TBCs were present between neighboring Sertoli cells where components of ESs could be identified (Fig. 3.5 B, D) and were frequently observed in folds or pockets within basal junction complexes. Basal TBCs in co-cultures were identified by their double-membrane tubular core (Fig. 3.5 B, D), coated pits at the tip of complexes (Fig. 3.5 B), and often by the presence of large bulbs or swellings (Fig. 3.5 A, C) in close association with cisternae of ER (Fig. 3.5 A, C). TBCs with putative bulbs were observed only in Sertoli-germ cell co-cultures (Fig. 3.5).

In primary Sertoli cell cultures without germ cells, TBCs in early stages of formation were present close to areas occupied by ESs (Fig. 3.6 A, D). These structures were identified by the presence of double-membrane coated pits (Fig. 3.6 A, D) and proximal tubule regions (Fig. 3.6 B, D) surrounded by a network of actin filaments (Fig. 3.6 B). TBCs that were slightly more developed with long tubular regions and coated pits that had moved away from the junction were also visible in these cultures (Fig. 3.6 C). TBCs in primary Sertoli cell cultures did not form large bulbs or swellings which is consistent with previous observations of this system[57].

When comparing the morphology of TBCs in both cultures, it was evident that the occurrence of fully developed bulbs was only observed in Sertoli-germ cell co-cultures as opposed to Sertoli cell-only cultures.

3.4 Discussion

The translocation of spermatocytes from basal to adluminal compartments of the seminiferous epithelium across basal junction complexes is essential for spermatogenesis to occur. During this process, massive junction complexes involving tight and adherens junctions disassemble above spermatocytes and reassemble below to facilitate the transport of the developing germ cells across the blood-testis barrier[6,55]. TBCs are unique sub-cellular structures that develop at sites of intercellular attachment in the seminiferous epithelium and are responsible for internalizing intact intercellular junctions[36,42,57–59,61]. Although there is substantial evidence that TBCs develop at basal junction complexes[4,33,57] and contain junction molecules[57], the link between basal TBCs and spermatocyte translocation has not been well established. This study explored the hypothesis that basal TBCs are associated with spermatogenic cell translocation through junction complexes between Sertoli cells in a primary co-culture system. A Sertoli-germ cell system was optimized and determined if the addition of early germ cells to a primary Sertoli cell culture system would stimulate basal junction remodeling by altering the morphology of TBCs present at basal junction complexes.

Germ cells were isolated specifically from early infantile rats (postnatal day (PND) 10), as during this infantile period, seminiferous tubules are predominantly composed of spermatogonia, and germ cells at later stages of differentiation are not present[155]. When isolated germ cells were added to primary Sertoli cell cultures, they often formed clusters and adhered to the surface of monolayers. Germ cells typically adhere to Sertoli cell monolayers *in vitro* by forming focal adhesion or desmosome-like junctions[156]. Some of the added germ cells

moved in between Sertoli cells and displayed the ability to migrate from the apical compartment towards basal regions of the monolayer, where spermatogonia usually reside[149]. Germ cell transplantation studies have reported the movement of SSCs towards spermatogonial stem cell niches from apical to basal parts of the seminiferous epithelium[157]. It has been proposed that chemotactic factors and chemokines produced by Sertoli cells are attracted to receptors present on the surface of spermatogonia and this controls germ cell migration[158,159].

In this developed co-culture system, the added germ cells were often not viable, posing a challenge in maintaining cultures for long periods of time. Germ cell death may have occurred due to enzymatic digestions during the isolation procedure or insufficient provision of specific nutrients or hormones in the culture media. The germline stem cell marker Sall4 was used to identify repopulating germ cells in co-cultures. Sall4 is a transcription factor that is required for the normal function SSCs and their renewal[153]. Positive Sall4 staining in the co-cultures confirmed the presence and entrance of germ cells into the monolayer of Sertoli cells. Sertoli cells cultured without germ cells served as a control. As expected, Sall4 stained cells were not observed in primary Sertoli cell cultures.

When Sertoli cells are cultured *in vitro*, they reportedly establish a functional permeability barrier within 3-4 days[90]. Consistent with this observation, the results showed that Sertoli cells in Sertoli-germ cell co-cultures formed well-developed ESs associated with actin filaments and ER and comprised of tight and gap junctions in basal regions of the monolayer.

The establishment of ESs indicates that this co-culture system can be used as a model to study junction dynamics *in vitro*. Du and colleagues[57] were the first to demonstrate that TBCs develop in basal regions of primary Sertoli cell cultures. They determined that the TBCs were generally tubular in nature and were capped by coated pits and cuffed by an actin network[57]. This was similarly observed in this study as TBCs were in early stages of development. Furthermore, it was observed that fully mature bulbs did not develop in primary Sertoli cell

cultures[57]. Due to the absence of complex somatic/germ cell interactions, these cultures do not accurately represent *in vivo* conditions.

Upon the addition of germ cells to the established primary Sertoli cell culture system, TBCs were consistently present in basal regions of monolayers in areas occupied by ESs. These TBCs seemed to be in more advanced stages of development compared to Sertoli cell-only cultures due to the presence of mature bulbs with ER membrane contacts reminiscent of those formed *in vivo*. In addition to bulbs, tubular regions of TBCs capped with double membrane-coated pits were observed. TBCs in co-cultures more closely resembled TBCs *in vivo* than in primary cultures to which germ cells were not added. These observations were made strictly using a qualitative approach. This is due to the fact that basal TBCs, unlike apical TBCs[57], do not cluster in predictable locations and generally occur in pockets or folds formed by intercellular junctions and cannot yet be adequately visualized at the light or fluorescence level to enable quantification.

These findings provide the first evidence that basal TBCs appear more mature in Sertoli-germ cell co-cultures than in Sertoli cell only primary cultures and may be related to germ cell induced junction turnover.

3.5 Chapter 3 Figures

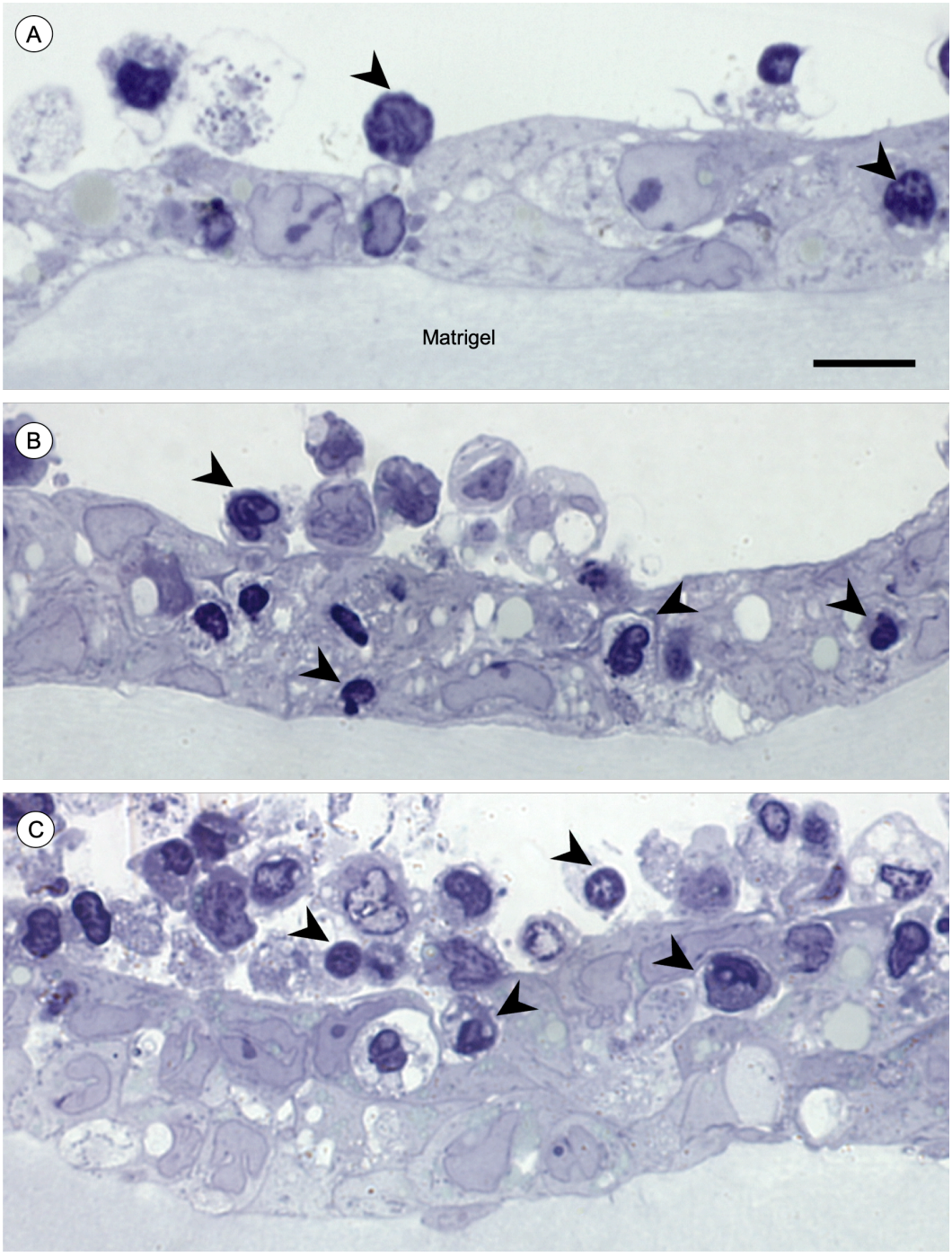

Figure 3.1 Light micrographs of Sertoli-germ cell co-cultures.
In Sertoli-germ cell co-cultures, the added germ cells (arrowheads) adhered to the apex of the Sertoli cell monolayer and some managed to enter the epithelium (A, B, C). All images were captured at 100X magnification. Bar = 10 µm.

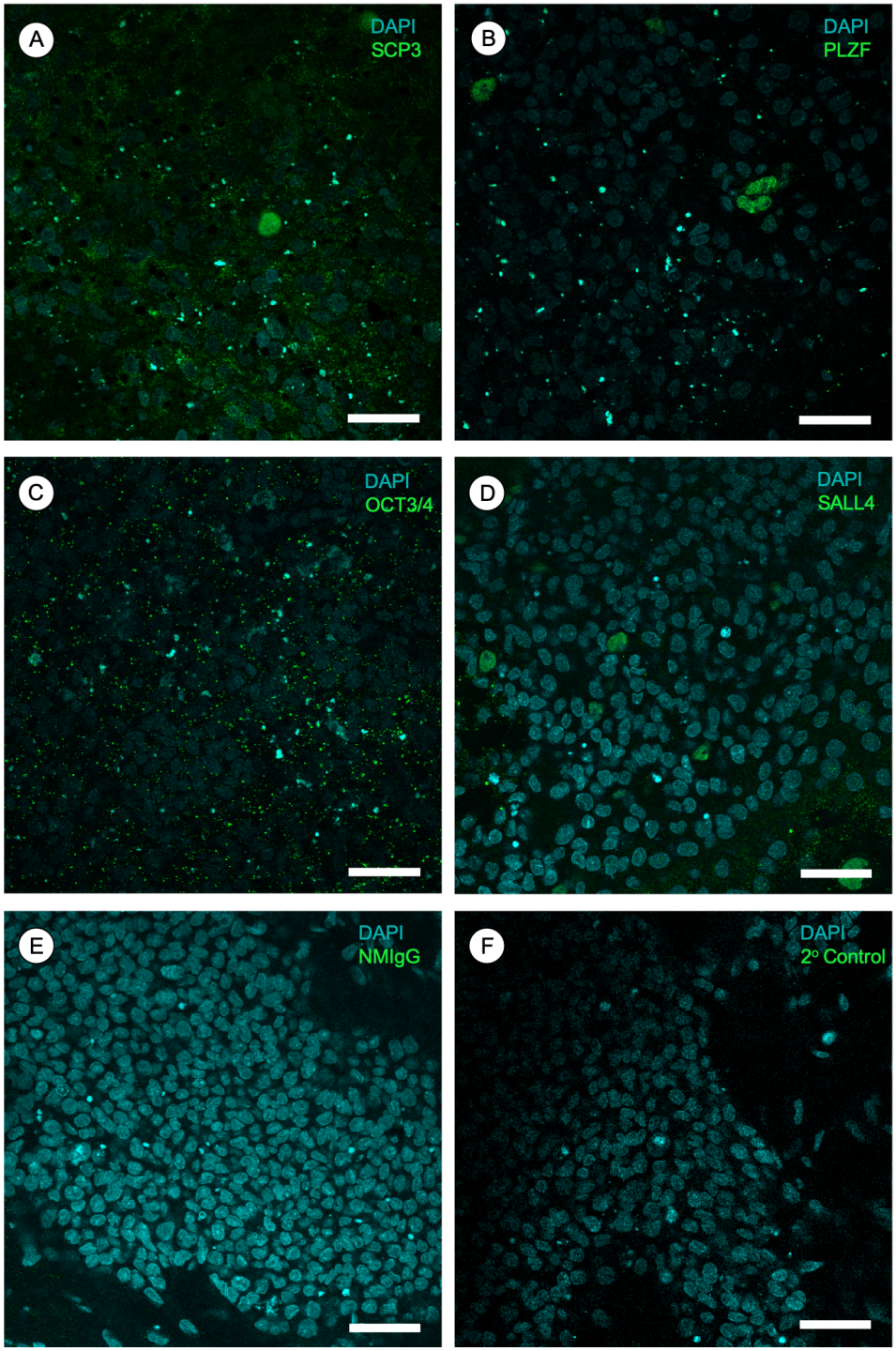

Figure 3.2 Testing germline stem cell markers.
(A – D) show the staining pattern (green) for SCP-3, PLZF, Oct-3/4 and Sall4, respectively. Nuclei of Sertoli cells were stained with DAPI (blue). (E) shows NMIgG control for germ cell markers and (F) shows secondary antibody control. All figures are maximum intensity projections of Z-stacks of immunofluorescently labeled Sertoli-germ cell co-cultures. For (A – C), Bars = 100 μm and for (D – F), Bars = 40 μm.

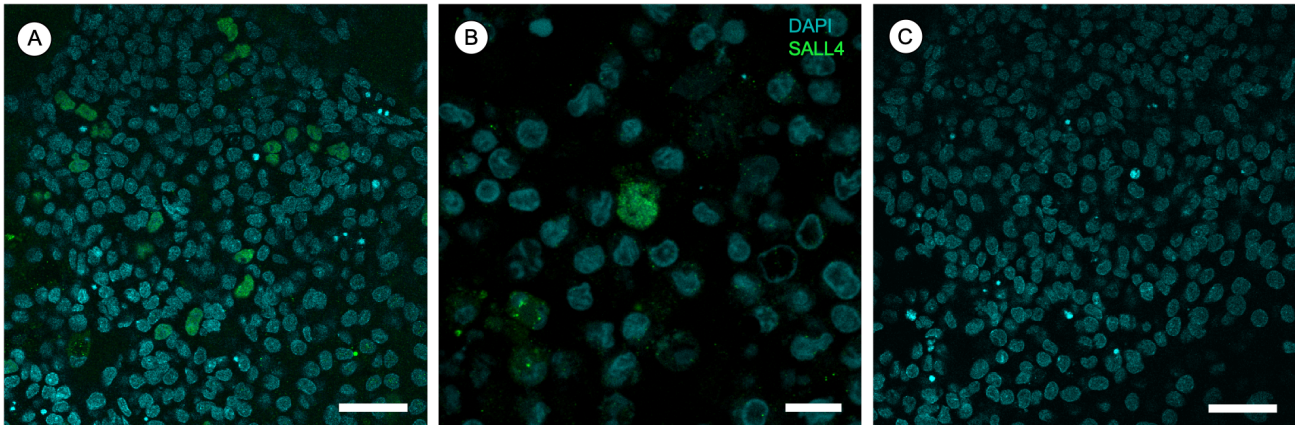

Figure 3.3 Immunofluorescence staining of re-populating germ cells in Sertoli-germ cell co-cultures.
Sall4 staining (green) confirmed the presence of repopulating germ cells in co-cultures (A, B). Sall4 staining was not observed in primary Sertoli cell cultures without added germ cells (C). The nuclei of Sertoli cells were stained with DAPI (blue). All figures are maximum intensity projections of Z-stacks of immunofluorescently labeled Sertoli-germ cell co-cultures. For (A, C), Bars = 40 μm, and for (B), Bar = 10 μm.

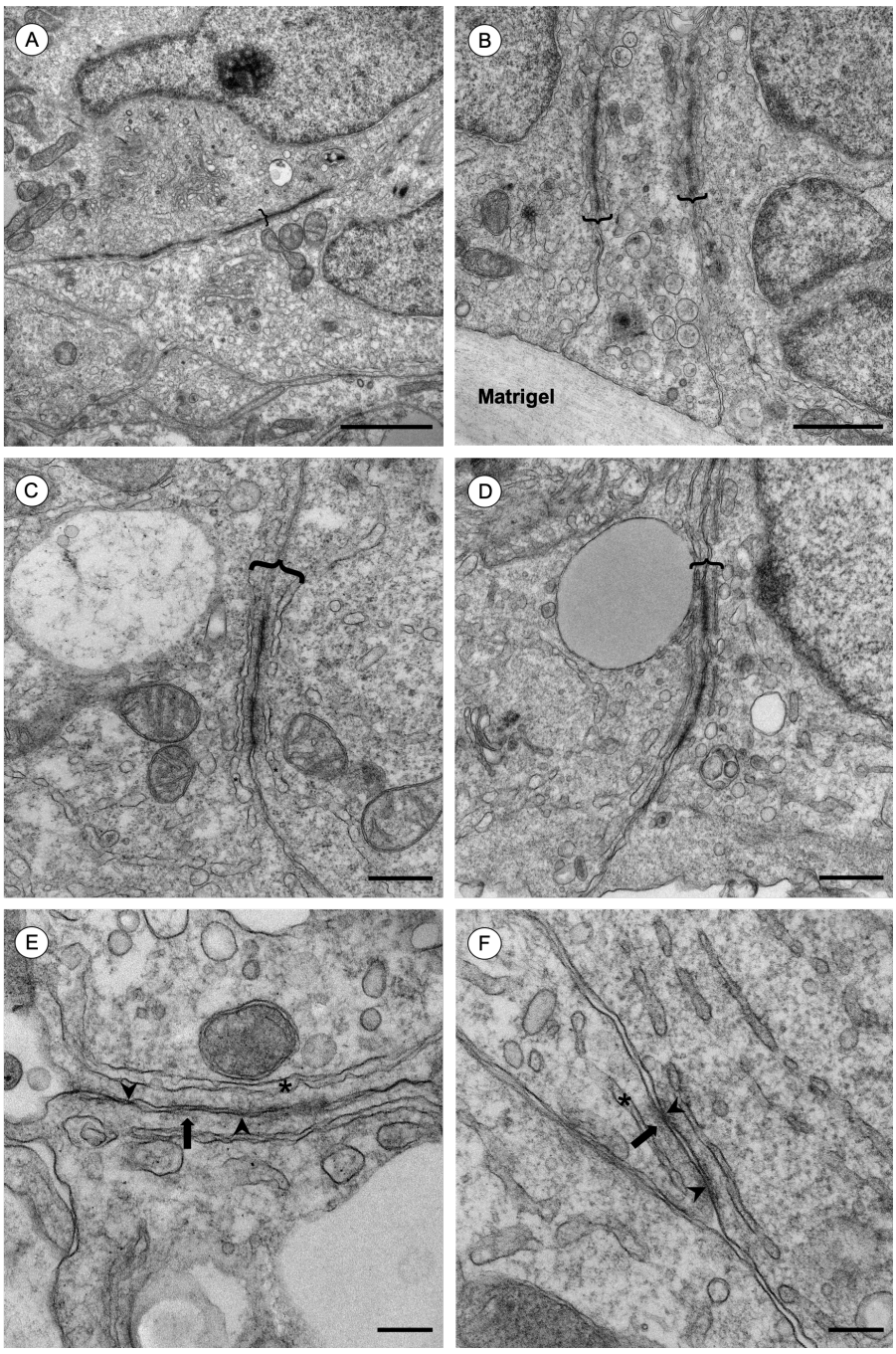

Figure 3.4 Sertoli-Sertoli interfaces in Sertoli-germ cell co-cultures as assessed by electron microscopy.
Ectoplasmic specializations (in brackets) occur at the base of Sertoli cell monolayers in co-cultures (A - D). They are characterized by the presence of actin filaments (arrows in E, F) between the plasma membrane of Sertoli cells and cisternae of endoplasmic reticulum (asterisks in E, F) and morphologically identifiable tight junctions (arrowheads in E, F) within the junction complexes. For (A), Bar = 2 µm, for (B), Bar = 1 µm, for (C, D), Bars = 500 nm, and for (E, F), Bars = 200 nm.

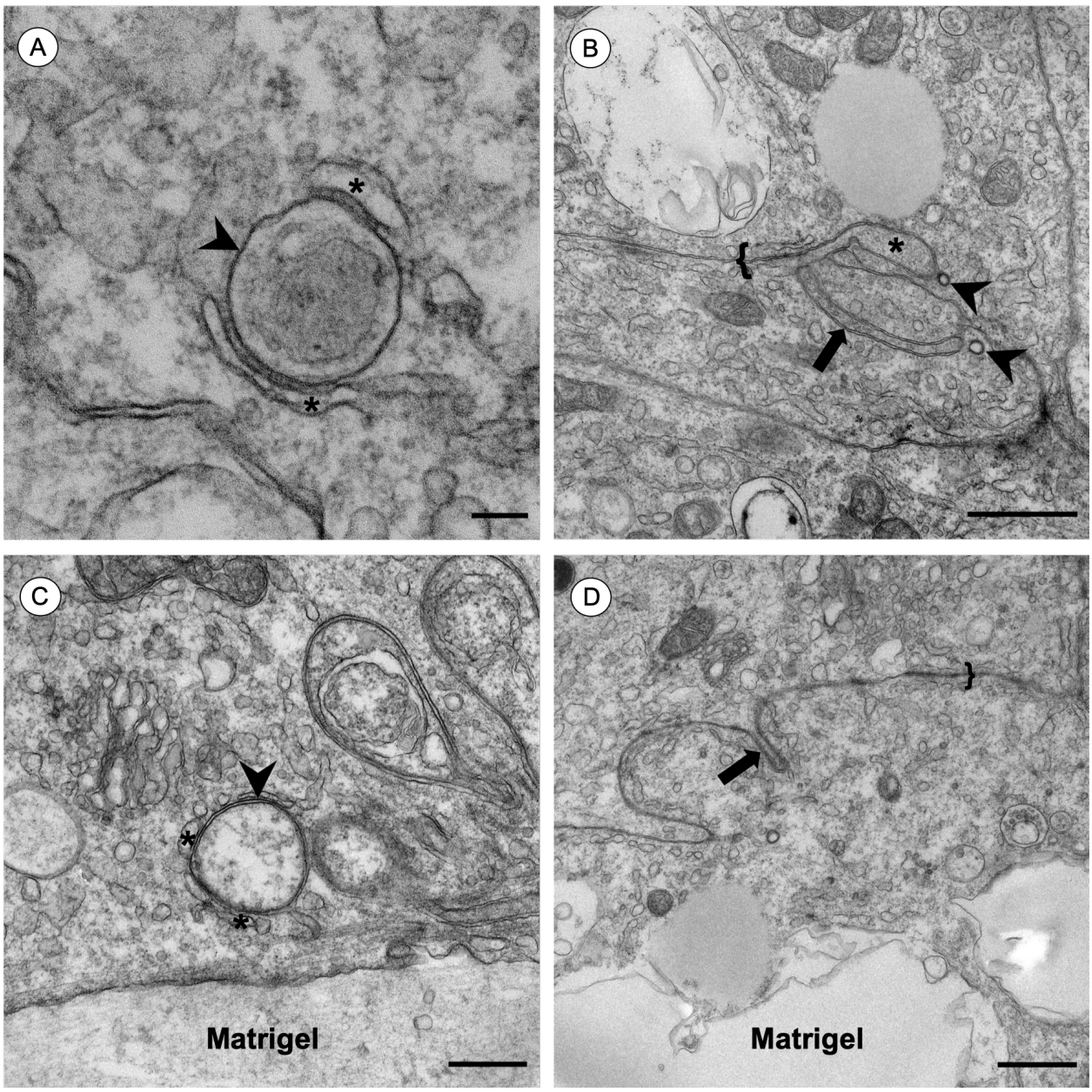

Figure 3.5 Electron micrographs of basal tubulobulbar complexes in Sertoli-germ cell co-cultures.
(A, C) show a cross-section of the bulbar region (arrowheads) of a basal tubulobulbar complex (TBC) in close association with endoplasmic reticulum (asterisks). (B, D) show TBCs that contain a proximal tubule region (arrows), a putative bulb (asterisk in B) and coated pits (arrowheads in B) and they develop in regions close to ectoplasmic specializations (brackets in B, D). For (A), Bar = 100 nm, for (B, D), Bars = 1 µm, and for (C), Bar = 500 nm.

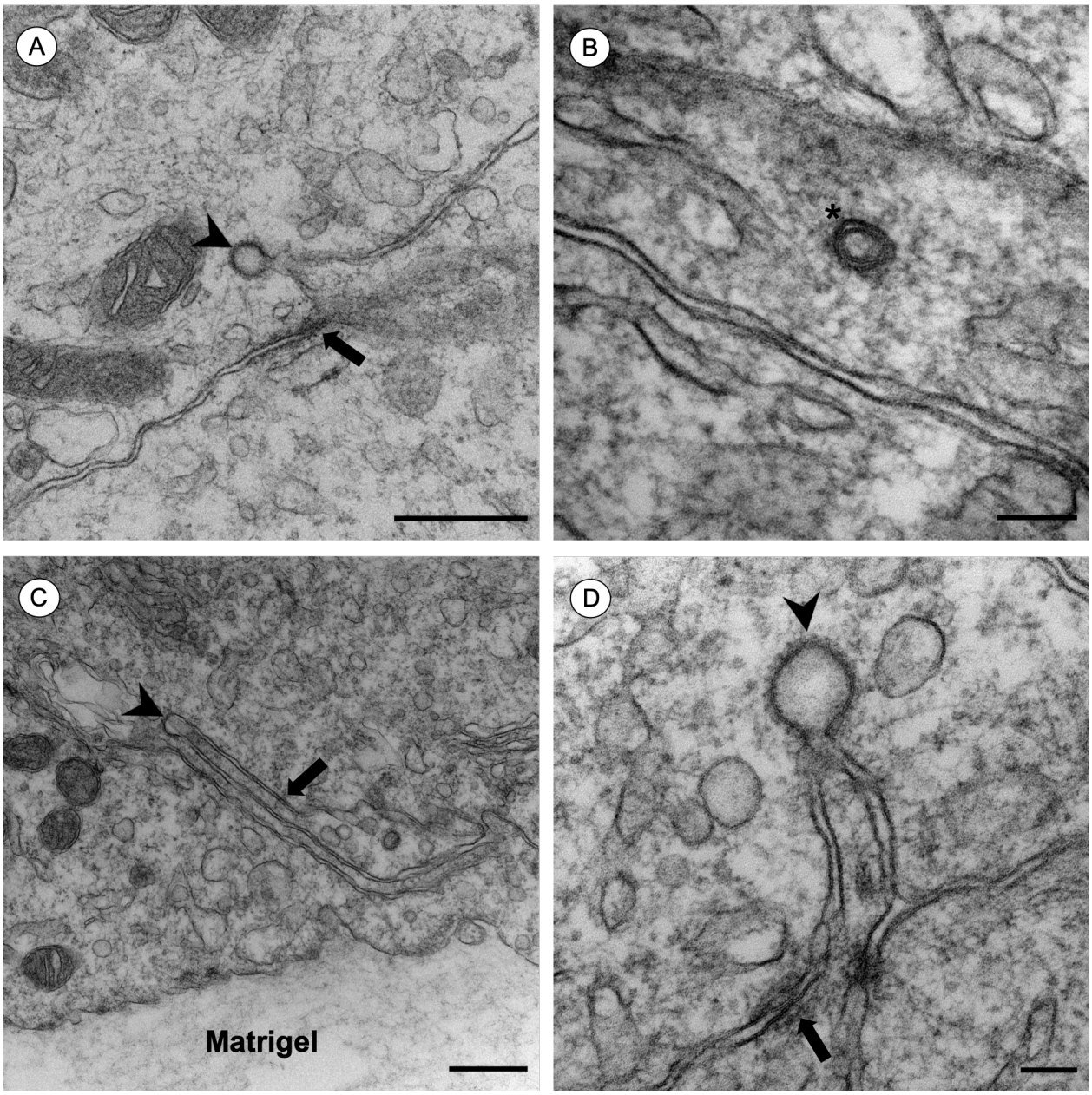

Figure 3.6 Electron micrographs of basal tubulobulbar complexes in primary Sertoli cell cultures without added germ cells.
(A, D) shows the start of formation of tubulobulbar complexes (TBCs) close to areas of ectoplasmic specializations (arrows indicate actin bundles) and the complexes are capped with coated pits (arrowheads). (B) shows the cross-section through the proximal tubular region surrounded by a network of actin filaments (asterisk). (C) shows a TBC close to the base of the Sertoli cells with a long proximal tubular region (arrow), capped by a coated pit (arrowhead). For (A, C), Bars = 500 nm, and for (B, D), Bars = 100 nm.

Chapter 4: Optimizing an *in vivo* RNAi technique to study basal junction turnover in the seminiferous epithelium

4.1 Background

The disassembly of intercellular junctions in the seminiferous epithelium plays a pivotal role during the release of mature spermatids (spermiation) at the apex, and during movement of spermatocytes through basal junction complexes. During these two major epithelial remodeling events, tubulobulbar complexes (TBCs) appear at both apical and basal junctions[62] to internalize intact intercellular attachments[36]. There is a large body of evidence supporting the fact that apical TBCs are subcellular machines that internalize junctions between Sertoli cells and mature spermatids[36,42,61] and that their proper functioning is an essential part of the sperm release mechanism. The absence of TBCs at apical sites of attachment between Sertoli cells and spermatids in estradiol treated rats[69] or in amphiphysin knockout mice[73] results in spermiation failure in the seminiferous epithelium. It also has been demonstrated that knocking down cortactin (a molecular component of TBCs) in rats by intratesticular injection of small interfering ribonucleic acid (siRNA) reagents results in shorter apical TBCs and a failure to release spermatids from the epithelium[79]. In knockdown rats, where the spermatids remained attached to the epithelium, ectoplasmic specializations (ESs) were also present suggesting that intercellular adhesion junctions had not been internalized[79]. These findings support the conclusion that apical TBCs are involved in internalizing intact junctions and are an integral part of the sperm release mechanism.

In comparison, almost nothing is known about basal TBCs, and the link between basal TBC function and the translocation of spermatocytes from basal to adluminal compartments has not yet been established. In rats, basal TBCs often appear in the early stages of spermatogenesis (stages III to VI)[4] and spermatocytes begin to translocate from basal to adluminal compartments

at stage VIII[6]. This suggests that basal junctions in between Sertoli cells begin to remodel well before the next generation of spermatocytes translocate upwards into the adluminal compartment[58]. At basal sites, TBCs have shown ultrastructurally identifiable tight and gap junctions, and immunofluorescence staining has revealed the presence of representative junction proteins such as nectin 2 (adhesion junctions), claudin-11 (tight junctions) and connexin-43 (gap junctions)[57,66]. In addition, markers for early endosomes such as early endosomal antigen 1 (EEA1) and ras-related protein Rab 5 (Rab5) are present in these structures[57]. These findings are consistent with the hypothesis that basal TBCs internalize intact junctions during spermatogenesis and function similarly to apical TBCs. If basal TBCs are responsible for internalizing intact basal junctions, then interfering with the formation of TBCs should result in the delay of spermatocyte translocation. Before exploring this prediction, it was important to optimize an *in vivo* ribonucleic acid interference (RNAi) technique to try and achieve long-term (up to nine days) silencing of cortactin (Cttn) in rats. The main aim of this study was to test the efficacy of the knockdown and determine if the knockdown of cortactin interfered with the morphology or formation of basal TBCs. A similar *in vivo* knockdown strategy successfully developed to study apical TBCs[79] was used to manipulate the expression of cortactin, and specifically looked at the effects on basal TBCs. This chapter reports and discusses the results obtained from the *in vivo* RNAi experiments. Knockdown of cortactin was observed 48 h post-siRNA treatment. This resulted in shorter TBCs at apical regions of the seminiferous epithelium as observed in the previous study[79]; however, at basal sites, differences in TBC morphology could not be detected.

4.2 Materials and Methods

4.2.1 Animals

All animals used for the *in vivo* RNAi experiments were reproductively active male Sprague Dawley rats, ranging anywhere from 300 – 400 g in weight, and were obtained from Charles River Laboratories (Sherbrooke, QC, Canada). The rats were maintained and used according to guidelines established by the Canadian Council on Animal Care, and using protocols approved by the Animal Care Committee of the University of British Columbia.

4.2.2 siRNA reagents and materials

Both ON-TARGETplus and Accell siRNA reagents were used for this study. An ON-TARGETplus SMARTpool siRNA (reagent comprised of a mixture of four siRNAs (Table 1)) (Dharmacon™ - A Horizon Discovery Group, Lafayette, CO, USA) was used to target rat cortactin. An ON-TARGETplus non-targeting pool of four siRNAs (Table 1) (Dharmacon™ - A Horizon Discovery Group) was used as a negative control. The ON-TARGETplus siRNAs were separately mixed with the transfection reagent, *in vivo*-jetPEI® (Polyplus transfection, Illkirch, France) at a nitrogen to phosphate (N/P) ratio of 1/8 at room temperature. Accell SMARTpool Cttn siRNA and Accell non-targeting control pool (Table 1) (Dharmacon™ - A Horizon Discovery Group) were used for experiments conducted later on in this study. The Accell siRNAs did not require any transfection reagent for delivery. Sterile 5X siRNA buffer (Dharmacon™ - A Horizon Discovery Group), Ribonuclease (RNase)-free water (Dharmacon™ - A Horizon Discovery Group) and 10% glucose solution (Polyplus transfection) were used for resuspending and preparing the siRNA reagents. RNase*Zap*® (ThermoFisher Scientific, Fife, WA, USA) was used to remove RNase contamination from equipment, work surfaces and pipettes. RNase-free tips (ThermoFisher Scientific) and tubes (Corning, Corning, NY, USA) were used for handling the

siRNA reagents. Syringes and needles for animal injections were purchased from the Hamilton Company (Reno, NV, USA).

4.2.3 Animal handling and preparation for intratesticular injections

All animals were handled daily for a week prior to conducting RNAi experiments in order to reduce animal anxiety around lab personnel. During the handling process, the animals were weighed, physically examined and given treats (Kellogs Fruit Loops). In preparation for intratesticular injections, animals were first weighed then anesthetized with isoflurane. Animals were placed on a thermal blanket to maintain body temperature. The animals were injected subcutaneously on the back with the analgesic ketaprophen (5.0 mg/kg) for pre-emptive pain management, and 5 ml of sterile saline to maintain hydration. Eye protection was applied to keep the eyes moist during injections. The injection sites were shaved and washed three times using warm soapy water and then swabbed with alcohol. The animal's color and respiratory rate was consistently monitored and the gas flow of oxygen was adjusted accordingly.

4.2.4 *In vivo* injection of siRNA reagents into the testis of rats

In each animal, the right testis was injected with 60 µl of Cttn-targeting siRNA (ON-TARGETplus or Accell siRNA reagent) and the left testis was injected with 60 µl of non-targeting siRNA (ON-TARGETplus or Accell siRNA reagent). The siRNA reagents were subcutaneously injected into the centre of the testis at a single site. The animals regained consciousness within 5 min post-injections and were gently handled, fed treats and placed in their home cages. Thereafter, they were monitored daily over the course of the experiment. The animals were re-injected with the same concentration of siRNA every three days if the duration of the RNAi treatment was nine days long.

4.2.5 Whole testis lysate and immunoblotting

All western blots were performed on whole testis. To obtain whole testis lysates, testes were removed from rats under deep anesthesia, and decapsulated. The whole testicular mass was immediately homogenized in cold RIPA lysis buffer (150 mM NaCl, 50 mM Tris, pH 7.5, 5mM EDTA, 1% NonIdet P-40, 1% deoxychloic acid [sodium salt], 0.1% SDS) with cOmplete™ ULTRA tablet EDTA-free protease inhibitor (Millipore Sigma, Oakville, ON, Canada). Lysate aliquots of both experimental and control testes were loaded into wells of 10% Tricine protein gels at equal concentrations determined by protein assay. The gels were run according to standard protocols[160]. Proteins were transferred to PVDF membranes (ThermoFisher Scientific) for 1 h and then the membranes were blocked overnight at 4^{o}C using 4% milk/TBST (25 mM Tris, pH 8.3, 150 mM NaCl, 0.1% Tween-20 (Millipore Sigma), 4% Milk). The next day, membranes were incubated with the primary antibody, rabbit-anti-cortactin (Millipore Sigma), at a concentration of 1:10,000 for 1 h at room temperature. Then, the membranes were washed 3 times, 10 min each with 4% milk/TBST. Following this, membranes were incubated with the secondary antibody, goat anti-rabbit horseradish peroxidase-conjugated antibody (Millipore Sigma), at a concentration of 1:40,000 for 1 h at room temperature. Following incubation, membranes were washed 3 times, 10 min each with TBST (25 mM Tris, pH 8.3, 150 mM NaCl, 0.1% Tween-20), and placed in ECL solution (GE Lifesciences, Pittsburgh, PA, USA) for 3 min before the bands were visualized and captured with the digital imaging system, ImageQuant LAS 4000 (GE Lifesciences). Loading controls were performed by first stripping the membranes with Restore Western Blot Stripping Buffer (ThermoFisher Scientific) for 30 min at room temperature. Then, the membranes were washed 3 times in TBST, for 5 min each. The membranes were blocked for 1 h in 4% Milk/TBST at room temperature, then incubated with the primary antibody, rabbit-anti-calnexin (Millipore Sigma), at a concentration of 1:40,000 for 1 h at room temperature. Membranes were then washed 3 times for 5 min each with 4% Milk/TBST,

followed by incubation with secondary antibody, goat anti-rabbit horseradish peroxidase-conjugated antibody (Millipore Sigma), at a concentration of 1:40,000 for 1 h at room temperature. Blots were washed 3 times for 5 min each with TBST, and then placed in ECL solution (GE Lifesciences) for 3 min before the bands were visualized and captured with the digital imaging system, ImageQuant LAS 4000 (GE Lifesciences). Densitometry analysis was conducted using the analyze gels function on ImageJ[126] to quantify western blot data.

4.2.6 Immunofluorescence

Testes were removed from anesthetised animals and perfused with PBS to clear blood. Then, the testes were perfused with fixative (PBS, 3% paraformaldehyde (Millipore Sigma), pH 7.3) for 30 min. Fixed testes were mounted onto aluminum stubs with OCT compound (Sakura Finetek USA, Torrence, CA) and frozen using liquid nitrogen. 10 µm thick tissue sections were cut using a cryo-microtome and placed onto poly-L-lysine coated glass slides. After sectioning, the slides were immediately submerged in cold (-20^{o}C) acetone for 5 min. Slides were removed from acetone and placed in 0.1%BSA/PBS, pH 7.3 bath for at least 5 min. A water-repellent circle was drawn around each tissue section using a liquid blocker super pap pen (Cedarlane, Burlington, ON, Canada) to retain the liquid over the sections. Blocking buffer (1% BSA/PBS, pH 7.3) was added to the tissue sections for 1 h at room temperature. After blocking, primary antibodies were diluted with 0.1% BSA/PBS, and were added to sections. The working concentration of the primary antibody, rabbit anti-cortactin (Millipore Sigma) was 0.005 mg/ml. Specificity control of antibody staining was prepared by using normal IgG serum from the same species in which the primary antibody was generated. The slides were left in 4^{o}C overnight. After overnight incubation with primary antibodies, the next day, the slides were washed three times with 0.1% BSA/PBS for 10 min. After washing, secondary antibody conjugated to a fluorochrome (Goat-anti-rabbit Alexa Fluor 488 (ThermoFisher Scientific) was diluted to a final

concentration of 1:100 using 0.1% BSA/PBS and added to the slides, followed by incubation at 37^{o}C for 1 h. Then, the slides were washed once with 0.1% BSA/PBS for 10 min. After washing, tissues sections were stained with diluted DAPI (ThermoFisher Scientific) for 10 min at room temperature. Then, the slides were washed with 0.1% BSA/PBS. The water-repellent circles were removed using a razor blade, and tissue sections were mounted in VectaShield mounting medium without DAPI (Vector Laboratories, Burlington, ON, Canada). Images were obtained using a Leica TCS SP5 Confocal laser-scanning microscope (Leica Microsystems Inc., Concord, Ontario, Canada). All fluorescence microscopy images were subsequently analyzed and processed using ImageJ software[126]. The Z-project function on ImageJ was used to create a max projection image of apical spermatid heads, which was a composite of the various stains from Z-stacks.

4.2.7 Electron microscopy

Animals were anesthetized with isoflurane and the testes were removed and perfused through spermatic artery for 1 min with warm PBS to clear blood. Then, the testes were perfused with fixative (1.5% paraformaldehyde/1.5% glutaraldehyde (Electron Microscopy Sciences, Hatfield, PA, USA), pH 7.3) for 30 min. After perfusion, the testes were cut to small pieces in fixative and left to sit for an additional 2-3 h. The testes were then washed three times, for 10 min each with 0.1 M sodium cacodylate (Electron Microscopy Sciences) and fixed on ice for 1 h in 1% osmium tetroxide (made up in sodium cacodylate buffer) (Electron Microscopy Sciences). The material was washed three times, 10 min each with ddH_2O and stained for 1 h with 1% aqueous uranyl acetate (Electron Microscopy Sciences). Following this, the material was washed again three times, 10 min each with ddH_2O and dehydrated with increasing concentrations of ethyl alcohol. This was followed by two 15 min incubations in propylene oxide (Fisher Scientific, Ottawa, ON, Canada). The blocks were left in 1:1 solution of propylene oxide:

polybed overnight. Finally, the material was embedded in 100% polybed (Electron Microscopy Sciences) and placed in a 60^{o}C oven for at least 24 h. Sections were evaluated and photographed using a FEI Tecnai G2 Spirit electron microscope.

4.3 Results

4.3.1 Intratesticular injection of ON-TARGETplus Cttn siRNA results in cortactin rebound phenomenon

The first set of *in vivo* RNAi experiments were conducted using ON-TARGETplus siRNA reagents. Animals were injected with close to maximum (0.45 µg/µl) concentration of siRNA and western blots were performed on whole testis lysates from experimental (injected with Cttn-targeting siRNA) and control (injected with non-targeting siRNA) testes. Immunoblots of whole testis lysates did not show any signs of cortactin knockdown in the experimental testes relative to control testes three (Fig. 4.1 A) (n = 1 rat) and nine days (Fig. 4.1 B) (n = 1 rat) following siRNA delivery. Instead, a cortactin 'rebound' phenomenon was observed in both animals. The protein rebound in experimental testis was more profound on day three as indicated by the higher intensity of the cortactin band on the blot (Fig. 4.1 A). By day nine, the intensity of the cortactin band was consistent in both experimental and control testes (Fig. 4.1 B). The rebound of cortactin was still observed in experimental testes after three (Fig. 4.2 A) (n = 6 rats) and nine days (Fig. 4.2 B) (n = 3 rats) when rats were administered with half the maximum concentration (0.25 µg/µl) of siRNA. A cortactin rebound phenomenon occurred in all the animals injected with maximum or half of maximum concentrations of ON-TARGETplus Cttn siRNA reagents.

4.3.2 Apical tubulobulbar complexes are shorter in testes injected with maximum concentration of ON-TARGETplus Cttn siRNA

The testes from one animal (n = 1 rat) injected with maximum concentration of ON-TARGETplus Cttn siRNA were processed for electron microscopy to examine the morphological effects of the siRNA. Cross sections through apical Sertoli cell processes containing mature spermatids at stage VII of spermatogenesis showed that fewer profiles of proximal tubular regions of TBCs were present in experimental tissue (Fig. 4.3, D, E, F) compared to control tissue (Fig. 4.3, A, B, C) nine days post siRNA delivery. This suggested that TBCs were shorter in Cttn siRNA-treated tissue.

4.3.3 Testing the long-term silencing efficacy of Accell siRNA

In vivo RNAi experiments were conducted using Accell siRNA reagents. Animals were injected with close to maximum concentration (0.45 µg/µl) of Accell siRNA. The cortactin rebound phenomenon continued to occur after nine days (Fig. 4.4) (n = 1 rat) with the use of Accell siRNA reagents. The intensity of the cortactin band was slightly higher in the lysate from experimental (injected with Accell Cttn siRNA) relative to lysate from contralateral control (injected with Accell non-targeting siRNA) (Fig. 4.4). An immunoblot time course analysis revealed that cortactin rebound occurs 8 h, 16 h, 24 h and 72 h after siRNA delivery (Fig. 4.5, A, B, C, E) (n = 1 rat per time point). The intensity of the cortactin band on the blot was slightly weaker in experimental testis relative to control testis only at the 48 h time point (Fig. 4.5 D). To confirm protein knockdown after 48 h, two more animals (n = 2 and 3) were administered with maximum concentration of Accell siRNA and the testes were prepared for western blot analysis. For comparison purposes, the lysates from these animals were run alongside the lysates from the animal used for the 48 h time course analysis (Fig. 4.6 A). In animal 2, the intensity of the cortactin band was slightly weaker in the experimental testis compared to control (Fig. 4.6 A). In

contrast, a cortactin rebound phenomenon was observed in the experimental testis of animal 3 (Fig. 4.6 A). A densitometry analysis was conducted on these triplicate samples (Fig. 4.6 B) to quantify the intensities of the bands, verifying the cortactin knockdown or rebound phenomenon.

4.3.4 Accell siRNA-induced cortactin knockdown results in shorter apical tubulobulbar complexes

An immunofluorescence experiment was conducted to stain for cortactin in apical regions of Accell siRNA-treated testes (n = 1 rat) after 48 h. This was done to verify that the intensity of cortactin is lower in knockdown tissue after 48 h. At stage VII, TBCs in the seminiferous epithelium appeared qualitatively shorter and less organized in experimental testes (Fig. 4.7, B, D, F) compared to control (Fig. 4.7, A, C, E). Primary (Fig. 4.7 G) and secondary antibody (Fig. 4.7 H) controls confirmed the specificity of the antibody targeting cortactin. Similarly, at the ultrastructural level, it was observed that at stage VII of spermatogenesis, fewer profiles of apical TBCs were visible in experimental tissue (Fig. 4.8 B, D) versus control tissue (Fig. 4.8 A, C). Furthermore, longitudinal sections of apical TBCs showing the proximal regions were visibly shorter in experimental (Fig. 4.8 G) than in control (Fig. 4.8 F) tissue. In some regions, the apical processes of Sertoli cells appeared abnormally narrow in experimental (Fig. 4.8 E) tissue compared to control (Fig. 4.8 A, C).

4.3.5 The morphology of basal tubulobulbar complexes in Accell siRNA-treated testes

Basal TBCs were present in both control and experimental tissue at stages III to V where they are reported to be most abundant[3]. They formed close to areas occupied by ESs (Fig. 4.9 B, D). Proximal tubular regions generally looked similar in both Accell siRNA-treated (Fig. 4.9 B, D and Fig. 4.10 B, D, E) and un-treated tissue (Fig. 4.9 A, C and Fig. 4.10 A, C) with the presence of a double membrane core surrounded by a network of actin filaments (Fig. 4.9 C, D).

Some proximal tubules appeared to be unusually long (Fig. 4.10 F) compared to control (Fig. 4.10 A, C).

4.4 Discussion

Although the link between apical TBCs and sperm release has been established[69,73,79], the link between basal TBCs and spermatocyte translocation remains to be confirmed. In an attempt to start exploring the role of basal TBCs in the translocation of spermatocytes out of the stem cell niche, an *in vivo* RNAi technique was used to deplete cortactin and determine if differences in the morphology or formation of basal TBCs occurs. Cortactin is a protein that is expressed in various tissues and organs and regulates actin polymerization and cytoskeletal dynamics[161,162]. The functional domains of cortactin bind to and activate actin-related protein 2/3 (Arp2/3), a molecular machine that nucleates actin filament assembly, and together they stabilize newly formed branches[163,164]. Other cortactin binding proteins include a large number of cytoskeletal, signaling and membrane-trafficking proteins[165]. Cortactin plays an important role in actin-based cellular processes such as cell migration, invasion and membrane protrusion[166,167]. Cells lacking cortactin display a defect in lamellopodial protrusions[166]. The knockdown of cortactin in osteoclasts prevents the formation of podosomes[167]. The morphology and molecular composition of TBCs closely resembles podosomes in osteoclasts[81]. Cortactin is concentrated at TBCs and is a key component of the three-dimensional network of actin filaments surrounding the proximal and distal parts of the structure[60]. It previously has been shown that depleting cortactin using RNAi results in stunted apical TBCs and the failure to release mature spermatids from the epithelium[79].

Here I attempted to knockdown the expression of cortactin in the seminiferous epithelium by using a similar *in vivo* RNAi technique developed to study apical TBCs[79] to specifically look at basal TBCs. High siRNA dosages were used in an attempt to achieve long-term silencing of

cortactin *in vivo*. Basal junction remodeling starts well before spermatocyte translocation in rats[4,6]. Therefore, siRNA reagents were injected nine days prior to terminating the animals. As the RNAi effect is usually transient, animals were re-injected three times over the course of nine days. Also, animals were processed for immunoblotting three days post siRNA delivery to confirm initial knockdown.

Animals injected with close to maximum concentration (0.45 µg/µl) of ON-TARGETplus Cttn siRNA demonstrated a cortactin rebound phenomenon in both three and nine days following siRNA delivery. This was indicated by the presence of a more intense cortactin band in lysates from experimental testes compared to lysates from control testes. The rebound of gene and protein expression due to siRNA has very rarely been investigated and reported in literature. Hong and colleagues have shown that in mice, high doses of siRNA cause a quicker and higher rebound of gene expression compared to lower doses of siRNA[168]. They suggested that high doses of siRNA triggered the RNAi machinery to undergo negative regulation and cause a decrease in the inhibitory effect by coding for destabilizing enzymes[168]. To check if the observed rebound phenomenon was dose-dependent, animals were injected with half the maximum concentration (0.25 µg/µl) of ON-TARGETplus Cttn siRNA. However, even at a lower concentration, the cortactin rebound phenomenon persisted and no knockdown was observed after three and nine days on the blots. A set of ON-TARGETplus siRNA reagents targeting cortactin were previously used to perform knockdown experiments on apical TBCs[79]. It is possible that in these earlier studies, a very low dosage of siRNA (lower than 0.25 µg/µl) was administered to the rats and this resulted in a knockdown being observed on the blots three days post siRNA delivery[79].

Interestingly, the phenotype of apical TBCs was altered when rats were administered with close to maximum concentration of ON-TARGETplus Cttn siRNA. Apical TBCs were shorter in experimental tissue compared to control tissue at stage VII of spermatogenesis. This was the

same phenotype that was observed in earlier studies[79]. Even though a phenotypic effect was present in apical regions, a concomitant decrease in cortactin expression could not be observed on blots. It is likely that a transient reduction in cortactin expression occurred at an earlier time point (between day 0 – day 3) and this resulted in the altered phenotype of apical TBCs. However, due to the quick rebound of cortactin *in vivo*, the knockdown was not captured on the blots. Based on these observations, it can be concluded that the cortactin rebound phenomenon may have not just been a result of the high dosage of siRNA but could have been occurring due to the instability of the ON-TARGETplus Cttn siRNAs *in vivo*.

To determine if a more stable type of siRNA reagent would result in long-term silencing, experiments using Accell siRNA were performed. Accell siRNA is chemically modified for stability, target specificity and designed to enable extended duration of silencing *in vivo* without a transfection reagent. This siRNA is designed for use in difficult-to-transfect cell types and can be used for reapplication without causing cytotoxic effects. Rats were administered with close to maximum concentration (0.45 µg/µl) of Accell Cttn siRNA due to the fact that a phenotypic effect was observed on apical TBCs using this siRNA concentration in previous experiments. Once again, a cortactin rebound phenomenon was observed on the blot nine days after Accell Cttn siRNA delivery. In an attempt to observe the knockdown of cortactin on the western blot, a time course analysis was conducted. The intensities of cortactin bands on the immunoblots were higher in experimental lysates 8 h, 16 h, 24 h and 72 h post Accell Cttn siRNA treatment. A slight knockdown was only observed at the 48 h time point. To verify this knockdown, two more animals were injected with high doses of Accell Cttn siRNA, and the testis was prepared for western blot analysis after 48 h. A slight knockdown was once again observed in one animal and a cortactin rebound phenomenon occurred in the other animal, despite keeping all experimental conditions consistent. Since separate animals were used for each immunoblotting analysis, several factors that mediate cellular uptake, degradation and clearance may have

affected the *in vivo* performance of the Accell siRNA. This probably contributed to the inconsistencies in cortactin knockdown on the blots. Since a knockdown was observed at the 48 h time point, an immunofluorescence experiment was conducted to stain for cortactin specifically at the apex of the seminiferous epithelium, where apical TBCs are present. This was done to verify that the intensity of cortactin is lower in knockdown tissue after 48 h. When TBCs were labeled for cortactin, they were qualitatively shorter in experimental tissue compared to control tissue, consistent with previous results[79].

Subsequently, the morphological effect on apical TBCs after 48 h was also observed at the ultrastructural level. Shorter apical TBCs were observed in the knockdown epithelia compared to control, also similar to what has previously been reported[79].

The aim of this study was to look at the morphological effect of cortactin knockdown on basal TBCs. Unlike apical TBCs that are clustered in large numbers at specific regions on the spermatid head, basal TBCs are often not found in large clusters are not at predictable regions of junction complexes. Therefore, basal TBCs are much more difficult to visualize using techniques other than electron microscopy. In this study, basal TBCs were observed close to areas occupied by ESs in both control and experimental tissue. Basal TBCs in these tissues were identified by the presence of double membrane tubular regions and surrounding network of actin filaments. It was difficult to discern any morphological differences between TBCs qualitatively in siRNA-treated and untreated tissues using electron microscopy. In order to obtain some form of quantitative data, techniques will have to be developed to visualize larger numbers of basal TBCs so that lengths and numbers can be determined.

In conclusion, a knockdown was achieved 48 h post Accell Cttn siRNA delivery but this was inconsistent amongst animals. This knockdown correlated with a phenotypic effect on TBCs in apical regions, where TBCs were shorter in siRNA-treated tissue. In comparison, morphological

differences in basal TBCs could not be observed. The data discussed in this chapter provides a framework for future *in vivo* RNAi long-term silencing experiments.

4.5 Chapter 4 Figures

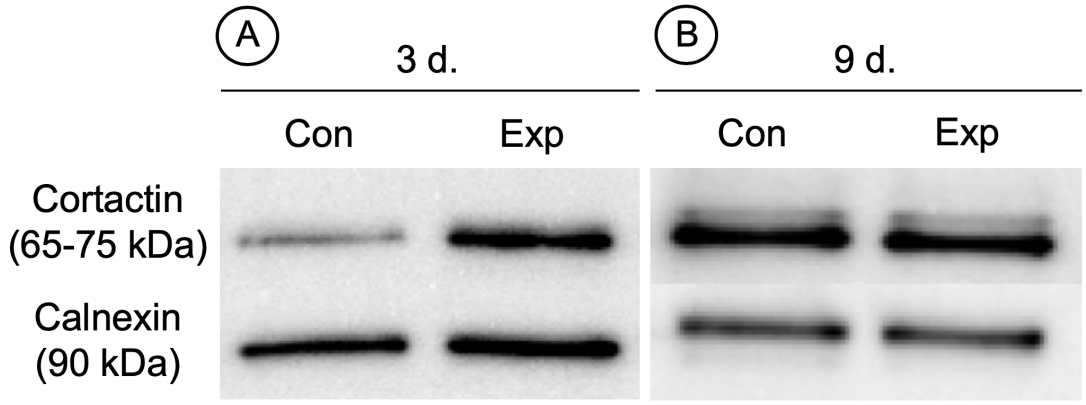

Figure 4.1 Western blots of whole testis lysates after intratesticular injection of maximum concentration of ON-TARGETplus siRNA.
A cortactin rebound phenomenon was observed when testes were injected with 0.45 µg/µl of ON-TARGETplus Cttn siRNA. Experimental testes were injected with ON-TARGETplus Cttn siRNA and control testes were injected with ON-TARGETplus non-targeting siRNA. (A) Western blot of whole testis lysate from one animal after three days shows that the intensity of the cortactin band is higher in experimental testis compared to control. (B) Western blot of whole testis lysate from another animal after nine days shows that the intensity of the cortactin band is consistent in both control and experimental testes. Calnexin was used as a loading control.

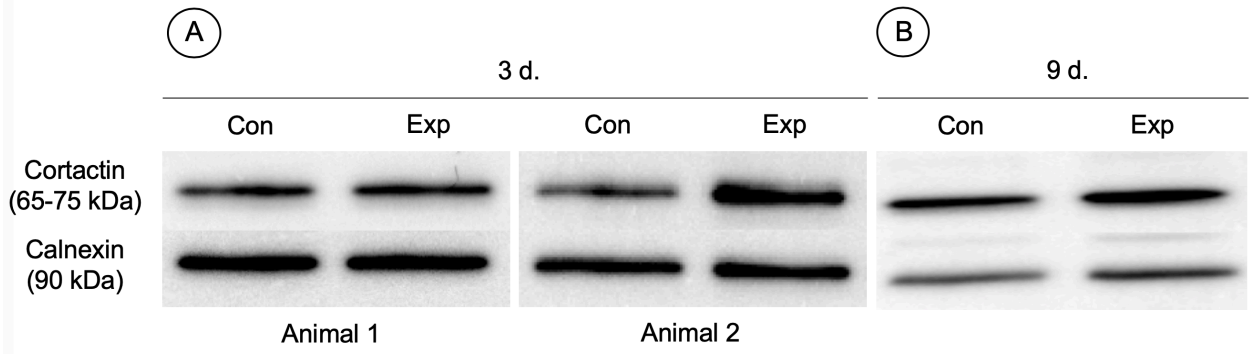

Figure 4.2 Western blots of whole testis lysates after intratesticular injection of half the maximum concentration of ON-TARGETplus siRNA.
A cortactin rebound phenomenon was observed when testes were injected with 0.25 µg/µl of ON-TARGETplus Cttn siRNA. Experimental testes were injected with ON-TARGETplus Cttn siRNA and control testes were injected with ON-TARGETplus non-targeting siRNA. (A) Western blot of whole testis lysates from two animals after three days shows that the intensity of the cortactin band is either consistent or slightly higher in experimental testis compared to control. (B) Western blot of whole testis lysate from another animal after nine days shows that the intensity of the cortactin band is slightly higher in experimental testis compared to control. Calnexin was used as a loading control.

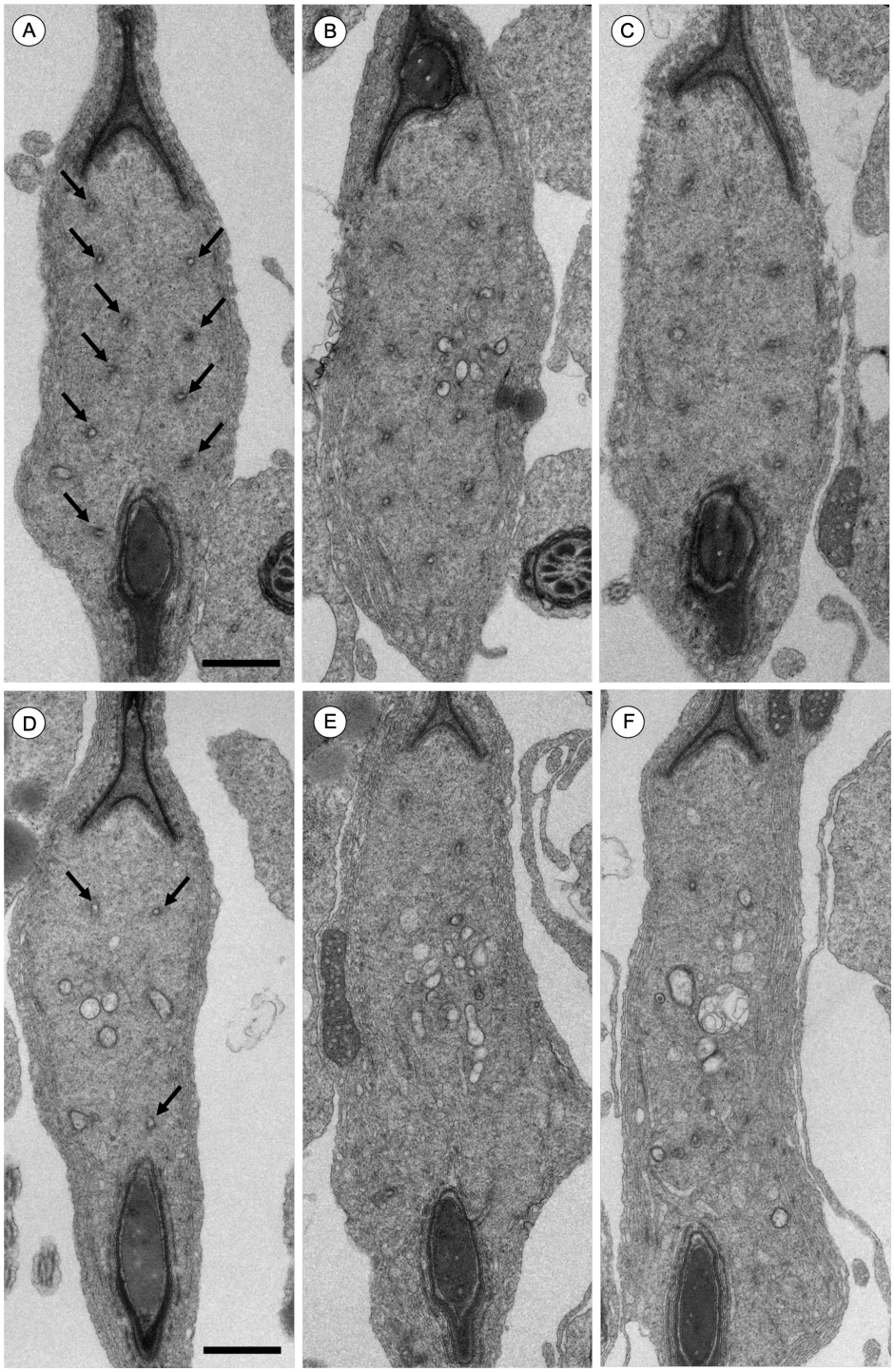

Figure 4.3 Cross sections through apical Sertoli cells testes treated with maximum concentration of ON-TARGETplus siRNA.
Apical Sertoli processes containing mature spermatids at stage VII of spermatogenesis showed that there were fewer profiles of proximal tubular regions of tubulobulbar complexes (TBCs) (arrows) in testis treated with ON-TARGETplus Cttn siRNA (D – F) relative to control testis (A – C). This indicates that TBCs are shorter in Cttn siRNA-treated testes. Bars = 500 nm.

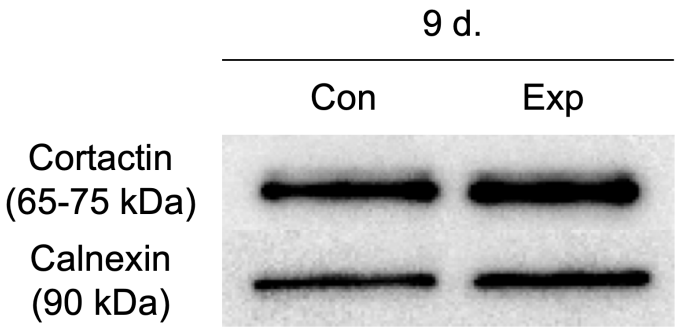

Figure 4.4 Western blots of whole testis lysates after intratesticular injection of maximum concentration of Accell siRNA.
A cortactin rebound phenomenon was observed when testes were injected with 0.45 µg/µl of Accell Cttn siRNA. Experimental testes were injected with Accell Cttn siRNA and control testes were injected with Accell non-targeting siRNA. Western blot of whole testis lysate from one animal after nine days shows that the intensity of the cortactin band is slightly higher in the experimental testis compared to control. Calnexin was used as a loading control.

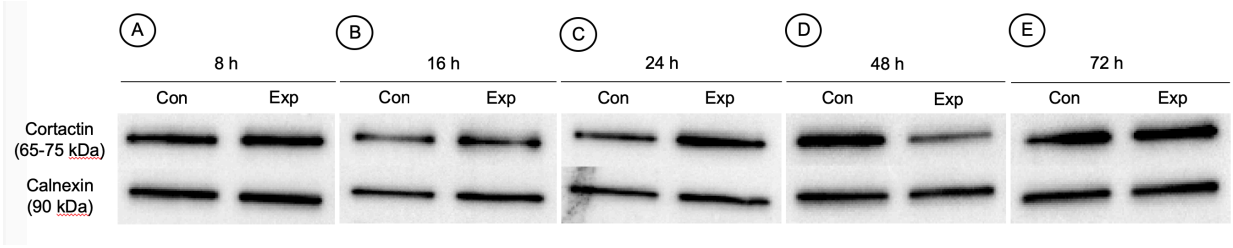

Figure 4.5 Western blot analysis of time course using Accell siRNA.
A cortactin rebound phenomenon was observed when testes were injected with 0.45 µg/µl of Accell Cttn siRNA (A) 8 h, (B) 16 h, (C) 24 h and (E) 72 h post siRNA delivery. The cortactin band on western blot of whole testis lysate from testis injected with Accell Cttn siRNA was weaker relative to similar lysate from contralateral control testis injected with non-targeting siRNA 48 h post siRNA delivery (D). Calnexin was used as a loading control.

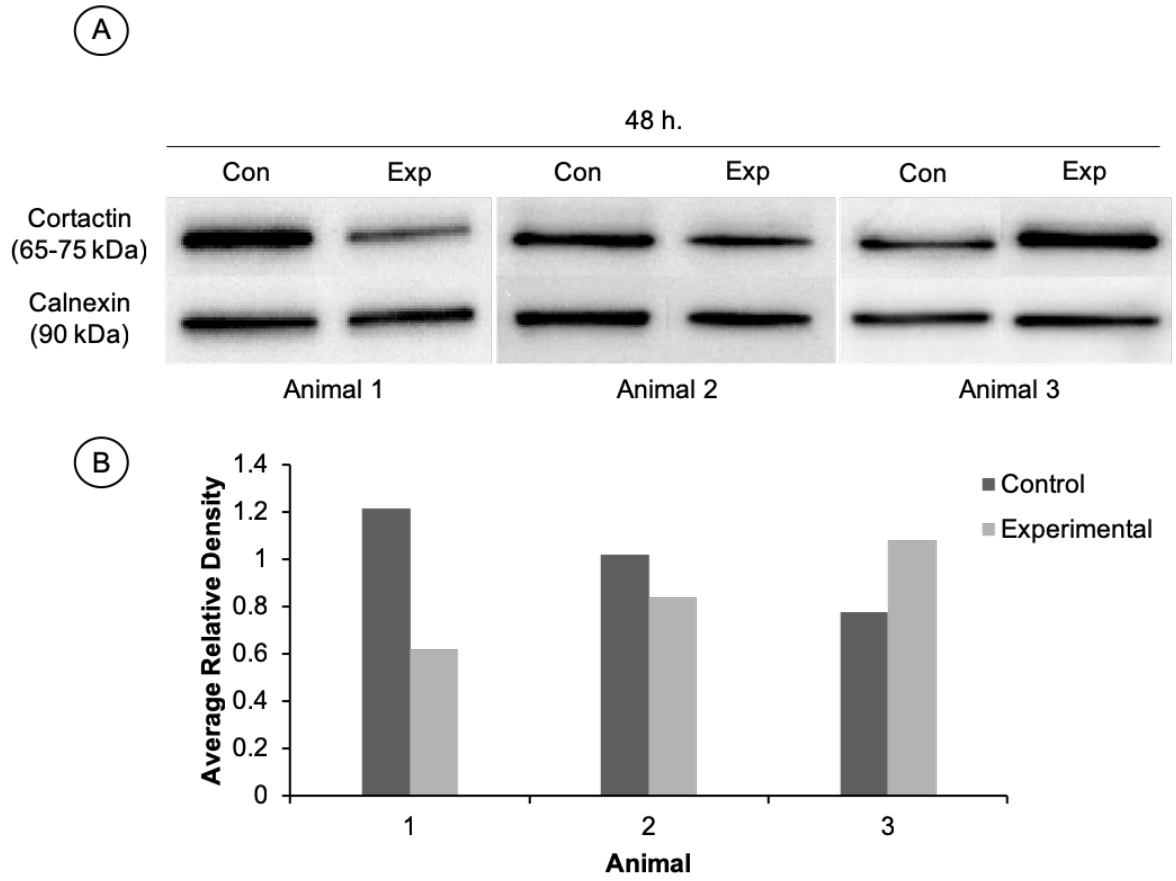

Figure 4.6 Western blots and densitometry analysis of whole testis lysates 48 h after intratesticular injection of maximum concentration of Accell siRNA.
A slight knockdown of cortactin was observed in experimental testes in (A) animals 1 and 2 compared to control testes 48 h post siRNA delivery. A rebound of cortactin was observed in the experimental testis of (A) animal 3. Calnexin was used as a loading control. (B) Densitometry analysis of western blots showed a reduction in cortactin levels in animals 1 and 2 and an increase in animal 3 when normalized to calnexin.

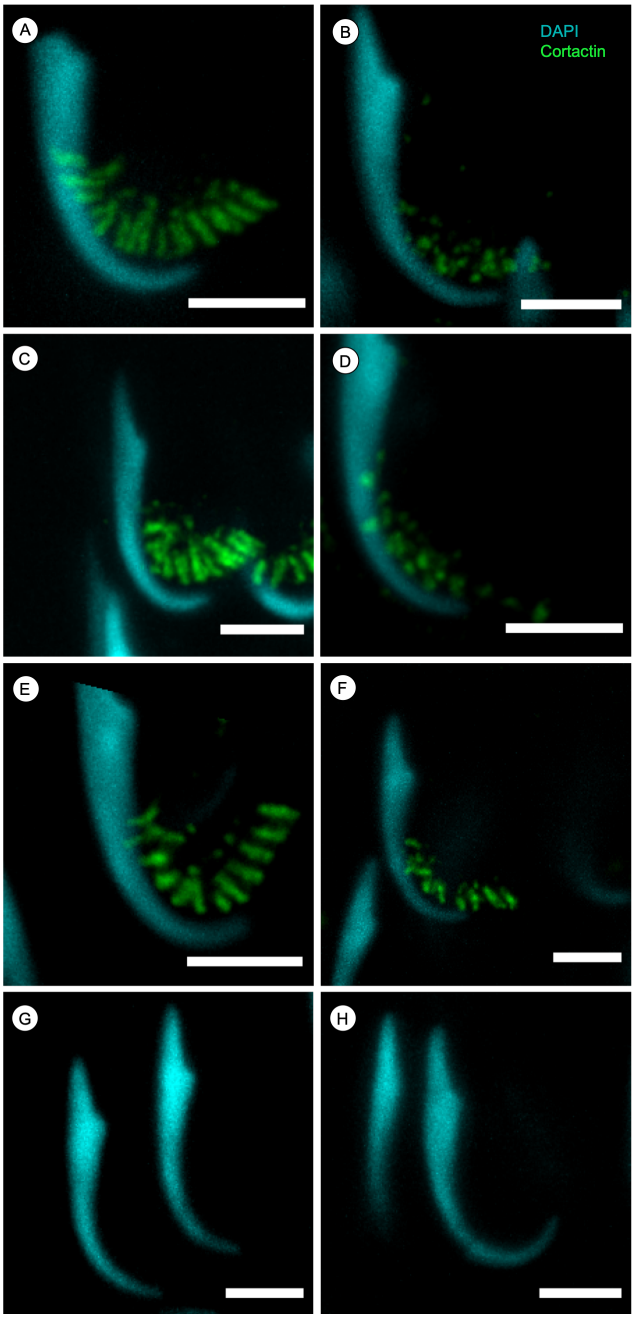

Figure 4.7 Immunofluorescence of stage VII spermatids 48 h post intratesticular injection with maximum concentration of Accell siRNA.
Tissue sections were labeled with cortactin (green) and DAPI (blue) after 48 h of injecting testis with 0.45 µg/µl of Accell siRNA. Experimental testes were injected with Accell Cttn siRNA and control testes were injected with Accell non-targeting siRNA. Cortactin staining outlines tubulobulbar complexes and was lower in experimental testis (B, D, F) compared to control (A, C, E) testis. (G) shows NRIgG control for cortactin staining and (H) shows secondary antibody control. All figures are maximum intensity projections of Z-stacks. For (A – H), Bars = 4 µm.

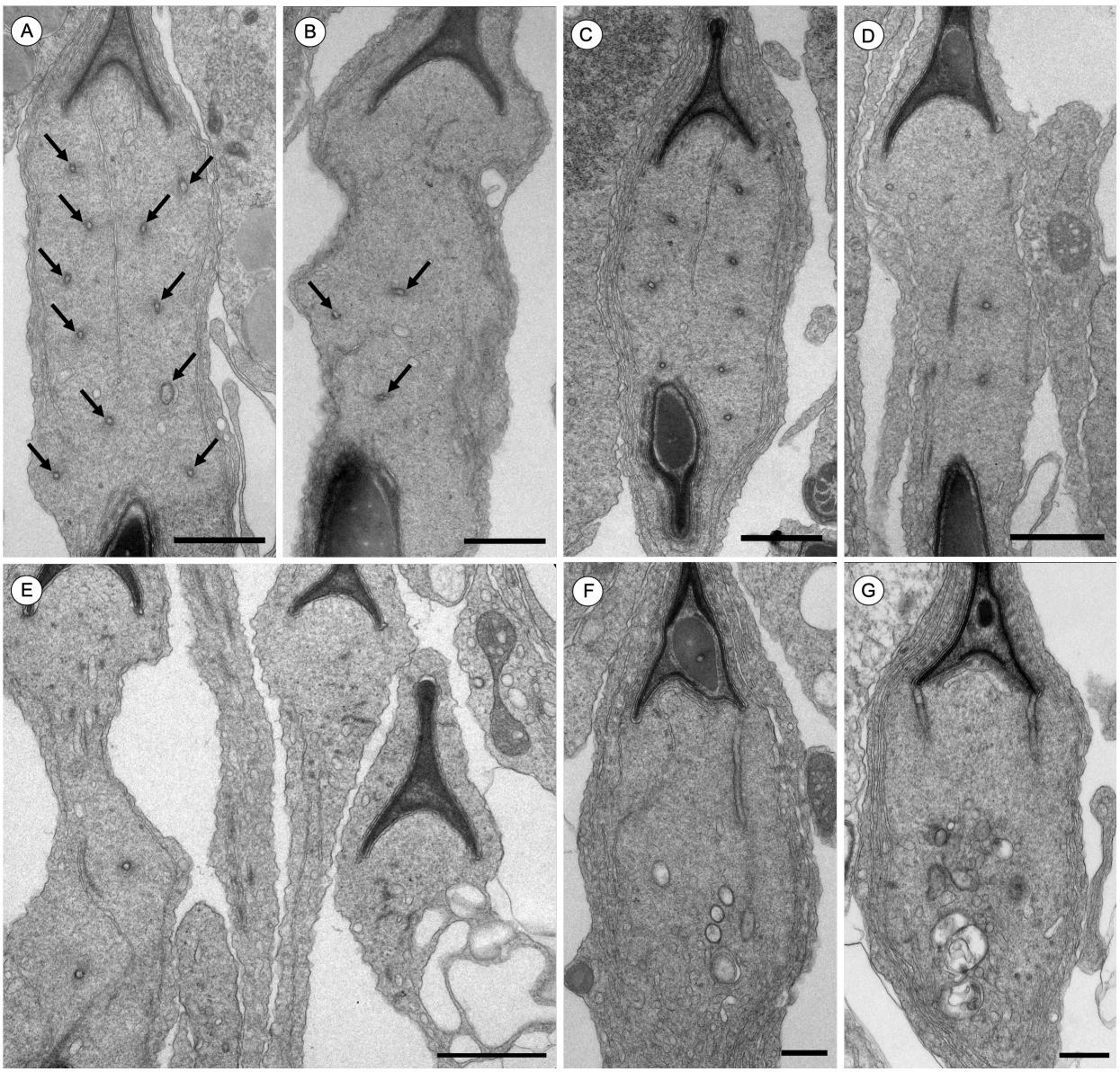

Figure 4.8 Sections of apical tubulobulbar complexes at stage VII of spermatogenesis in control and Accell siRNA treated testes.
(A – D) show cross-sections through apical Sertoli cell lobules. Fewer profiles of proximal tubular regions of tubulobulbar complexes (TBCs) were present in experimental (B, D) tissue compared to control (A, C). Apical processes in some regions appeared abnormally narrow in experimental tissue (E) compared to control (A, C). Longitudinal sections of TBCs show shorter proximal tubular regions in experimental (G) versus control (F) tissue. For (A – E), Bars = 1 μm, and for (F, G), Bars = 500 nm.

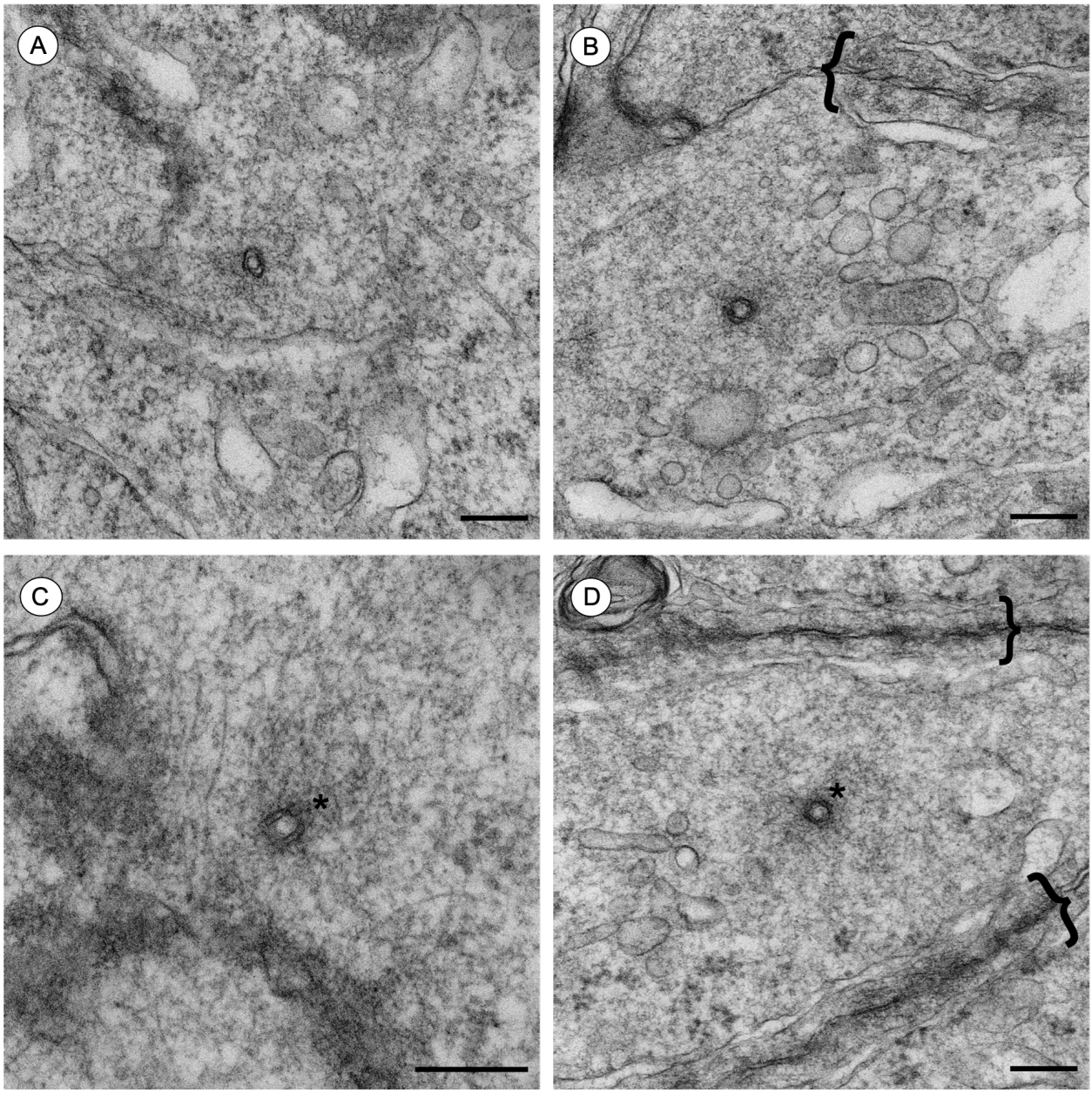

Figure 4.9 Cross sections of basal tubulobulbar complexes at stages III-V in control and cortactin Accell siRNA-treated testes.
(A – D) show cross-sections of proximal tubular regions surrounded by a network of actin filaments (asterisks in C, D) close to ectoplasmic specializations (brackets) in both siRNA-treated (B, D) and un-treated tissue (A, C). Bars = 200 nm.

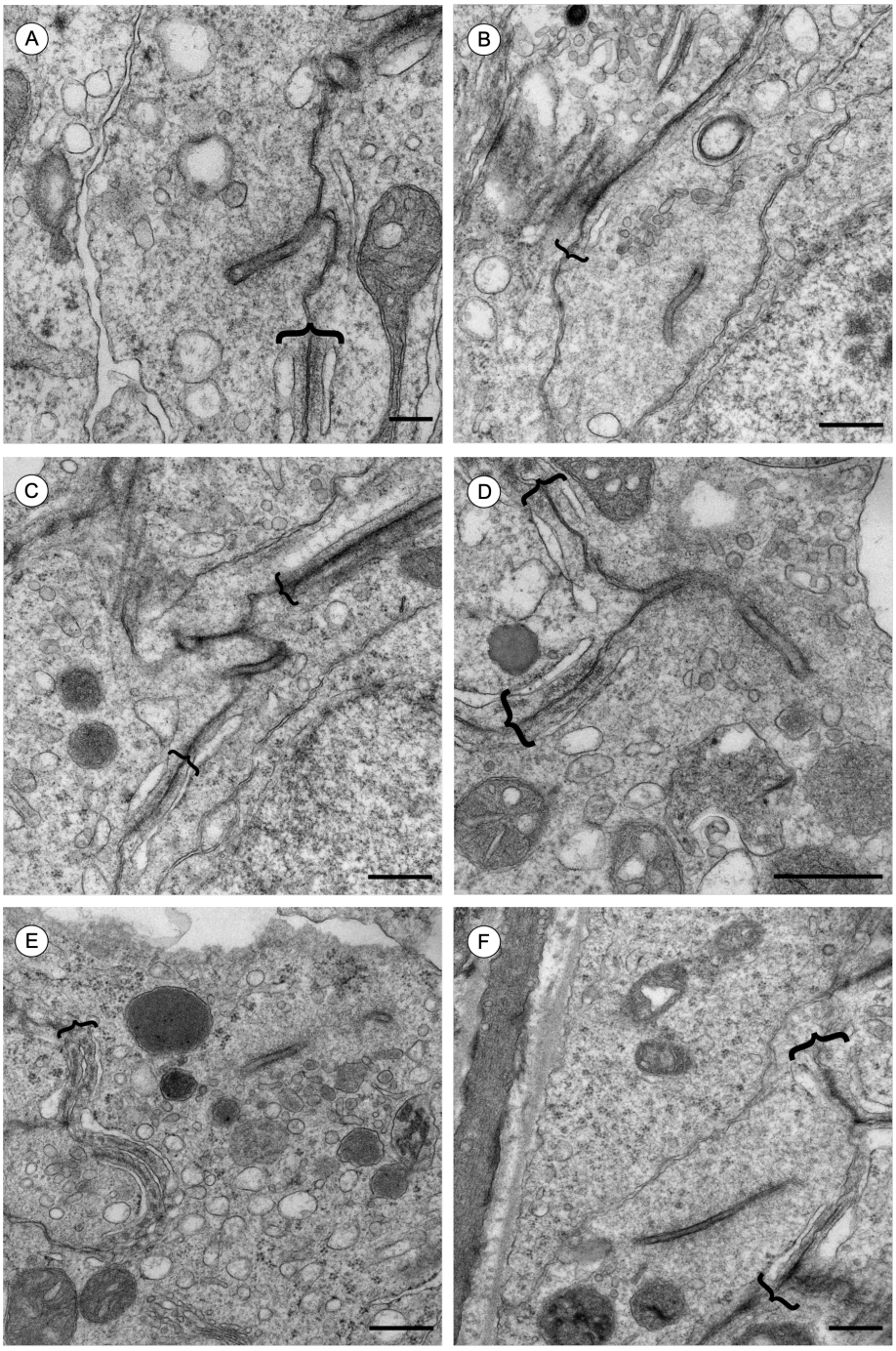

Figure 4.10 Proximal regions of basal tubulobulbar complexes at stages III-V in Accell siRNA-treated and untreated testes.
(A - F) shows the presence of proximal tubular regions of basal tubulobulbar complexes close to ectoplasmic specializations (brackets) in control (A, C) and experimental (B, D, E, F) tissue. Some of the proximal tubular regions were unusually long in experimental tissue (F). For (A), Bar = 200, and for (B – F), Bars = 500 nm.

Table 4.1 siRNA duplexes used for RNAi experiment

Gene	Product	Catalog number	Target sequences
Rat Cttn	ON-TARGETplus SMARTpool Cttn siRNA	L-080141-02-0020	CCGAGAGAGCUCAGCGGAU CGGAUGGACAAGAACGCAU AUACACAAGCUUCGAGAGA CAUCAGAGCCUGUUUACGA
Non-targeting	ON-TARGETplus Non-targeting pool	D-001810-10-20	UGGUUUACAUGUCGACUAA UGGUUUACAUGUUGUGUGA UGGUUUACAUGUUUUCUGA UGGUUUACAUGUUUUCCUA
Rat Cttn	Accell SMARTpool Cttn siRNA	E-080141-00-0020	CAAUUAUAGUCAGUUGAUA UGCGUGUGUUGAAUUGGUU GGUUGGGUUUUCUAUAUGA CCAGCAUCCUUGAUCAACU
Non-targeting	Accell Non-targeting control pool	D-001910-10-50	UGGUUUACAUGUCGACUAA UGGUUUACAUGUUUUCUGA UGGUUUACAUGUUUUCCUA UGGUUUACAUGUUGUGUGA

Chapter 5: Actin disruption results in altered morphology of basal tubulobulbar complexes in rat seminiferous epithelium

5.1 Background

Junction remodeling during spermatogenesis at both basal and apical sites of the seminiferous epithelium involves unique structures called tubulobulbar complexes (TBCs)[36,42,57,58,61,77]. TBCs are proposed to be subcellular machines that internalize intact intercellular junctions during spermatocyte translocation and release of mature spermatids[58,59,77]. These structures consist of elongate tubular extensions that project from a Sertoli cell or a spermatid into corresponding invaginations of a neighbouring Sertoli cell[62]. TBCs have three distinct regions: a proximal tubule, a bulb, and a distal tubule that is capped with a clathrin-coated pit. The tubular region is cuffed by a three-dimensional network of actin-filaments[38,66,169], which in turn is surrounded by a cytoskeletal shell consisting of spectrin and plectin[64,72]. The bulb region lacks an actin cuff but is closely associated with cisternae of endoplasmic reticulum. The bulb eventually buds off the complex, enters endocytic compartments of the Sertoli cell, and is degraded[62,66]. TBCs share morphological and molecular similarities with clathrin-mediated endocytic structures generally present in cells[80]. Except for the presence of double-membrane cores and bulbs, TBCs closely resemble clathrin-coated pits with extremely long necks.

A growing body of evidence supports the fact that TBCs that form at apical sites internalize intercellular junctions between mature spermatids and Sertoli cells[36,42,61] and that their proper functioning is critical for normal spermiation[69,73,79]. Although basal TBCs also internalize intercellular junctions[57,62] and have been suggested to play a role in spermatocyte translocation[57], they have been much less studied than apical TBCs for a number of reasons. It is difficult to predict exactly where basal TBCs occur at basal junction complexes, and often the

actin cuffs of the structures cannot be clearly distinguished from actin bundles associated with the junctions when using fluorescence microscopy. In addition, and unlike apical clusters of TBCs, basal TBCs cannot be isolated and fragmented away from the seminiferous epithelium for visualization.

Actin filament networks are a significant component of TBCs. Knocking down cortactin, a key regulator of cytoskeletal remodeling and membrane dynamics in other systems[170], results in shorter TBCs[79]. Previous research has shown that when the actin filament–disruptor cytochalasin D is injected into the testis, the tubular and bulbous regions of the complex are absent and typical TBCs do not occur[78]. Disruption of actin networks at apical TBCs with cytochalasin D, using an *ex vivo* perfusion approach, resulted in short, swollen tubular regions and abnormally shaped TBCs with ectopic bulbs[68]. Apical TBCs associated with spermatids were associated with lower levels of actin and patchy actin networks.[68,78] These results suggested that actin is involved in the formation, elongation, and maintenance of the tubular regions of the complex. Furthermore, a new model of TBC formation and vesiculation was proposed in which the disassembly of the actin cuff results in formation and enlargement of the bulb that eventually separates from the complex at a single scission site[68].

This study revisited perturbing actin filament networks in testes using the same *ex vivo* perfusion technique to administer cytochalasin D in order to determine if the effects observed at apical TBCs also occur at basal TBCs. Specifically, the aim of this study was to explore the effects of actin network perturbation on the morphology of basal TBCs. As predicted, treatment with cytochalasin D resulted in basal tubulobulbar complexes with swollen tubular regions and patchy actin networks. The results are consistent with the conclusion that basal and apical tubulobulbar complexes respond in a similar way to actin disruption and that actin networks are necessary for maintaining the normal architecture of the structures. In addition, the results

suggested that the mechanism of bulb formation, enlargement and scission are similar at the two sites.

5.2 Materials and Methods

5.2.1 Animals

The animals used in this study were reproductively active male Sprague Dawley rats, obtained from Charles River Laboratories (Sherbrooke, QC, Canada). The animals were maintained according to the guidelines established by the Canadian Council on Animal Care. They were housed in OptiRAT cages, had *ad libitum* access to food (Teklad global protein 18% - diet 2918) and water, and were maintained in a 12/12 light cycle with lights on at 0700 h and off at 1900 h. All the protocols used in this study were approved by the Animal Care Committee of the University of British Columbia.

5.2.2 Reagents

Unless otherwise indicated, all the reagents were obtained from Millipore Sigma (Oakville, ON, Canada).

5.2.3 *Ex-vivo* drug perfusion of the whole testis

The perfusion protocol used in this study was similar to that published previously[68,171].

Rats were deeply anesthetized using isoflurane inhalation. The testes were removed, and the spermatic arteries were cannulised using 27-gauge syringe needles attached to three-way valves. The valves received inputs from the perfusion buffer containing drug or vehicle and fixative. When possible, both testes from the same animal were cannulised, one for treatment

and one for control. Following removal of the testes, animals were euthanized while under deep anesthesia by opening the thorax and cutting the heart.

The perfusion buffer was comprised of modified Krebs-Henseleit buffer (11 mM D-glucose, 1.2 mM $MgSO_4$, 1.2 mM KH_2PO_4, 4.7 mM KCl, 120 mM NaCl, 0.63 mM $CaCl_2$, 6.2 mM $NaHCO_3$, 4% bovine serum albumin (BSA), pH 7.3) containing either 40 µM of cytochalasin D or dimethyl sulfoxide (DMSO) as a vehicle control. We maintained the perfusion buffers at 33°C and aerated them with 5% CO_2 in O_2. The testes were perfused with the treatment or control buffer using a two-channel peristaltic pump set to deliver 1 ml/min for 1 h followed by 30 min perfusion with a fixative solution (1.5% paraformaldehyde, 1.5% glutaraldehyde (Electron Microscopy Sciences, Hatfield, PA, USA), 0.1M sodium cacodylate (Electron Microscopy Sciences), pH 7.3).

5.2.4 Electron microscopy

After the 30 min perfusion-fix, the testes were cut into small pieces and placed into fresh fixative solution for 2 h. Following this, tissue was washed three times for 10 min each with 0.1 M sodium cacodylate at pH 7.3. The tissue was then fixed with 1% osmium tetroxide (Electron Microscopy Sciences) in 0.1 M sodium cacodylate for 1 h on ice. After osmium fixation, the tissue was washed another three times for 10 min each with ddH_2O and then stained for 1 h with 1% aqueous uranyl acetate solution (Canemco-Marivac Inc., Canton De Gore (Lakefield), QC, Canada). The tissue was washed another three times with ddH_2O and dehydrated in a series of ascending concentrations of ethanol (30%, 50%, 70%, 95%, 100%) for 10 min, each with an additional two washes in 100% ethanol. This was followed by two 30 min washes with 100% propylene oxide, and then the tissue was placed in a solution of 50% propylene oxide and EMbed-812 (Electron Microscopy Sciences) overnight. The following day, the tissue was placed

into 100% EMbed-812 for 1 h and replaced with fresh EMbed-812 for another hour. Finally, the tissue was embedded in fresh EMbed-812 and allowed to polymerize for 48 h at 60°C.

Thin sections were stained with saturated uranyl acetate in 75% methanol for 4 min, followed by lead citrate for another 4 min. The stained sections were then imaged using a Tecnai G2 Spirit electron microscope (FEI™ North America NanoPort, Hillsboro, Oregon, USA), operated at 120 kV.

5.2.5 Quantification of tubular region diameters

Electron micrographs of tubular regions of TBCs in either longitudinal or cross-sections were used to measure the diameters. Most micrographs used for quantification were imaged at 68,000X magnification on the microscope. The diameters of the tubular regions were measured using ImageJ software[126] version 1.48. Significant differences between the diameters of the tubular regions from control and drug-treated tissues were evaluated using a two-tailed, unpaired t-test with Welch's correction. Statistical analysis was carried out using the software Prism 6 by GraphPad version 6.0b.

Qualitative observations were based on a total of 34 control basal TBCs and 27 drug-treated TBCs. From these, a total of 23 control and 24 drug-treated basal TBCs were used for quantification of tubular region diameters. TBCs for quantification were chosen on the basis of an identifiable tubular region with clearly visible plasma membrane.

5.3 Results

5.3.1 Cytochalasin D disrupts actin cuffs at basal tubulobulbar complexes

The overall seminiferous epithelial architecture appeared normal in cytochalasin D – treated tissue, however major effects on TBCs were observed.

At the ultrastructural level, the actin cuffs associated with tubular regions of basal TBCs appeared disrupted in drug-treated tissues. In control tissues, the actin cuffs appeared as uniform filament networks or halos surrounding the tubular membrane cores and were less dense in the periphery (Fig. 5.1, A, B). In drug-treated tissues, the actin in cuffs appeared patchy. Often these patches or actin foci were found in regions distant from the complexes (Fig. 5.1, C - F).

5.3.2 Actin disruption results in swollen tubular regions and abnormal bulbs

In drug-treated tissues, the tubular regions of complexes appeared swollen or larger (Fig. 5.2, F - J) relative to controls (Fig. 5.2, A - E) in longitudinal sections of TBCs. In cross-sections of control tissues, the proximal tubular regions appeared uniform in diameter. When the diameters of the proximal tubular regions were measured, the differences between diameters in drug-treated and control testes (Fig. 5.3, A, B) were statistically significant in each of the animals. The diameters of the tubules were enlarged in drug-treated tissues.

In addition to swollen tubular regions, abnormal and malformed bulbs were also present in cytochalasin D-treated material. In control tissues, the bulbar region of basal TBCs were in close contact with cisternae of endoplasmic reticulum (ER) (Fig. 5.4, A, B), whereas in cytochalasin D-treated tissues, the plasma membrane of TBCs appeared branched and the cisternae of ER were not as tightly opposed to the bulbs (Fig. 5.4, C, D).

5.4 Discussion

To date, there have only been a few studies on basal TBCs[4,57,62] and the structures have mostly been ignored due to the difficulties associated with studying them. Apical TBCs are much easier to study because they are consistently clustered at specific locations around spermatid heads, and the spermatid heads together with associated regions of the Sertoli cell containing

the TBCs can be easily isolated from the seminiferous epithelium for visualization at high resolution[36]. In comparison, the positions of basal TBCs cannot be accurately predicted as they often occur in pockets or folds in the junction complexes, making it difficult to distinguish them from the junction complexes themselves[57]. This is particularly problematic when fluorescence labeling of actin is used as a marker because actin filaments are a major component of ectoplasmic specializations (ESs) that are associated with the junctions[172]. As a result, much less is known about the function and general regulation of basal TBCs. In fact, many of the proposed specific functions attributed to TBCs generally are 'spermatid' centric[63,173,174] and do not account for the presence of TBCs at basal Sertoli/Sertoli junctions. In this study, it was demonstrated, as predicted, that basal TBCs react to the actin filament disrupting drug cytochalasin D in a similar way to apical ones. Cytochalasin D is a compound that interferes with actin-related processes by binding to the growing end of actin filaments, causing depolymerization[175].

At apical TBCs, *ex vivo* perfusion of testes with cytochalasin D results in patchy actin networks, increased diameters of tubular regions, and enlarged and branched bulbs[68]. This study demonstrated that basal TBCs react to actin disruption in a generally similar way; that is with patchy actin concentrated into foci, swollen tubular regions resulting in increased diameters, and the formation of abnormal bulbs. In fact, the increases in diameter of tubular regions at apical and basal regions are of the same order of magnitude [apical 1.6-fold increase[68], basal 1.7-fold increase] when exposed to 40 μM of cytochalasin D. Cytochalasin D significantly altered but did not completely eliminate the actin network surrounding TBCs or at ESs at basal junctions in the seminiferous epithelium. These results were consistent with the conclusion that a normal actin network is necessary for maintaining the structural integrity of tubulobulbar complexes, both at apical and basal sites.

The observation that actin disruption has similar effects at apical and basal TBCs is not unexpected since both have similar architecture. Also, the results are consistent with the hypothesis that both structures have similar functions; that is, TBCs generally are modified clathrin-based endocytosis structures that internalize intercellular junctions. TBCs begin as coated pits that project into Sertoli cells at sites of intercellular attachment in the mammalian seminiferous epithelium. As the pits mature, the plasma membrane of the two cells remain attached and the necks continue to elongate, forming double-membrane tubes, each surrounded by a cuff of actin filaments. These complexes can extend up to 2-3 μm in Sertoli cells in rats[62]. As TBCs mature, bulbs develop near the end of the complexes. Eventually, these bulbs bud off and are degraded by Sertoli cells as part of the junction remodeling process that occurs before translocation of spermatocytes through basal junction complexes at the base of the epithelium, and preceding spermiation at the apex[58].

Based on the observations of actin disruption with cytochalasin D in two previous studies[68,77], a model was proposed for the formation of the bulb and internalization of apical TBCs by the Sertoli cell[68]. The results obtained in this study indicate that this model applies to basal TBCs as well (Fig. 5.5). The model suggests that the actin cuffs surrounding TBCs are actively involved in the formation and maintenance of the narrow diameters of the tubular regions. The focal and progressive disassembly of the actin networks results in the formation and enlargement of the bulbs. The observation that tubular regions expand after cytochalasin D treatment is consistent with the proposal that actin network disassembly is involved with bulb formation and elongation, both at apical and basal TBCs. As bulbs enlarge along proximal tubules, the latter are reduced to small ‘necks’ that remains at the sites where the TBCs originate from the intercellular junctions, and the coated pits at the distal ends of TBCs are resolved into the bulb as well. Eventually, a single scission occurs at the neck, resulting in the bulbs getting internalized into the Sertoli cells and entering endocytic compartments. This model

(Fig. 5.5) differs from the original TBC internalization model that suggests that there are multiple scission sites along the length of each TBC[62,66,74]. The bulb buds off of the complexes and the remaining tubular regions and coated pits undergo scission at multiple sites, forming numerous double-membrane vesicles. In clathrin-mediated endocytosis, an intact actin network participates in constricting necks of forming vesicles and scission of vesicles from the plasma membrane[176,177]. TBCs in the seminiferous epithelium are similar in morphology and molecular composition to elements of the clathrin-mediated endocytosis pathway present in cells, indicating that these structures likely evolved from this basic system.

This study demonstrated that actin disruption at basal TBCs results in similar phenotypic changes that have previously been observed at apical sites[68]. This is consistent with the conclusion that the function of actin networks at both locations is similar.

5.5 Chapter 5 Figures

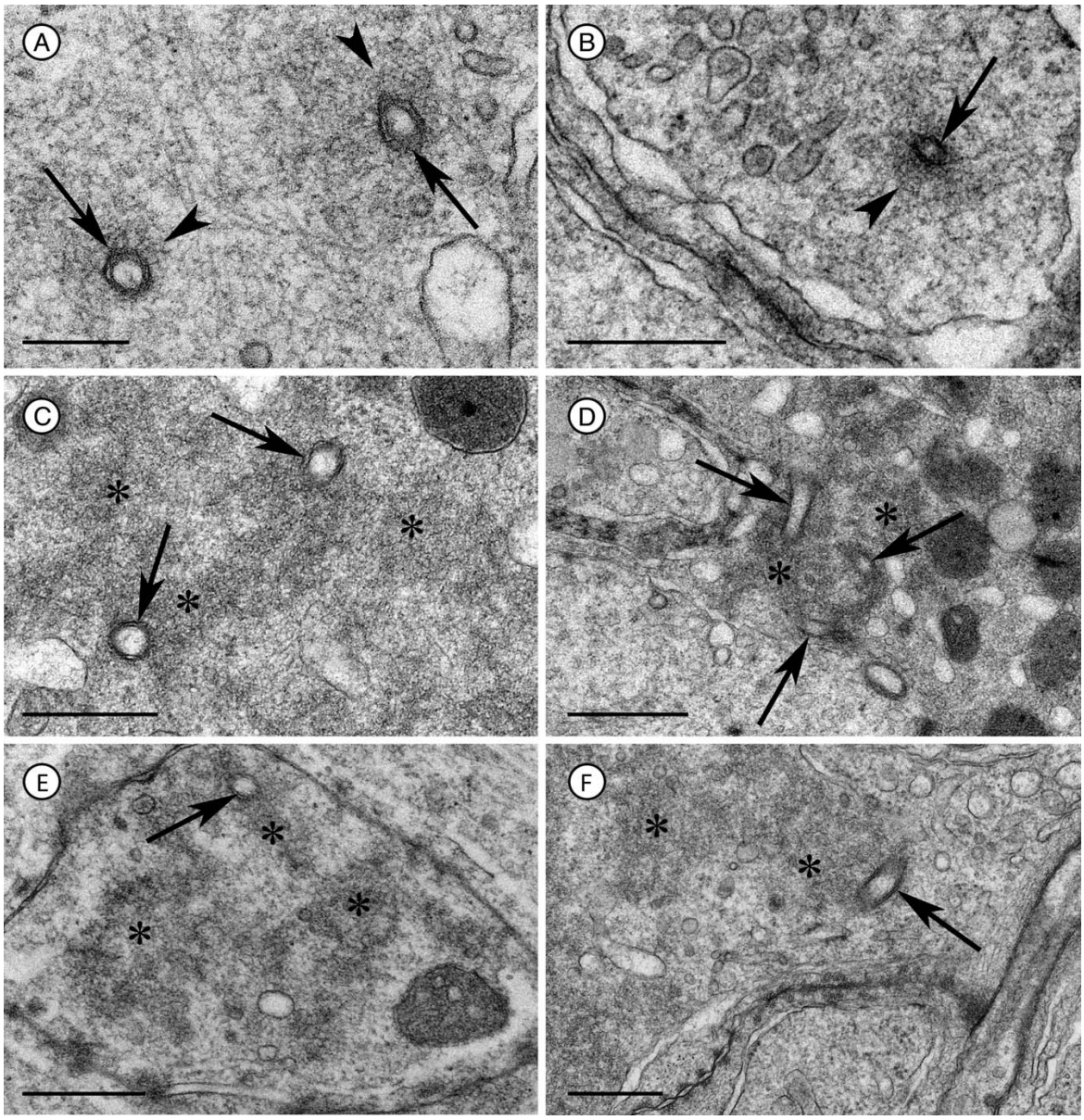

Figure 5.1 Actin networks at basal tubulobulbar complexes in vehicle control and drug-treated testes.
Electron micrographs of controls (A, B) showing the actin networks (arrowheads) surrounding the tubular regions of basal tubulobulbar complexes (TBCs) (arrows). In drug-treated tissue, the actin networks at the tubular regions are disrupted (C - F) and appear patchy. The actin patches, or foci, in drug-treated tissue are found in regions adjacent to the tubular regions of TBCs (arrows) as well as in regions distant from TBCs (C - F asterisks). For (A), Bar = 200 nm, for (B, C), Bars = 500 nm, for (D), Bar = 1 μm, and for (E, F), Bars = 500 nm. Figure 5.1 from © Sriram *et al.* (2016)[178]. Actin Disruption Results in Altered Morphology of Basal Tubulobulbar Complexes in Rat Seminiferous Epithelium. The Anatomical Record, 299(10) 1449-1455. Page 1452. Adapted with permission from publisher.

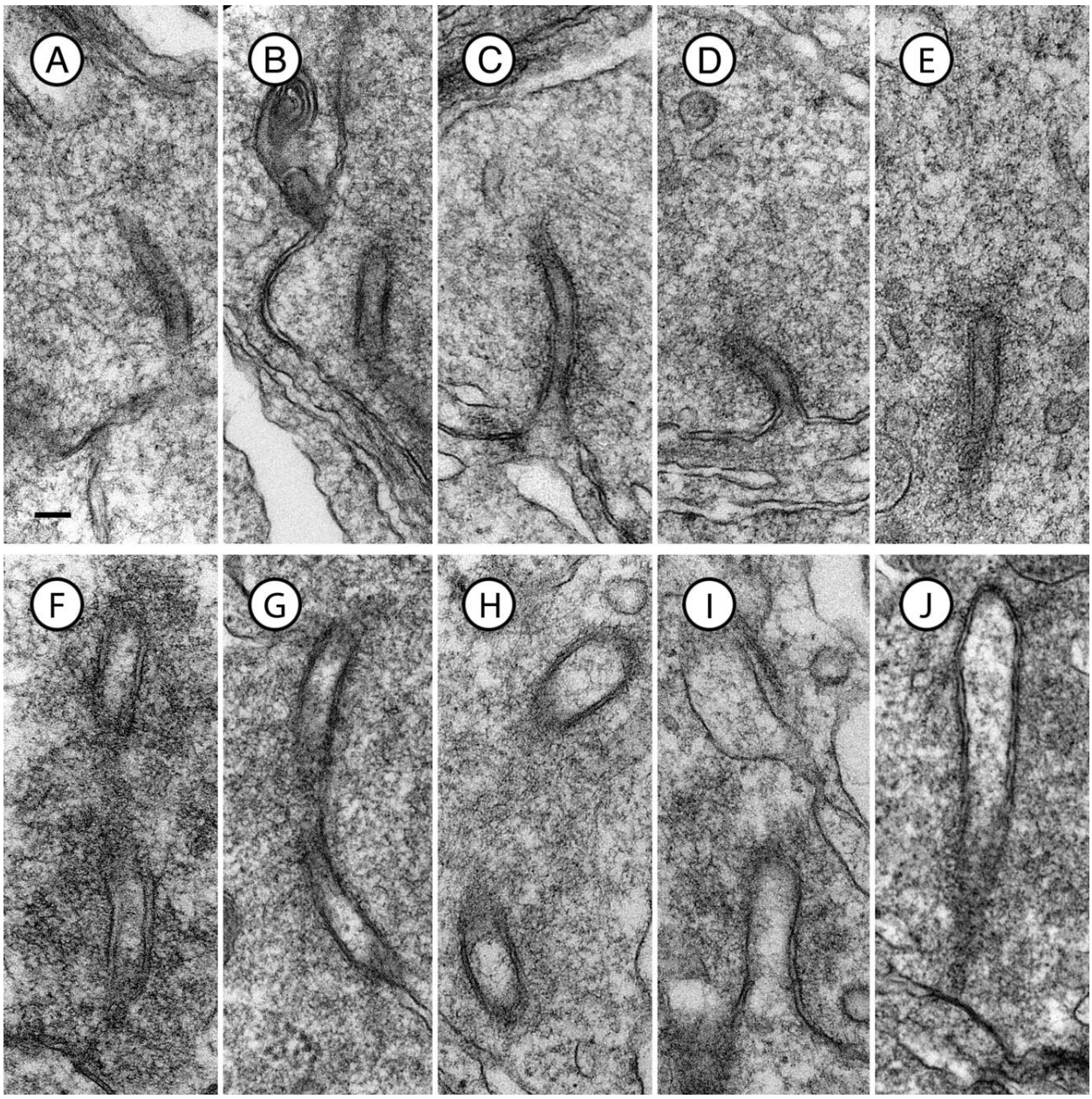

Figure 5.2 Tubular regions of basal tubulobulbar complexes are swollen in drug-treated testes.
Electron micrographs of basal tubulobulbar complexes (TBCs) in vehicle control testes appeared narrow and uniform in diameter (A - E). Basal TBCs in drug-treated testes (F - J) appeared swollen and larger in diameter compared to controls. Bar = 100 nm. All micrographs are at the same magnification. Figure 5.2 from © Sriram *et al.* (2016)[178]. Actin Disruption Results in Altered Morphology of Basal Tubulobulbar Complexes in Rat Seminiferous Epithelium. The Anatomical Record, 299(10) 1449-1455. Page 1453. Adapted with permission from publisher.

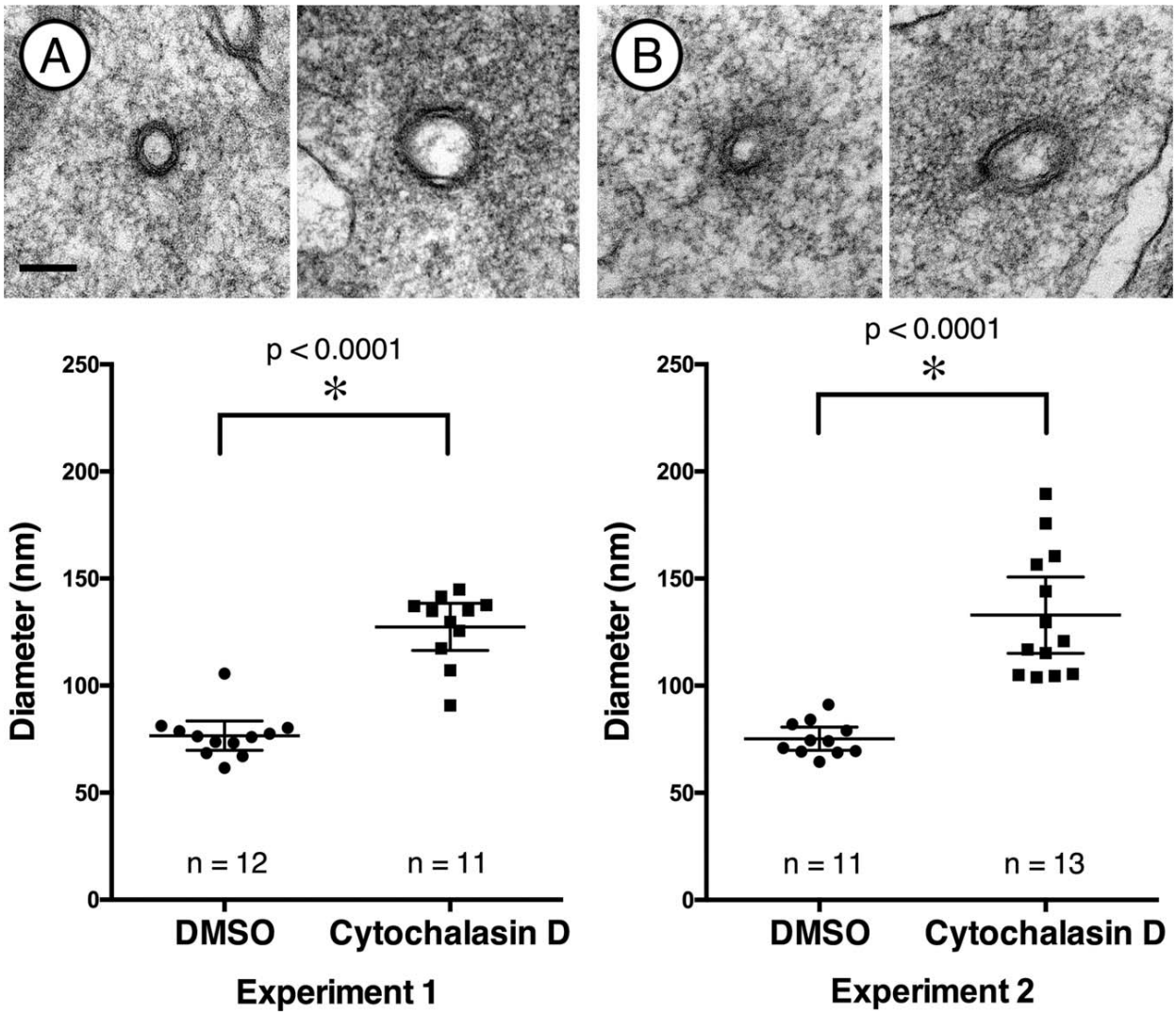

Figure 5.3 Diameters of the tubular regions of basal tubulobulbar complexes are larger in drug-treated testes.
The diameters of tubular regions from vehicle control (DMSO) and drug-treated testes were measured in two independent experiments (A and B). All individual data points are shown on scatter plots along with the mean and 95% confidence intervals. In each experiment, there was a significant difference between the tubular region diameters of control and drug-treated testes. Representative electron micrographs of the tubular regions from control and drug-treated tissues are shown for each experiment. Bar = 100 nm. All micrographs are at the same magnification. Figure 5.3 from © Sriram *et al.* (2016)[178]. Actin Disruption Results in Altered Morphology of Basal Tubulobulbar Complexes in Rat Seminiferous Epithelium. The Anatomical Record, 299(10) 1449-1455. Page 1454. Adapted with permission from publisher.

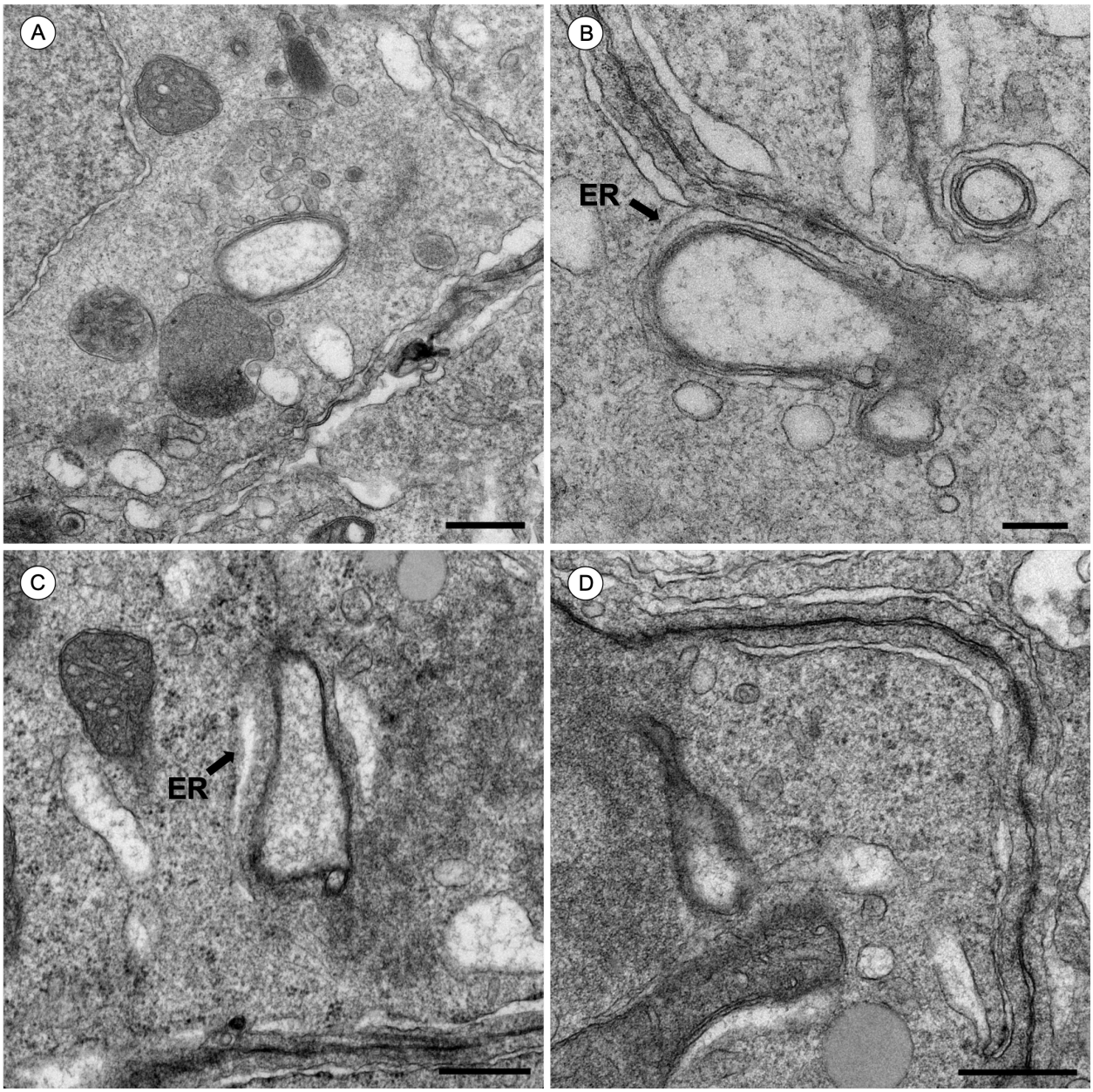

Figure 5.4 Abnormal bulbar regions occur in basal tubulobulbar complexes in drug-treated testes.
Normal basal tubulobulbar complexes (TBCs) from control epithelia are shown in (A, B). The bulb regions of normal TBCs are closely associated with a cisterna of endoplasmic reticulum (ER) and the two plasma membranes that make the structure of TBCs are tightly apposed (A, B). In drug-treated tissue, the bulb regions of TBCs appear abnormal (C, D). The plasma membrane of TBCs from drug-treated tissue branches abnormally (D) and the cisternae of ER is not as clearly opposed to the bulbs (C). For (A, C, D), Bars = 500 nm, and for (B), Bar = 200 nm.

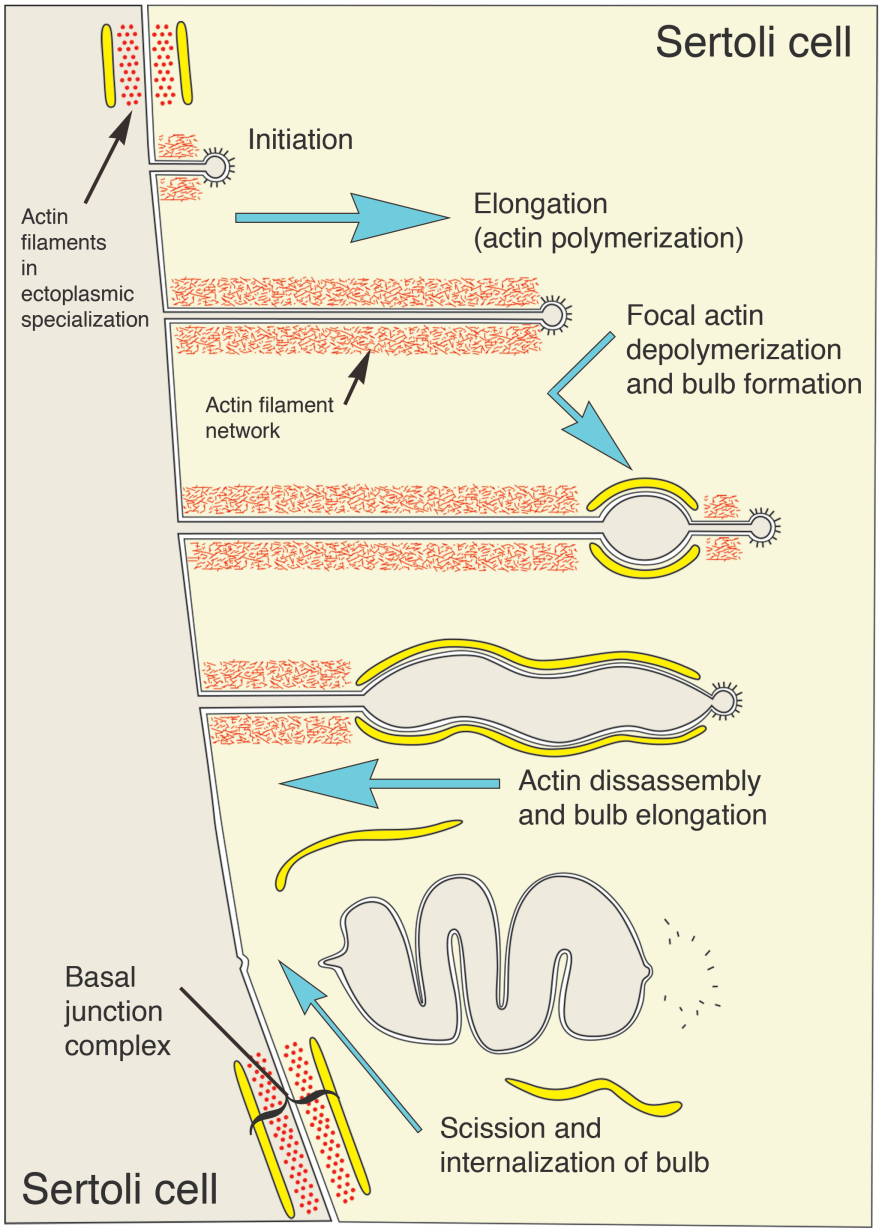

Figure 5.5 Model of basal tubulobulbar complex internalization.
Basal tubulobulbar complexes initially form as coated pits at basal junction complexes. Actin filaments in the Sertoli cell polymerize to elongate the complex. Actin filaments begin to depolymerize near the distal end of the complex resulting in a swelling that forms a bulb. As the actin filaments progressively depolymerize, the bulb elongates to incorporate the coated-pit as well as the tubular regions. Scission occurs at the base of the complex resulting in the internalization of the bulb into the endocytic compartments of the Sertoli cell. Figure 5.5 from © Sriram *et al.* (2016)[178]. Actin Disruption Results in Altered Morphology of Basal Tubulobulbar Complexes in Rat Seminiferous Epithelium. The Anatomical Record, 299(10) 1449-1455. Page 1455. Adapted with permission from publisher.

Chapter 6: Conclusion

6.1 Overview of results and conclusion

Tubulobulbar complexes (TBCs) are actin-related endocytic structures that form at ectoplasmic specializations (ESs) and are responsible for internalizing intact junctions during sperm release at the apex and during the translocation of spermatocytes from basal to adluminal compartments of the seminiferous epithelium. To date, the link between TBC formation and sperm release at apical sites has been well documented[69,73,79]. In comparison, due to the difficulties associated with studying basal TBCs, the link between basal TBC function and spermatocyte translocation through basal junctions has not yet been established. This thesis explored the role of basal TBCs in the internalization of basal junction complexes.

An improved morphologically differentiated primary Sertoli cell culture system was successfully established using 20-day-old rats and was optimized to form polarized monolayers with nuclei and junctions located basally. The presence of well-developed ESs and tight junctions as part of the basal junction complexes indicated Sertoli cell differentiation *in vitro*. TBCs at early stages of development were observed at basal junctions in these primary Sertoli cell cultures, similar to what has been previously reported[57]. Also, it was demonstrated that when the age of rats used for isolating Sertoli cells is older than 20 days, the cells respond much differently to the same culture conditions than cells from younger animals. Sertoli cells isolated from 30-day-old rats resulted in the formation of cord-like structures surrounded by remodeled Matrigel (three-dimensional (3D) culture system). Sertoli cells within the cords were columnar, polarized and basal junctions at the base of the cords functionally compartmentalized the cords into apical and basal compartments. The two-dimensional (2D) culture system, which was established using 20-day-old rats, was used for co-culturing with germ cells and studying

basal junction turnover *in vitro* as it provided easy access to the apical and basal environments for experimental manipulation.

A primary Sertoli-germ cell co-culture system was developed to determine if the presence of spermatogenic cells, in this case spermatogonia, influences the structure or development of TBCs at basal junctions between Sertoli cells. The data in this thesis provides the first evidence that the presence of spermatogenic cells in primary Sertoli cell cultures results in the formation of mature TBCs with bulbar regions, which is not seen in TBCs present in cultures without germ cells[57]. The basal TBCs that develop in Sertoli-germ cell co-cultures more closely resemble their *in vivo* counterparts. This finding adds a new dimension to our understanding of basal junction remodeling as it relates to spermatocyte translocation. With further modifications that include co-culturing with other cell types found in the seminiferous epithelium, this *in vitro* Sertoli-germ cell co-culture system could serve as a valuable model for studying junction remodeling in the future.

In vivo ribonucleic acid interference (RNAi) testicular injections were conducted on Sprague Dawley rats to perturb TBCs by knocking down cortactin, ultimately to test the prediction that impaired TBC structure would prevent junction internalization at basal sites and delay spermatocyte translocation. In this thesis, results are presented of attempts to optimize an *in vivo* RNAi procedure to achieve long term silencing of cortactin in rats and determine if knockdown of cortactin interferes with the morphology or formation of basal TBCs. A rebound of cortactin expression was consistently observed by immunoblotting despite multiple injections over a nine-day period. A slight knockdown of cortactin was only achieved on blots 48 h post small interfering ribonucleic acid (siRNA) treatment though this was not consistent over the course of trials. This knockdown was correlated with shorter TBCs in apical regions of the seminiferous epithelium, confirming earlier findings[79]. However, at basal sites, significant differences in TBC morphology could not be detected. This may be due to the fact that

compared to apical TBCs, basal TBCs are not clustered at predictable locations in the seminiferous epithelium, making it difficult to visualize large numbers of TBCs in basal regions for comparative purposes. The prediction that spermatocyte translocation across the blood-testis barrier (BTB) would be delayed due to the perturbation of basal TBCs has yet to be verified experimentally. The results presented in this thesis serve as a precursor for future research to establish the link between basal TBC function and spermatocyte translocation.

The effects of actin network perturbation on the morphology of basal TBCs in the seminiferous epithelium was also explored. Compared to control, the actin cuffs around basal TBCs in cytochalasin D-treated testes appeared patchy and less obvious. In addition, abnormal bulbs were observed, and the tubular regions of the complexes appeared swollen with an increase in diameter. These results suggest that intact networks of actin filaments are required for maintaining the structural integrity of both apical[68] and basal TBCs[178] and that the actin networks have similar functions in the seminiferous epithelium. Furthermore, these results also indicate that the model for the formation of the bulb and internalization of TBCs is similar at both apical[68] and basal sites of the seminiferous epithelium[178].

In conclusion, the results obtained from the *in vitro* and *in vivo* studies are generally consistent with the hypothesis that basal TBCs that form in areas of contact between Sertoli cells in basal regions of the seminiferous epithelium are involved with the internalization of junctions during junction turnover and function similarly to apical TBCs.

6.2 Limitations and future directions

The *in vitro* primary Sertoli cell culture studies led to the discovery that Sertoli cells isolated from mature animals (30-day-old rats) formed cord-like structures with a highly polarized and differentiated phenotype *in vitro*. However, the cords in this culture system were atypical as they were devoid of germ cells and failed to form a central lumen even with time in culture. In the

future, further development of cords in this culture system would be possible by co-culturing with other testicular cell types (germ cells, peritubular myoid cells or Leydig cells). To more accurately represent the *in vivo* condition, Sertoli cells isolated from 30-day-old rats could be cultured along with the endogenous contaminating germ cells and not be exposed to a hypotonic wash to remove germ cells. These cultures could then be evaluated for their ability to form cords and support germ cell growth and later stages of differentiation.

The data presented in this thesis lay the foundation for testing the hypothesis that basal TBCs are necessary for the normal turnover of the BTB. First, an *in vitro* Sertoli-germ cell co-culture system was developed to recreate the complex Sertoli-germ cell organization and study basal junction turnover. One of the major limitations of this culture system was the lack of viability of germ cells. Germ cell death in co-cultures may be avoided by reducing exposure to trypsin during the germ cell isolation procedure. Surface components on germ cells are involved in recognizing and binding to Sertoli cells *in vitro*[137,179]. It has been shown that proteolytic digestion of germ cells by trypsin inhibits the ability of spermatogenic cells to adhere to Sertoli cell monolayers[179]. Exposure to high concentrations of trypsin for prolonged periods can damage cell membranes and result in cell death. An alternative approach to enzymatic digestion may be a more mechanical isolation technique.

In this thesis, only a qualitative approach was employed to compare the morphology of basal TBCs in Sertoli-germ cell co-cultures and Sertoli cell cultures without germ cells. In the future, to determine if TBCs are more prevalent after germ cell addition, the number of basal TBCs in these cultures may be compared by staining and probing for molecular components (cortactin or adaptor protein 2 (AP2)) or markers of early endosomes (ras-related protein Rab5 (Rab5) and early endosomal antigen 1 (EEA1)) that associate with TBCs[36,42,61].

Finally, this thesis discussed the optimization of an *in vivo* RNAi method to achieve long term silencing of cortactin. The main limitation of this method was that the knockdown results

obtained using immunoblotting were inconsistent and could not be correlated to phenotypic effects. In addition, the knockdown of cortactin could not be maintained for a period of nine days despite re-injecting the animals every three days. The duration of the RNAi depends on the turnover rate of the protein of interest. Messenger RNAs (mRNA) with high turnover rates are resistant to silencing by siRNAs. The instability of the siRNA together with the protein turnover rate *in vivo* may have impaired the ability to achieve protein knockdown even though a phenotypic effect could be observed in apical regions of the seminiferous epithelium. Since a slight knockdown was observed 48 h post Accell siRNA treatment, in the future, RNAi reagents could be injected every two days to sustain long-term silencing. Immunoblotting techniques in conjunction with quantitative polymerase chain reaction (qPCR) could be employed to confirm knockdown of the protein and mRNA. The testes can then be examined for delayed spermatocyte translocation by comparing the number of preleptotene or leptotene spermatocytes that move upwards away from the base of the epithelium at stages IX and X in toluidine blue stained plastic sections of perfusion fixed control and knockdown testes. In addition, cryosections of seminiferous epithelium could be labeled with phalloidin (to label actin filaments) or claudin-11 (to label tight junctions) and thresholding techniques (using ImageJ software) could be utilized to compare the number of basal junctions present at stage VII in control and knockdown testes[57]. If TBCs function to internalize junctions during spermatocyte translocation, then interfering with basal TBCs should result in more junctions present at stage VII and delayed spermatocyte translocation at stage IX or X. In these experiments, it will be necessary to develop techniques to evaluate TBCs at basal junctions in a way that will enable detecting any differences in TBC numbers and morphology between control and knocked down testes, so that any results can be correlated with changes in junctions and spermatocyte translocation.

6.3 Significance of work and contributions to the field

Results presented in this thesis are consistent with the hypothesis that basal TBCs are linked to basal junction turnover in the seminiferous epithelium. Significantly, this work has contributed to the first development of a new *in vitro* Sertoli-germ cell co-culture system that shows that the presence of germ cells affects the morphology of basal TBCs, which has not yet been established. Furthermore, this work has formed the foundation for doing crucial *in vivo* experiments to eventually link basal TBC function to the turnover of the BTB and spermatocyte translocation in the future. Moreover, the work on actin network perturbation provides evidence that the function of actin networks at apical and basal TBCs are similar, therefore they function similarly in the seminiferous epithelium.

A better understanding of the functional role of TBCs and the cellular processes underlying spermatogenic cell migration between Sertoli cells will further our understanding of the process of spermatogenesis generally in mammals. Also, it will add a new dimension of understanding to how intercellular junctions and the cytoskeleton function co-operatively to generate complex remodeling events in the seminiferous epithelium. It could lead to the identification and characterization of molecular targets (within TBCs) for the development of male contraceptives. Furthermore, this work has the potential to provide insight into the causes of certain forms of male infertility, which has a profound impact on human populations. Infertility affects approximately 15% of couples (48.5 million) worldwide and males are responsible for almost 50% of cases overall[180]. Studies have shown that the mean sperm count in healthy men has declined by 1% per year between 1938 and 1990[181]. Furthermore, sperm density has decreased globally by approximately 50% over the past 50-60 years[182]. Infertility is an alarming global health issue that requires further research to understand its prevalence and develop effective treatments.

Bibliography

1. França, L.R., Hess, R. A., Dufour, J.M., Hofmann, M.C. & Griswold, M.D. The Sertoli cell: one hundred fifty years of beauty and plasticity. *Andrology* **4**, 189–212 (2016).

2. Griswold, M.D. 50 years of spermatogenesis: Sertoli cells and their interactions with germ cells. *Biol. Reprod.* **99**, 87-100 (2018).

3. Griswold, M.D. Interactions between germ cells and Sertoli cells in the testis. *Biol. Reprod.* **52**, 211–216 (1995).

4. Russell, L.D. Observations on the inter-relationships of Sertoli cells at the level of the blood- testis barrier: evidence for formation and resorption of Sertoli-Sertoli tubulobulbar complexes during the spermatogenic cycle of the rat. *Am. J. Anat.* **155**, 259–79 (1979).

5. Dym, M. & Fawcett, D.W. The blood-testis barrier in the rat and the physiological compartmentation of the seminiferous epithelium. *Biol. Reprod.* **3**, 308–326 (1970).

6. Russell, L.D. Movement of spermatocytes from the basal to the adluminal compartment of the rat testis. *Am. J. Anat.* **148**, 313–328 (1977).

7. O'Donnell, L., Nicholls, P.K., O'Bryan, M.K., McLachlan, R.I. & Stanton, P.G. Spermiation. *Spermatogenesis* **1**, 14–35 (2011).

8. Liang, G.H. & Weber, C.R. Molecular aspects of tight junction barrier function. *Curr. Opin. Pharmacol.* **19,** 84–89 (2014).

9. Furuse, M., Hirase, T., Itoh, M., Nagafuchi, A., Yonemura, S., Tsukita, S., & Tsukita, S. Occludin: A novel integral membrane protein localizing at tight junctions. *J. Cell Biol.* **123**, 1777–1788 (1993).

10. Yokouchi, M. & Kubo, A. Maintenance of tight junction barrier integrity in cell turnover and skin diseases. *Exp. Dermatol.* **27**, 876–883 (2018).

11. Furuse, M., Fujita, K., Hiiragi, T., Fujimoto, K. & Tsukita, S. Claudin-1 and -2: Novel integral membrane proteins localizing at tight junctions with no sequence similarity to occludin. *J. Cell Biol.* **141**, 1539–1550 (1998).

12. Tsukita, S., Tanaka, H. & Tamura, A. The Claudins: From Tight Junctions to Biological Systems. *Trends Biochem. Sci.* **44**, 141–152 (2019).

13. Naik, U.P. & Eckfeld, K. Junctional adhesion molecule 1 (JAM-1). *J. Biol. Homeost. Agents* **17**, 341–347 (2003).

14. Coyne, C.B. & Bergelson, J.M. CAR: a virus receptor within the tight junction *Adv. Drug Deliv. Rev.* **57**, 869–882 (2005).

15. Ramena, Y. & Ramena, G. Cell-Cell Junctions and Epithelial Differentiation. *J Morphol Anat* **2**, 111 (2018).

16. Cheng, C.Y. & Mruk, D.D. Cell Junction Dynamics in the Testis: Sertoli-Germ Cell Interactions and Male Contraceptive Development. *Physiol. Rev.* **82**, 825–874 (2002).

17. Cheng, C.Y. & Mruk, D.D. The Blood-Testis Barrier and Its Implications for Male Contraception. *Pharmacol. Rev.* **64**, 16–64 (2011).

18. Mruk, D.D. & Cheng, C.Y. The mammalian blood-testis barrier: Its biology and regulation. *Endocr. Rev.* **36**, 564–591 (2015).

19. Kumar, N.M. & Gilula, N.B. The gap junction communication channel. *Cell* **84**, 381–388 (1996).

20. Carette, D., Weider, K., Gilleron, J., Giese, S., Dompierre, J., Bergmann, M., Brehm, R., Denizot, J.P., Segretain, D., & Pointis, G. Major involvement of connexin 43 in seminiferous epithelial junction dynamics and male fertility. *Dev. Biol.* **346**, 54–67 (2010).

21. Giepmans, B.N.G. & van IJzendoorn, S.C.D. Epithelial cell-cell junctions and plasma membrane domains. *Biochim. Biophys. Acta - Biomembr.* **1788**, 820–831 (2009).

22. Goodenough, D.A., Goliger, J.A., & Paul, D.L. Connexins, Connexons, and Intercellular Communication. *Annu. Rev. Biochem.* **65**, 475–502 (2002).

23. Van Zeijl, L., Ponsioen, B., Giepmans, B.N.G., Ariaens, A., Postma, F.R., Várnai, P., Balla, T., Divecha, N., Jalink, K., & Moolennar, W.H. Regulation of connexin43 gap junctional communication by phosphatidylinositol 4,5-bisphosphate. *J. Cell Biol.* **177**, 881–891 (2007).

24. Giepmans, B.N.G. Role of connexin43-interacting proteins at gap junctions. *Adv. Cardiol.* **42**, 41–56 (2006).

25. Harris, T.J.C. & Tepass, U. Adherens junctions: From molecules to morphogenesis. *Nat. Rev. Mol. Cell Biol.* **11**, 502–514 (2010).

26. Pokutta, S. & Weis, W.I. Structure and Mechanism of Cadherins and Catenins in Cell-Cell Contacts. *Annu. Rev. Cell Dev. Biol.* **23**, 237–261 (2007).

27. Ozaki-Kuroda, K., Nakanishi, H., Tanaka, H., Kurihara, H., Mueller, S., Irie, K., Ikeda, W., Sakai, T., Wimmer, E., Nishimune, Y., & Takai, Y. Nectin couples cell-cell adhesion and the actin scaffold at heterotypic testicular junctions. *Curr. Biol.* **12**, 1145–1150 (2002).

28. Fujiwara, Y., Goda, N., Tomonari, T., Narita, H., Satomura, K., Tenno, T., Nakagawa, A., Oda, M., Suzuki, M., Sakisaka, T., Takai, Y., & Hiroaki, H. Crystal structure of afadin PDZ domain-nectin-3 complex shows the structural plasticity of the ligand-binding site. *Protein Sci.* **24**, 376–385 (2015).

29. Indra, I., Troyanovsky, R., & Troyanovsky, S.M. Afadin controls cadherin cluster stability using clathrin-independent mechanism. *Tissue Barriers* **2**, e28687 (2014).

30. Indra, I., Choi, J., Chen, C.S., Troyanovsky, R.B., Shapiro, L., Honig, B., & Troyanovsky, S.M. Spatial and temporal organization of cadherin in punctate adherens junctions. *Proc. Natl. Acad. Sci.* **115**, e(4406-4415) (2018).

31. Hess, R.A. & Vogl, A.W. Sertoli cell anatomy and cytoskeleton. *Sertoli Cell Biology* (2015). doi:10.1016/b978-0-12-417047-6.00001-6

32. Cheng, C.Y. & Mruk, D.D. Biochemistry of Sertoli cell/germ cell junctions, germ cell transport, and spermiation in the seminiferous epithelium. *Sertoli Cell Biology* (2015). doi:10.1016/b978-0-12-417047-6.00012-0

33. Vogl, A.W., Vaid, K.S. & Guttman, J.A. The Sertoli cell cytoskeleton. *Adv. Exp. Med. Biol.* **636**, 186–211 (2008).

34. Russell, L.D. Observations on rat sertoli ectoplasmic ('junctional') specializations in their association with germ cells of the rat testis. *Tissue Cell* **9**, 475–498 (1977).

35. Vogl, A.W., Pfeiffer, D.C. & Redenbach, D.M. Ectoplasmic ("Junctional") Specializations in Mammalian Sertoli Cells: Influence on Spermatogenic Cells. *Ann. N. Y. Acad. Sci.* **637**, 175–202 (1991).

36. Guttman, J.A., Takai, Y. & Vogl, A.W. Evidence That Tubulobulbar Complexes in the Seminiferous Epithelium Are Involved with Internalization of Adhesion Junctions. *Biol. Reprod.* **71**, 548–559 (2004).

37. Lee, N.P.Y. & Cheng, C.Y. Ectoplasmic specialization, a testis-specific cell-cell actin-based adherens junction type: Is this a potential target for male contraceptive development? *Hum. Reprod. Update* **10**, 349–369 (2004).

38. Vogl, A.W. Distribution and Function of Organized Concentrations of Actin Filaments in Mammalian Spermatogenic Cells and Sertoli Cells. *Int. Rev. Cytol.* **119**, 1–56 (1989).

39. Salanova, M., Stefanini, M., De Curtis, I. & Palombi, F. Integrin receptor alpha 6 beta 1 is localized at specific sites of cell-to-cell contact in rat seminiferous epithelium. *Biol. Reprod.* **52**, 79–87 (1995).

40. Siu, M.K. & Cheng, C.Y. Interactions of Proteases, Protease Inhibitors, and the β1 Integrin/Laminin γ3 Protein Complex in the Regulation of Ectoplasmic Specialization Dynamics in the Rat Testis. *Biol. Reprod.* **70**, 945–964 (2004).

41. Yan, H.H.Y. & Cheng, C.Y. Blood-testis barrier dynamics are regulated by an engagement/disengagement mechanism between tight and adherens junctions via peripheral adaptors. *Proc. Natl. Acad. Sci.* **102**, 11722–11727 (2005).

42. Young, J.S., Guttman, J.A., Vaid, K.S., & Vogl, A.W. Tubulobulbar complexes are intercellular podosome-like structures that internalize intact intercellular junctions during epithelial remodeling events in the rat testis. *Biol. Reprod.* **80**, 162–174 (2009).

43. Morita, K., Sasaki, H., Fujimoto, K., Furuse, M. & Tsukita, S. Claudin-11/OSP-based tight junctions of myelin sheaths in brain and Sertoli cells in testis. *J. Cell Biol.* **145**, 579–588 (1999).

44. McCabe, M.J., Allan, C.M., Foo, C.F., Nicholls, P.K., McTavish, K.J., & Stanton, P.G. Androgen Initiates Sertoli Cell Tight Junction Formation in the Hypogonadal (hpg) Mouse. *Biol. Reprod.* **87**, 1–8 (2012).

45. Decrouy, X., Gasc, J.M., Pointis, G., & Sgretain, D. Functional characterization of Cx43 based gap junctions during spermatogenesis. *J. Cell. Physiol.* **200**, 146–154 (2004).

46. Risley, M.S. Connexin gene expression in seminiferous tubules of the Sprague-Dawley rat. *Biol Reprod* **62**, 748–754 (2000).

47. Mok, K.W., Lie, P.P.Y., Mruk, D.D, Mannu, J., Mathur, P.P., Silvestrini, B., & Cheng, C.Y. The apical ectoplasmic specialization-blood-testis barrier functional axis is A novel target for male contraception. *Adv. Exp. Med. Biol.* **763**, 334–355 (2012).

48. Akhtar, N. & Hotchin, N.A. RAC1 regulates adherens junctions through endocytosis of E-cadherin. *Mol. Biol. Cell* **12**, 847–862 (2001).

49. Ivanov, A. I., Nusrat, A., & Parkos, C.A. Endocytosis of Epithelial Apical Junctional Proteins by a Clathrin-mediated Pathway into a Unique Storage Compartment. *Mol. Biol. Cell* **15**, 176–188 (2004).

50. Shen, L., & Turner, J.R. Actin Depolymerization Disrupts Tight Junctions via Caveolae-mediated Endocytosis. *Mol. Biol. Cell* **16**, 3919–3936 (2005).

51. Troyanovsky, R.B., Sokolov, E.P., & Troyanovsky, S.M. Endocytosis of Cadherin from Intracellular Junctions Is the Driving Force for Cadherin Adhesive Dimer Disassembly. *Mol. Biol. Cell* **17**, 3484–3493 (2006).

52. Paterson, A.D., Parton, R.G., Ferguson, C., Stow, J.L., & Yap, A.S. Characterization of E-cadherin Endocytosis in Isolated MCF-7 and Chinese Hamster Ovary Cells. *J Biol Chem* **278**, 21050–21057 (2003).

53. Berthoud, V.M., Minogue, P.J., Laing, J.G., & Beyer, E.C. Pathways for degradation of connexins and gap junctions. *Cardiovasc. Res.* **62**, 256–267 (2004).

54. Piehl, M., Lehmann, C., Gumpert, A., Denizot, J., Segretain, D., & Falk, M.M. Internalization of Large Double-Membrane Intercellular Vesicles by a Clathrin-dependent Endocytic Process. *Mol. Biol. Cell* **18**, 337–347 (2007).

55. Smith, B.E. & Braun, R.E. Germ cell migration across sertoli cell tight junctions. *Science* **338**, 798–802 (2012).

56. Leblond, C.P. & Clermont, Y. Definition of the stages of the cycle of the seminiferous epithelium in the rat. *Ann. N. Y. Acad. Sci.* **55**, 548–573 (1952).

57. Du, M., Young, J., De Asis, M., Cipollone, J., Roskelley, C., Takai, Y., Nicholls, P.K., Stanton, P.G., Deng, W., Finlay, B.B., & Vogl, A.W. A Novel Subcellular Machine Contributes to Basal Junction Remodeling in the Seminiferous Epithelium. *Biol. Reprod.* **88**, 1–17 (2013).

58. Vogl, A.W., Du, M., Wang, X.Y., & Young, J.S. Novel clathrin/actin-based endocytic machinery associated with junction turnover in the seminiferous epithelium. *Semin. Cell Dev. Biol.* **30**, 55–64 (2014).

59. Vogl, A.W., Young, J.S. & Du, M. New Insights into Roles of Tubulobulbar Complexes in Sperm Release and Turnover of Blood-Testis Barrier. *Int. Rev. Cell Mol. Biol.* **303**, 319–355 (2013).

60. Young, J.S., Guttman, J.A., Vaid, K.S., Shahinian, H., & Vogl, A.W. Cortactin (CTTN), N-WASP (WASL), and clathrin (CLTC) are present at podosome-like tubulobulbar complexes in the rat testis. *Biol. Reprod.* **80**, 153–161 (2009).

61. Young, J.S., Takai, Y., Kojic, K.L., & Vogl, A. W. Internalization of adhesion junction proteins and their association with recycling endosome marker proteins in rat seminiferous epithelium. *Reproduction* **143**, 347–357 (2012).

62. Russell, L. & Clermont, Y. Anchoring device between Sertoli cells and late spermatids in rat seminiferous tubules. *Anat. Rec.* **185**, 259–277 (1976).

63. Kierszenbaum, A.L. & Tres, L.L. The acrosome-acroplaxome-manchette complex and the shaping of the spermatid head. *Arch. Histol. Cytol.* **67**, 271–284 (2004).

64. Upadhyay, R.D., Kumar, A.V., Ganeshan, M., & Balasinor, N.H. Tubulobulbar complex: Cytoskeletal remodeling to release spermatozoa. *Reprod. Biol. Endocrinol.* **10**, 27 (2012).

65. Russell, L.D. & Malone, J.P. A study of Sertoli-spermatid tubulobulbar complexes in selected mammals. *Tissue Cell* **12**, 263–285 (1980).

66. Russell, L.D. Further observations on tubulobulbar complexes formed by late spermatids and sertoli cells in the rat testis. *Anat. Rec.* **194**, 213–232 (1979).

67. Vogl, A.W., Grove, B.D. & Lew, G.J. Distribution of actin in sertoli cell ectoplasmic specializations and associated spermatids in the ground squirrel testis. *Anat. Rec.* **215**, 331–341 (1986).

68. Lyon, K.R., Bosseboeuf, E., & Vogl, A.W. An Alternative Model of Tubulobulbar Complex Internalization During Junction Remodeling in the Seminiferous Epithelium of the Rat Testis. *Biol. Reprod.* **93**, 1–12 (2015).

69. D'Souza, R., Pathak, S., Upadhyay, R., Gaonkar, R., D'Souza, S., Sonawane, S., Gill-Sharma, M., & Balasinor, N.H. Disruption of tubulobulbar complex by high intratesticular estrogens leading to failed spermiation. *Endocrinology* **150**, 1861–1869 (2009).

70. Guttman, J.A., Obinata, T., Shima, J., Griswold, M., & Vogl, A. W. Non-muscle cofilin is a component of tubulobulbar complexes in the testis. *Biol. Reprod.* **70**, 805–812 (2004).

71. Mulholland, D.J., Dedhar, S., & Vogl, A.W. Rat Seminiferous Epithelium Contains a Unique Junction (Ectoplasmic Specialization) with Signaling Properties Both of Cell/Cell and Cell/Matrix Junctions. *Biol. Reprod.* **64**, 396–407 (2001).

72. Aristaeus de Asis, M., Pires, M., Lyon, K. & Vogl, A.W. A network of spectrin and plectin surrounds the actin cuffs of apical tubulobulbar complexes in the rat. *Spermatogenesis* **3**, e25733 (2013).

73. Kusumi, N., Watanabe, M., Yamada, H., Li, S.A., Kashiwakura, Y., Matsukawa, T., Nagai, A., Nasu, Y., Kumon, H., & Takei, K. Implication of amphiphysin 1 and dynamin 2 in tubulobulbar complex formation and spermatid release. *Cell Struct. Funct.* **32**, 101–113 (2007).

74. Vaid, K.S., Guttman, J.A., Babyak, N., Deng, W., McNiven, M.A., Mochizuki, N., Finlay, B.B., & Vogl, A.W. The role of dynamin 3 in the testis. *J. Cell. Physiol.* **210**, 644–654 (2007).

75. Adams, A. & Vogl, A.W. High Resolution Localization of Rab5, EEA1, and Nectin-3 to Tubulobulbar Complexes in the Rat Testis. *Anat. Rec.* **300**, 1160–1170 (2017).

76. Lyon, K., Adams, A., Piva, M., Asghari, P., Moore, E.D., & Vogl, A.W. Ca^{2+} signaling machinery is present at intercellular junctions and structures associated with junction turnover in rat Sertoli cells. *Biol. Reprod.* **96**, 1288–1302 (2017).

77. Russell, L.D., Goh, J.C., Rashed, R.M., & Vogl, A.W. The consequences of actin disruption at Sertoli ectoplasmic specialization sites facing spermatids after in vivo exposure of rat testis to cytochalasin D. *Biol. Reprod.* **39**, 105–118 (1988).

78. Russell, L.D., Saxena, N.K., & Turner, T.T. Cytoskeletal involvement in spermiation and sperm transport. *Tissue Cell* **21**, 361–379 (1989).

79. Young, J.S., de Asis, M., Guttman, J., & Vogl, A.W. Cortactin depletion results in short tubulobulbar complexes and spermiation failure in rat testes. *Biol. Open* **1**, 1069–1077 (2012).

80. Taylor, M.J., Perrais, D., & Merrifield, C.J. A High Precision Survey of the Molecular Dynamics of Mammalian Clathrin-Mediated Endocytosis. *PLoS Biol.* **9**, e1000604 (2011).

81. Ochoa, G.C., Slepnev, V.I., Neff, L., Ringstad, N., Takei, K., Daniell, L., Kim, W., Cao, H., McNiven, M., Baron, R., & De Camilli, P. A functional link between dynamin and the actin cytoskeleton at podosomes. *J. Cell Biol.* **150**, 377–389 (2000).

82. Adams, A., Sriram, A. & Vogl, A. W. Internalization of Intact Intercellular Junctions in the Testis by Clathrin/Actin-Mediated Endocytic Structures: Tubulobulbar Complexes. *Anat. Rec. (Hoboken)* **301**, 2080–2085 (2018).

83. Byers, S.W., Hadley, M.A., Djakiew, D., & Dym, M. Growth and Characterization of Polarized Monolayers of Epididymal Epithelial Cells and Sertoli Cells in Dual Environment Culture Chambers. *J. Androl.* **7**, 59–68 (1986).

84. Dorrington, J.H., Roller, N.F., & Fritz, I.B. Effects of follicle-stimulating hormone on cultures of sertoli cell preparations. *Mol. Cell. Endocrinol.* **3**, 57–70 (1975).

85. Steinberger, A., Heindel, J.J., Lindsey, J.N., Elkington, J.S., Sanborn, B.M., & Steinberger, E. Isolation and culture of FSH responsive Sertoli cells. *Endocr Res Commun* **2**, 261–272 (1975).

86. Steinberger, A.J. Polarized New Functions Culture and Sertoli in a System. **6**, 69–71 (1985).

87. Hadley, M.A., Byers, S.W., Suárez-Quian, C.A., Djakiew, D., & Dym, M. In vitro models of differentiated Sertoli cell structure and function. **24**, 550–557 (1988).

88. Suárez-Quian, C.A. Sertoli cell culture in dual compartment chambers (including ECM). *Protoc. Cult. Tissue John G* 1–22 (1992).

89. Alves, M.G. & Oliveira, P. F. *Sertoli Cells Methods and Protocols (Methods in Molecular Biology - Book 1748)* (Humana, 2018).

90. Mruk, D.D. & Cheng, C.Y. An in vitro system to study Sertoli cell blood-testis barrier dynamics. *Methods Mol. Biol.* **763**, 237-252 (2011).

91. Mather, J.P., Wolpe, S.D., Gunsalus, G.L., Bardin, C.W. & Phillips, D.M. Effect of purified and cell-produced extracellular matrix components on Sertoli cell function. *Ann. N. Y. Acad. Sci.* **438**, 572–575 (1984).

92. Suárez-Quian, C.A., Hadley, M.A., & Dym, M. Effect of substrate on the shape of Sertoli cells in vitro. *Ann. N. Y. Acad. Sci.* **438**, 417–434 (1984).

93. Tung, P.S. & Fritz, I.B. Extracellular Matrix Promotes Rat Sertoli Cell Histotypic Expression In Vitro. *Biol. Reprod.* **30**, 213-229 (1984).

94. Janecki, A. & Steinberger, A. Polarized Sertoli cell functions in a new two-compartment culture system. *J. Androl.* **7**, 69-71 (1986).

95. Hadley, M.A., Byers, S.W., Suarez-Quian, C.A., Kleinman, H.K. & Dym, M. Extracellular matrix regulates Sertoli cell differentiation, testicular cord formation, and germ cell development in vitro. *J. Cell Biol.* **101**, 1511–1522 (1985).

96. Kleinman, H.K., McGarvey, M.L., Hassell, J.R., Star, V.L., Cannon, F.B., Laurie, G.W., & Martin, G.R. Basement Membrane Complexes with Biological Activity. *Biochemistry* **25**, 312-318 (1986).

97. Hadley, M.A., Djakiew, D., Byers, S.W. & Dym, M. Polarized secretion of androgen-binding protein and transferrin by Sertoli cells grown in a bicameral culture system. *Endocrinology* **120**, 1097-1103 (1987).

98. Djakiew, D., Hadley, A., Byers, W., & Dym, M. Transferrin-mediated of ^{59}Fe across confluent epithelial sheets of Sertoli cells grown in bicameral culture chambers. *J. Androl.* **7**, 355-366 (1986).

99. Kohno, S., Ziparo, E., Marek, L.F., & Tung, K.S.K. Murine Sertoli cells: major histocompatibility antigens and glycoconjugates. *J. Reprod. Immunol.* **5**, 339-350 (1983).

100. Majumdar, S.S., Tsuruta, J., Griswold, M.D., & Bartke, A. Isolation and culture of Sertoli cells from the testes of adult Siberian hamsters: analysis of proteins synthesized and secreted by Sertoli cells cultured from hamsters raised in a long or a short photoperiod. *Biol. Reprod.* **52**, 658-666 (1995).

101. Zhang, H., Liu, B., Qiu, Y., Fan, J.f., & Yu, S.j. Pure cultures and characterization of yak Sertoli cells. *Tissue Cell* **45**, 414-420 (2013).

102. Teng, Y., Xue, W.J., Ding, X.M., Feng, X.S., Xiang, H.L., Jiang, Y.Z., & Tian, P.X. Isolation and culture of adult Sertoli cells and their effects on the function of co-cultured allogeneic islets in vitro. *Chin. Med. J. (Engl.)* **118**, 1857-1862 (2005).

103. Clermont, Y. & Perey, B. Quantitative study of the cell population of the seminiferous tubules in immature rats. *Am. J. Anat.* **100**, 241-267 (1957).

104. Vitale, R., Fawcett, D.W., & Dym, M. The normal development of the blood-testis barrier and the effects of clomiphene and estrogen treatment. *Anat. Rec.* **176**, 331-344 (1973).

105. Mather, J.P. Establishment and Characterization of Two Distinct Mouse Testicular Epithelial Cell Lines. *Biol. Reprod.* **23**, 243-252 (1980).

106. Jégou, B. The Sertoli cell in vivo and in vitro. *Cell Biol. Toxicol.* **8**, 49–54 (1992).

107. Sluka, P., O'Donnell, L., Bartles, J.R., & Stanton, P.G. FSH regulates the formation of adherens junctions and ectoplasmic specialisations between rat Sertoli cells in vitro and in vivo. *J. Endocrinol.* **189**, 381-395 (2006).

108. Galdieri, M., Ziparo, E., Palombi, F., Russo, M.A. & Stefanini, M. Pure Sertoli Cell Cultures: A New Model for the Study of Somatic—Germ Cell Interactions. *J. Androl.* **2**, 249-254 (1981).

109. Hynes, R.O. Integrins: A family of cell surface receptors. *Cell.* **48**, 549-554 (1987).

110. Tamkun, J.W., DeSimone, D.W., Fonda, D., Patel, R.S., Buck, C., Horwitz, A.F., & Hynes, R.O. Structure of integrin, a glycoprotein involved in the transmembrane linkage between fibronectin and actin. *Cell.* **46**, 271-282 (1986).

111. Nelson, C.M. & Bissell, M.J. Modeling dynamic reciprocity: engineering three-dimensional culture models of breast architecture, function, and neoplastic transformation. *Seminars in Cancer Biology*. **15**, 342-352 (2005).

112. Streuli, C.H., Bailey, N., & Bissell, M.J. Control of mammary epithelial differentiation: Basement membrane induces tissue-specific gene expression in the absence of cell-cell interaction and morphological polarity. *J. Cell Biol.* **115**, 1383-1395 (1991).

113. Emerman, J.T. & Pitelka, D.R. Maintenance and induction of morphological differentiation in dissociated mammary epithelium on floating collagen membranes. *In Vitro.* **13**, 316–328 (1977).

114. Ross, A.J. & Capel, B. Signaling at the crossroads of gonad development. *Trends Endocrinol. Metab.* **16**, 19-25 (2005).

115. Hadley, M.A., Weeks, B.S., Kleinman, H.K., & Dym, M. Laminin promotes formation of cord-like structures by sertoli cells in vitro. *Dev. Biol.* **140**, 318-327 (1990).

116. Mackay, S., Booth, S.H., MacGowan, A., & Smith, R.A. Ultrastructural studies demonstrate that epithelial polarity is established in cultured mouse pre-Sertoli cells by extracellular matrix components. *J. Electron Microsc. (Tokyo)* **48**, 159-165 (1999).

117. Gassei, K., Schlatt, S., & Ehmcke, J. De novo morphogenesis of seminiferous tubules from dissociated immature rat testicular cells in xenografts. *J. Androl.* **27**, 611-618 (2006).

118. Gassei, K., Ehmcke, J., Wood, M.A., Walker, W.H. & Schlatt, S. Immature rat seminiferous tubules reconstructed in vitro express markers of Sertoli cell maturation after xenografting into nude mouse hosts. *Mol. Hum. Reprod.* **16**, 97-110 (2010).

119. Reuter, K., Ehmcke, J., Stukenborg, J.B., Simoni, M., Damm, O.S., Redmann, K., Schlatt, S., & Wistuba, J. Reassembly of somatic cells and testicular organogenesis in vitro. *Tissue Cell* **46**, 86–96 (2014).

120. Legendre, A., Froment, P., Desmots, S., Lecomte, A., Habert, R., & Lemazurier, E. An engineered 3D blood-testis barrier model for the assessment of reproductive toxicity potential. *Biomaterials* **31**, 4492-4505 (2010).

121. Gassei, K., Ehmcke, J., & Schlatt, S. Initiation of testicular tubulogenesis is controlled by neurotrophic tyrosine receptor kinases in a three-dimensional Sertoli cell aggregation assay. *Reproduction* **136**, 459-469 (2008).

122. Wegner, S., Hong, S., Yu, X., & Faustman, E.M. Preparation of rodent testis co-cultures. *Curr. Protoc. Toxicol.* **55**, 16.10.1-16.10.7 (2013).

123. Zhang, X., Wang, L., Zhang, X., Ren, L., Shi, W., Tian, Y., Zhu, J., & Zhang, T. The use of KnockOut serum replacement (KSR) in three dimensional rat testicular cells co-culture model: An improved male reproductive toxicity testing system. *Food Chem. Toxicol.* **106**, 487-495 (2017).

124. Alves-Lopes, J.P., Söder, O. & Stukenborg, J.B. Testicular organoid generation by a novel in vitro three-layer gradient system. *Biomaterials* **130**, 76-89 (2017).

125. Bhushan, S., Aslani, F., Zhang, Z., Sebastian, T., Elsässer, H.P., & Klug, J. Isolation of Sertoli Cells and Peritubular Cells from Rat Testes. *J. Vis. Exp.* **8**, e53389 (2016).

126. Abràmoff, M.D., Magalhães, P.J. & Ram, S.J. Image processing with ImageJ. *Biophotonics International* (2004).

127. Tung, P.S. & Fritz, I.B. Extracellular matrix components and testicular peritubular cells influence the rate and pattern of Sertoli cell migration in vitro. *Dev. Biol.* **113**, 119-134 (1986).

128. Schlatt, S., de Kretser, D.M. & Loveland, K.L. Discriminative analysis of rat Sertoli and peritubular cells and their proliferation in vitro: evidence for follicle-stimulating hormone-mediated contact inhibition of Sertoli cell mitosis. *Biol. Reprod.* **55**, 227-235 (1996).

129. Griswold, M.D. The central role of Sertoli cells in spermatogenesis. *Semin. Cell Dev. Biol.* **9**, 411–416 (1998).

130. de Rooij, D.G. Proliferation and differentiation of spermatogonial stem cells. *Reproduction* **121**, 347–354 (2001).

131. Wistuba, J., Stukenborg, J.B., & Luetjens, C.M. Mammalian Spermatogenesis. *Funct. Dev. Embryol.* **1**, 99–117 (2007).

132. Oatley, J.M. & Brinster, R.L. Regulation of Spermatogonial Stem Cell Self-Renewal in Mammals. *Annu. Rev. Cell Dev. Biol.* **24**, 263–286 (2008).

133. Oatley, J.M. & Brinster, R.L. The Germline Stem Cell Niche Unit in Mammalian Testes. *Physiol. Rev.* **92**, 577–595 (2012).

134. Meachem, S., von Schönfeldt, V., & Schlatt, S. Spermatogonia: stem cells with a great perspective. *Reproduction* **121**, 825–834 (2001).

135. de Rooij, D.G. The spermatogonial stem cell niche. *Microsc. Res. Tech.* **72**, 580–585 (2009).

136. Stukenborg, J.B., Colón, E., & Söder, O. Ontogenesis of testis development and function in humans. *New Concepts Hum. Disord. Sex. Dev.* **4**, 199–212 (2010).

137. Palombi, F., Ziparo, E., Rommerts, F.F., Grootegoed, J.A., Antonini, M., & Stefanini, M. Morphological characteristics of male germ cells of rats in contact with Sertoli cells in vitro. *Reproduction* **57**, 325–330 (1979).

138. Skinner, M.K. Cell-cell interactions in the testis. *Endocr. Rev.* **12**, 45–77 (1991).

139. Iwanami, Y., Kobayashi, T., Kato, M., Hirabayashi, M., & Hochi, S. Characteristics of rat round spermatids differentiated from spermatogonial cells during co-culture with Sertoli cells, assessed by flow cytometry, microinsemination and RT-PCR. *Theriogenology* **65**, 288–298 (2006).

140. Le Magueresse-Battistoni, B., Gérard, N., & Jégou, B. Pachytene spermatocytes can achieve meiotic process in vitro. *Biochem. Biophys. Res. Commun.* **179**, 1115–1121 (1991).

141. Tres, L.L. & Kierszenbaum, A.L. Viability of rat spermatogenic cells in vitro is facilitated by their coculture with Sertoli cells in serum-free hormone-supplemented medium. *Proc. Natl. Acad. Sci. U. S. A.* **80**, 3377–3381 (1983).

142. Boitani, C., Politi, M.G., & Menna, T. Spermatogonial cell proliferation in organ culture of immature rat testis. *Biol. Reprod.* **48**, 761–767 (1993).

143. Lambrot, R., Coffigny, H., Pairault, C., Donnadieu, A.C., Frydman, R., Habert, R., & Rouiller-Fabre, V. Use of organ culture to study the human fetal testis development: Effect of retinoic acid. *J. Clin. Endocrinol. Metab.* **91**, 2696–2703 (2006).

144. Schlatt, S., Zhengwei, Y., Meehan, T., De Kretser, D.M. & Loveland, K.L. Application of morphometric techniques to postnatal rat testes in organ culture: Insights into testis growth. *Cell Tissue Res.* **298**, 335–343 (1999).

145. Steinberger, A., Steinberger, E., & Perloff, W. H. Mammalian testes in organ culture. *Exp. Cell Res.* **36**, 19–27 (1964).

146. Abu Elhija, M., Lunenfeld, E., Schlatt, S., & Huleihel, M. Differentiation of murine male germ cells to spermatozoa in a soft agar culture system. *Asian J. Androl.* **14**, 285–293 (2012).

147. Boucheron, C. & Baxendale, V. Isolation and purification of murine male germ cells. *Methods Mol. Biol.* **825**, 59–66 (2012).

148. Brinster, R.L. & Zimmermannt, J.W. Spermatogenesis following male germ-cell transplantation. *Dev. Biol.* **91**, 11298–11302 (1994).

149. Nagano, M., Avarbock, M.R., & Brinster, R.L. Pattern and kinetics of mouse donor spermatogonial stem cell colonization in recipient testes. *Biol. Reprod.* **60**, 1429–1436 (1999).

150. Li, M.W., Mruk, D.D., Lee, W.M., & Cheng, C.Y. Disruption of the blood-testis barrier integrity by bisphenol A in vitro: Is this a suitable model for studying blood-testis barrier dynamics? *Int. J. Biochem. Cell Biol.* **41**, 2302–2314 (2009).

151. Su, L., Kopera-Sobota, I.A., Bilinska, B., Cheng, C.Y., & Mruk, D.D. Germ cells contribute to the function of the Sertoli cell barrier. *Spermatogenesis* **3**, e26460 (2013).

152. Di Carlo, A.D., Travia, G., & De Felici, M. The meiotic specific synaptonemal complex protein SCP3 is expressed by female and male primordial germ cells of the mouse embryo. *Int. J. Dev Biol.* **44**, 241–244 (2000).

153. Lovelace, D.L., Gao, Z., Mutoji, K., Song, Y.C., Ruan, J., & Hermann, B.P. The regulatory repertoire of PLZF and SALL4 in undifferentiated spermatogonia. *Development* **143**, 1893–1906 (2016).

154. Pesce, M., Wang, X., Wolgemuth, D.J., & Schöler, H. Differential expression of the Oct-4 transcription factor during mouse germ cell differentiation. *Mech Dev.* **71**, 89–98 (1998).

155. Picut, C. A., Remick, A.K., de Rijik, E.P., Simons, M.L., Stump, D.G., & Parker, G.A. Postnatal Development of the Testis in the Rat: Morphologic Study and Correlation of Morphology to Neuroendocrine Parameters. *Toxicol. Pathol.* **43**, 326–342 (2015).

156. Siu, M.K., Wong, C.H., Lee, W.M. & Cheng, C.Y. Sertoli-germ cell anchoring junction dynamics in the testis are regulated by an interplay of lipid and protein kinases. *J. Biol. Chem.* **280**, 25029–25047 (2005).

157. Carrell, D.T. & Aston, K.I. *Spermatogenesis - Methods and Protocols. Methods in Molecular Biology* **927** (Humana Press, 2013).

158. Chen, C., Ouyang, W., Grigura, V., Zhou, Q., Carnes, K., Lim, H., Zhao, G.Q., Arber, S., Kurpios, N., Murphy, T.L., Cheng, A.M., Hassell, J.A., Chandrashekar, V., Hofmann, M.C.,

Hess, R.A., & Murphy, K.M. ERM is required for transcriptional control of the spermatogonial stem cell niche. *Nature* **436**, 1030–1034 (2005).

159. Simon, L., Ekman, G.C., Garcia, T., Carnes, K., Zhang, Z., Murphy, T., Murphy, K.M., Hess, R.A., Cooke, P.S., & Hofmann, M.C. ETV5 regulates sertoli cell chemokines involved in mouse stem/progenitor spermatogonia maintenance. *Stem Cells* **28**, 1882–1892 (2010).

160. Laemmli, U.K. Cleavage of structural proteins during the assembly of the head of bacteriophage T4. *Nature* **227**, 680–685 (1970).

161. Schafer, D.A. Coupling actin dynamics and membrane dynamics during endocytosis. *Curr. Opin. Cell Biol.* **14**, 76–81 (2002).

162. Miyaso, H., Komiyama, M., Matsuno, Y., Naito, M., Hirai, S., Itoh, M., & Mori, C. The changes of cortactin p80/85 isoform profiles and tyrosine phosphorylation status during spermatogenesis in the mouse testis. *J. Androl.* **31**, 507–518 (2010).

163. Weaver, A.M., Karginov, A.V., Kinley, A.W., Weed, S.A., Li, Y., Parsons, J.T., & Cooper, J.A. Cortactin promotes and stabilizes Arp2/3-induced actin filament network formation. *Curr. Biol.* **11**, 370–374 (2001).

164. Daly, R.J. Cortactin signalling and dynamic actin networks. *Biochem. J.* **382**, 13–25 (2004).

165. Kirkbride, K.C., Sung, B.H., Sinha, S., & Weaver, A.M. Cortactin: A multifunctional regulator of cellular invasiveness. *Cell Adh Migr.* **5**, 187–198 (2011).

166. Bryce, N.S., Clark, E.S., Leysath, J.L., Currie, J.D., Webb, D.J., & Weaver, A.M. Cortactin promotes cell motility by enhancing lamellipodial persistence. *Curr. Biol.* **15**, 1276–1285 (2005).

167. Tehrani, S., Faccio, R., Chandrasekar, I., Ross, F.P., & Cooper, J.A. Cortactin Has an Essential and Specific Role in Osteoclast Actin Assembly. *Mol. Biol. Cell* **17**, 2882–2895 (2006).

168. Hong, J., Qian, Z., Shen, S., Min, T., Tan, C., Xu, J., Zhao, Y., & Huang, W. High doses of siRNAs induce eri-1 and adar-1 gene expression and reduce the efficiency of RNA interference in the mouse. *Biochem. J.* **390**, 675–679 (2005).

169. Vogl, A.W., Soucy, L.J., & Lew, G.J. Distribution of actin in isolated seminiferous epithelia and denuded tubule walls of the rat. *Anat. Rec.* **213**, 63–71 (1985).

170. Schafer, D.A., Weed, S.A., Binns, D., Karginov, A.V., Parsons, J.T., & Cooper, J.A. Dynamin2 and cortactin regulate actin assembly and filament organization. *Curr. Biol. CB* **12**, 1852–1857 (2002).

171. Hoffer, A.P., Carlton, B.D., & Brunengraber, H. Ultrastructure and intercellular vacuolization of isolated perfused and control rat testes. *J. Androl.* **4**, 361–370 (1983).

172. Franke, W.W., Grund, C., & Fink, A. Location of actin in the microfilament bundles associated with the junctional specializations between Sertoli cells and spermatids. *Biol Cell* **31**, 7–13 (1978).

173. Russell, L.D. Spermatid-Sertoli tubulobulbar complexes as devices for elimination of cytoplasm from the head region late spermatids of the rat. *Anat. Rec.* **194**, 233–246 (1979).

174. Tanii, I., Yoshinaga, K., & Toshimori, K. Morphogenesis of the acrosome during the final steps of rat spermiogenesis with special reference to tubulobulbar complexes. *Anat. Rec.* **256**, 195–201 (1999).

175. Weber, J.E., Turner, T.T., Tung, K.S. & Russell, L.D. Effects of cytochalasin D on the integrity of the Sertoli cell (blood-testis) barrier. *Am. J. Anat.* **182**, 130–147 (1988).

176. Collins, A., Warrington, A., Taylor, K.A. & Svitkina, T. Structural organization of the actin cytoskeleton at sites of clathrin-mediated endocytosis. *Curr. Biol. CB* **21**, 1167–1175 (2011).

177. Kaksonen, M., Toret, C.P., & Drubin, D.G. Harnessing actin dynamics for clathrin-mediated endocytosis. *Nat. Rev. Mol. Cell Biol.* **7**, 404–414 (2006).

178. Sriram, A., Lyon, K.R., Ho, C.D., Huynh, N. & Vogl, A.W. Actin Disruption Results in Altered Morphology of Basal Tubulobulbar Complexes in Rat Seminiferous Epithelium. *Anat. Rec.* **299**, 1449–1455 (2016).

179. D'Agostino, A., Monaco, L., Stefanini, M., & Geremia, R. Study of the interaction between germ cells and Sertoli cells in vitro. *Exp. Cell Res.* **150**, 430–435 (1984).

180. Agarwal, A., Mulgund, A., Hamada, A., & Chyatte, M.R. A unique view on male infertility around the globe. *Reproductive Biology and Endocrinology.* **13**(1), 37 (2015).

181. Carlsen, E., Giwercman, A., Keiding, N., & Skakebaek, N.E. Evidence for decreasing quality of semen during past 50 years. *BMJ.* **305**, 609-613 (1992).

182. Fisch, H. Declining Worldwide Sperm Counts: Disproving a Myth. *Urologic Clinics of North America.* **35**, 137-146 (2008).